The Role of Forkhead Box Transcription Factors in Zebrafish Ocular Development and the Superior Ocular Fissure

By

Tara Rachel Stach

A thesis submitted in partial fulfillment of the requirements for the degree of

Master of Science

In

Medical Sciences - Medical Genetics

University of Alberta

Abstract

Ocular development is a tightly orchestrated process that is dependent upon precise environmental and genetic factors. Disruption of this can result in microphthalmia, anophthalmia and coloboma (MAC), which is a spectrum of congenital ocular disease with lifelong consequences affecting sight. In particular, coding anomalies in a member of the Bone Morphogenetic Protein family, *GDF6*, results in MAC in patients. Using zebrafish *gdf6a*$^{-/-}$ mutants, we have found that the microphthalmia present in both patients and model organisms appears to be due the requirement for Gdf6a in the regulation of ocular proliferation, progenitor cell survival, and apoptosis in the developing eye. Additionally, we have found that Gdf6a is located upstream of two forkhead box (FOX) transcription factor genes, *foxi1* and *foxi2*, which provide dorsal-ventral polarity to a region where ocular progenitor cells reside, the ciliary marginal zone (CMZ). This is the first report of its kind regarding spatio-temporal identity of the CMZ, and we show that *foxi2* and *gdf6a* lie on converging genetic pathways that regulate ocular size.

The forkhead box (FOX) proteins are a family of transcription factors with diverse roles in development such as patterning of neural tissue, cell migration, proliferation, differentiation and survival. Mutations in FOX genes are associated with blinding ocular disorders that occur due to malformation of anterior segment components, and the failure of the optic nerve to correctly innervate the brain. Based on expression patterns and a regulation by Gdf6a, we hypothesized that *foxi1* and *foxi2* have roles in the patterning and growth of the retina. Knockdown of either *foxi1* or *foxi2* expression using morpholino (MO) technology resulted in aberrant dorsal-ventral ocular patterning and MAC phenotypes. However, *foxi1*$^{-/-}$ embryos do not have ocular phenotypes similar to those of the morphant, suggesting compensation by redundant genes, an allele that is not fully disruptive to protein function, or off-target MO effects.

The choroid fissure is a well-recognized developmental structure whose failure to close results in coloboma affecting structures of the inferior eye. However, patients with coloboma affecting structures of the superior eye led us to discover the superior ocular fissure, present during zebrafish ocular development and indicative of ~450 million years of evolutionary conservation. Biochemical modeling of transheterozygous *CYP1B1* coding anomalies in a proband indicated these might underlie the pathogenicity of superior coloboma, with a requirement for this enzyme to metabolize vitamin A to its active derivative, retinoic acid (RA). Examination of the developing zebrafish retina shows expression of *cyp1b1* and other RA metabolism enzymes at the locations of the ocular fissures, and supplementation of vitamin A to a coloboma model during development rescued the phenotype by facilitating closure of the inferior ocular fissure. Finally, I find that antagonism between the FOX genes *foxg1* and *foxd1* determine the location of fissure formation, with knockdown resulting in superior fissure shift to the nasal axis, or duplication, respectively.

Preface

This thesis is an original work by Tara Stach. The research project, of which this thesis is a part, received research ethics approval from the University of Alberta Animal Policy and Welfare Committee. The author has met the Canadian Council on Animal Care (CCAC) mandatory training requirements for animal users on the Care and Use of Animals in Research, Teaching and Testing.

Portions of Chapter 2 and Chapter 3 have been modified from the publication:

French CR, **Stach TR**, March LD, Lehmann OJ, Waskiewicz AJ. Apoptotic and Proliferative Defects Characterize Ocular Development in a Microphthalmic BMP Model. Invest Ophthalmol Vis Sci. 2013 Jul 10;54(7):4636-47

Please note that ARVO is the copyright holder of this publication

C.R. French and myself are co-first authors of this paper. C.R. French is responsible for Figures 1, 2, 4, the majority of 5, 6, and Supplementary Figure 1. I am responsible for Figures 7 and 8, panels M – T in Figure 5, and aiding L.D. March with preliminary experiments leading to Figure 3, of which she is responsible. This manuscript was written and assembled by myself, with aid in figure assembly and manuscript edits from C.R. French and L.D. March. A.J. Waskiewicz was the supervisory author and was involved with concept formation, manuscript composition and edits. O.J. Lehmann provided manuscript edits and was the co-supervisor of this project.

Please note that the R368H (c.1103G>A) and A287Pfsx6 (c.859delG) *CYP1B1* mutations in the proband were diagnosed and interpreted by the Molecular Diagnostic Laboratory in the Department of Medical Genetics at the University of Alberta and confirmed by Erin Strachan.

Please note that Caroline Cheng owns the copyrights to Figure 1-1 and the DNA double helix in Figure 1-3.

Dedication

I dedicate this thesis to my mother and father, for nothing would have been possible without the lifetime of immeasurable support that they have provided.

Acknowledgements

I would like to thank my supervisor, Dr. Ordan Lehmann, and my committee members, Dr. Andrew Waskiewicz and Dr. David Eisenstat for their direction and support during my degree. Thanks to Dr. Sarah Hughes, Dr. Andrew Simmonds, Dr. Fred Berry and Dr. Michael Walter for their guidance.

Thanks to Aleah McCorry for the maintenance of fish stocks.

Thanks to the funding agencies that made this work possible: Women and Children's Health Research Institute, Canadian Institutes of Health Research, the Faculty of Medicine & Dentistry, the Government of Alberta, and Alberta Innovates-Health Solutions.

I would like to acknowledge my friends and family who made the course of my degree not only bearable, but also enjoyable.

My mother Belinda and father Mark, my sister Alyse and brother Konrad, my grandparents Jeanette and Phil Stach, and Martha and Richard Blair.

Thanks to my fellow graduate students and lab mates, to whom I cannot say enough of: Jen W., Caroline, Lindsey, Lyndsay, Jen H., Jakub, Laura, Vanessa, Danna, Curtis, Tim, Jamie, Chloe, Ping, Mika, Prajakta, Sam, Erin, Yoko, Phil, Michelle, and Namal.

Table of Contents

List of Tables

Table of Figures

List of Abbreviations

aldh1a2: Aldehyde dehydrogenase 1a2

aldh1a3: Aldehyde dehydrogenase 1a3

APS: ammonium persulfate

BAMBI: BMP and activin membrane-bound inhibitor

BCOR: BCL6 Co-repressor

BSA: Bovine serum albumin

BMP: bone morphogenetic protein

BP: base pair

CHARGE: Coloboma, heart anomaly, choanal atresia, growth or mental retardation, genital and ear anomalies

CHD7: Chromodomain helicase DNA binding protein 7

CMZ: ciliary marginal zone

CNC: Cranial neural crest cell

Cos-7: CV-1 in Origin, carrying SV40, 7

CRABP: cellular RA-binding protein

CRBP: cellular retinol-binding protein

CYP: Cytochrome P450

DMEM: Dulbecco's Modified Eagle Medium

DMSO: dimethyl sulfoxide

dpf: days post fertilization

Efn: Ephrin ligands

EGFP: enhanced green fluorescent protein

EM: embryo media

Eph: Eph receptors – receptor tyrosine kinases

FGFs: fibroblast growth factors

FOX: forkhead box

Gdf: growth and differentiation factor

hpf: hours post fertilization

HRM: high resolution melt

IF: immunofluorescence

ISH: in situ hybridization

MAC: microphthalmia, anophthalmia and coloboma

MO: morpholino oligonucleotide

NCCs: Neural crest cells

Otx2: Orthodenticle homeobox 2

Pax2: Paired homeobox 2

Pax6: Paired homeobox 6

PBS: phosphate buffered saline

PBSDTT: 1 X PBS, 1% DMSO, 1% Tween-20 & 1% Triton

PBST: phosphate buffered saline with 0.1% Tween-20

PFA: paraformaldehyde

PH3: phosphohistone H3

PIC: protease inhibitor cocktail

PMSF: phenylmethylsulfonyl floride

POM: periocular mesenchyme

PTU: 1-phenyl 2-thiourea

RA: retinoic acid

RAR: retinoic acid receptor

RARE: Retinoic acid –responsive element

RAX/Rx/rx3: retina and anterior neural fold homeobox

RIPA: radio-immunoprecipitation assay

RPE: retinal pigment epithelium

RPC: retinal progenitor cell

RT: room temperature

RXR: retinoid X receptor

SEM: scanning electron microscopy

SDS-PAGE: sodium dodecyl sulfate-polyacrylamide gel electrophoresis

SFRP: secreted frizzed-related protein

SHH: sonic hedgehog

Six3: SIX homeobox 3

Six6: SIX homeobox 6

Sox2: SRY (sex determining region Y)-box 2

SSC: saline sodium citrate buffer

STRA6: Stimulated by retinoic acid 6

TGFβ: transforming growth factor-β

TBST: Tris-buffered saline with Tween-20

TBX: T-box transcription factor

TEMED: tetramethylethlenediamine

UTR: untranslated region

VAX2: ventral homeobox 2

WT: wild type

ZIRC: Zebrafish International Resource Center

Chapter 1

Introduction

Microphthalmia, anophthalmia and coloboma

Microphthalmia, anophthalmia and coloboma (MAC) lie on a phenotypic spectrum of ocular disease that occurs in approximately 30/100 000 births, with microphthalmia present in up to 11% of blind children (MORRISON *et al.* 2002; VERMA AND FITZPATRICK 2007; PARKER *et al.* 2010). Pathogenicity of this disease remains to be fully discerned, but is thought to be due to either failed optic vesicle formation (primary), failed anterior neural tube formation (secondary), or the subsequent degeneration of optic vesicles after development (VERMA AND FITZPATRICK 2007). Disease etiology is complex, with a combination of environmental causes such as gestational infection, solvent exposure and vitamin A deficiency implicated, in addition to genetic causes that can be heritable or spontaneous (VERMA AND FITZPATRICK 2007; WILLIAMSON AND FITZPATRICK 2014).

MAC can be monogenetic or chromosomal, present in an isolated fashion, or with multisystem defects. Autosomal dominant mutations in *Chromodomain helicase DNA binding protein 7* (*CHD7)* and *Paired Box 2* (*PAX2*) both result in coloboma, with the former present in CHARGE (coloboma, heart anomaly, choanal atresia, growth or mental retardation, genital and ear anomalies) syndrome (JANSSEN et al. 2012), and the latter in papillorenal syndrome (BOWER et al. 2012). MAC can also occur in patients with X-linked oculofaciocardiodental syndrome (DAVOODY *et al.* 2012), and with partial penetrance with holoprosencephaly as a result of *Sonic Hedgehog* (*SHH)* and *SIX homeobox 3* (*SIX3)* mutations (MERCIER *et al.* 2010). However, the majority of MAC cases are due to coding anomalies in genes with roles in ocular development (VERMA AND FITZPATRICK 2007; WILLIAMSON AND FITZPATRICK 2014). Specification of the retinal anlage requires expression of the homeodomain transcription factors *Six3, Orthodenticle homeobox 2 (Otx2), Paired homeobox 6 (Pax6),* and *Retina and anterior neural fold homeobox (Rax),* with the ability of *Six3* and *Rax* expression to induce ectopic ocular vesicles (ZUBER et al.

2003). *RAX/Rx/rx3* is required for evagination, proliferation and differentiation of retinal progenitor cells, with anophthalmia and microphthalmia present in humans, mice and zebrafish when this gene is disrupted (MATHERS *et al.* 1997; CHUANG AND RAYMOND 2001; LOOSLI *et al.* 2003; VORONINA *et al.* 2004). *Otx2* is required for ocular tissue specification and patterning the optic primordia, and for cell cycle regulation of neural retina progenitors. Carriers of heterozygous mutations of *OTX2* are afflicted with severe ocular defects, in both patients and model organisms (MARTINEZ-MORALES *et al.* 2001; MARTINEZ-MORALES *et al.* 2003; ZUBER *et al.* 2003; RAGGE *et al.* 2005; SCHILTER *et al.* 2011). Later stages in ocular development also require the aforementioned transcription factors. Lens placode induction and subsequent growth is a critical step during ocular development and, in a dose-dependent manner, requires *Six3, Forkhead box E3 (Foxe3), Pax6* and *SRY (sex determining region Y)-box 2* (*Sox2). FOXE3* mutations are causative of microphthalmia and inherited in an autosomal dominant or recessive manner, with disruption of this gene similarly resulting in small eyes in murine and zebrafish models (SHI *et al.* 2006; REIS *et al.* 2010). Heterozygous mutations, whether inherited or *de novo*, in *SOX2* are the cause of the majority of human cases of anophthalmia and microphthalmia (GERTH-KAHLERT *et al.* 2013; WILLIAMSON AND FITZPATRICK 2014). Haploinsufficiency of *Sox2, Pax6, Six3* and *Otx2* results in MAC phenotypes in both murine and zebrafish models (LIU *et al.* 2006; SMITH *et al.* 2009), which can be further attributed to their additional roles in progenitor cell competence and differentiation into the inner neural retina and outer retinal pigmented epithelium (RPE) of the bi-layered optic cup (HILL *et al.* 1992; OLIVER *et al.* 1996; LOOSLI *et al.* 1999; VAN RAAMSDONK AND TILGHMAN 2000; LAGUTIN *et al.* 2001; MARTINEZ-MORALES *et al.* 2003; WARGELIUS *et al.* 2003; TARANOVA *et al.* 2006; WEN *et al.* 2008; WESTENSKOW *et al.* 2009; MATSUSHIMA *et al.* 2011; WILLIAMSON AND FITZPATRICK 2014).

A number of MAC cases have been attributed to defects in members of the Vitamin A (retinol) metabolism pathway, as well as to deficiencies and excess of Vitamin A during gestation (HORNBY *et al.* 2000; WILLIAMSON AND FITZPATRICK 2014). Specifically, MAC has been linked to coding anomalies in three pathway members, *Stimulated by retinoic acid 6* (*STRA6), Retinoic acid receptor, beta (RARB),* and *Aldehyde dehydrogenase 1A3* (*ALDH1A3*) (WILLIAMSON AND FITZPATRICK 2014). In these cases, MAC presented in both non-syndromic and syndromic fashion, was typically bilateral, with *ALDH1A3* mutations more viable, or having higher patient survival, than those of *STRA6* and *RARB* (WILLIAMSON AND FITZPATRICK 2014). This is likely due to their positions in the metabolic pathway, as ALDH1a3 is an enzyme required for an intermediate step and is partially redundant, while STRA6 is a cell membrane receptor for cellular-retinol binding protein to uptake retinol from the blood stream, and RARB binds RA in the cytoplasm (Figure 1-3). *STRA6* and *RARB* coding anomalies can result in pulmonary, diaphragmatic, anophthalmia and cardiac (PDAC) syndrome or in isolated MAC, with *STRA6* mutations transmitted recessively, and *RARB* mutations dominant, recessive, or *de novo* (CASEY *et al.* 2011; CHASSAING *et al.* 2013; SROUR *et al.* 2013; WILLIAMSON AND FITZPATRICK 2014). In contrast, MAC cases resulting from *ALDH1A3* coding anomalies appear to be a result of consanguinity and are autosomal recessive and typically result in MAC in a non-syndromic fashion (FARES-TAIE *et al.* 2013; ABOUZEID *et al.* 2014; MORY *et al.* 2014; SEMERCI *et al.* 2014). Knockdown of *aldh1a3* and *stra6* in zebrafish results in microphthalmia (ISKEN *et al.* 2008; YAHYAVI *et al.* 2013) and *RBP*$^{-/-}$ mice have reduced eye function early in development (QUADRO *et al.* 1999; FARES-TAIE *et al.* 2013; WILLIAMSON AND FITZPATRICK 2014).

A number of MAC cases can also be attributed to monoallelic inheritance or *de novo* occurrence of variants in members of the Bone Morphogenetic (BMP) family, *BMP4, BMP7, GDF3* and *GDF6*. For *BMP4* and *BMP7,* only a handful of alleles have been identified, and only nonsynonymous variant alleles have been identified for *GDF3* and *GDF6* (WILLIAMSON AND

FITZPATRICK 2014). Due to the roles of the BMPs in a host of other developmental processes, such as embryonic patterning and the cell cycle, MAC patients in this group often present with other anomalies of the brain, digits, and skeleton such as Klippel-Feil syndrome (BAKRANIA *et al.* 2008). *BMP4* alleles are typically heterozygous loss of function alleles, although they do arise *de novo,* and result in a range of MAC phenotypes present with anterior segment, brain, and digit phenotypes (BAKRANIA *et al.* 2008; REIS *et al.* 2011). There have been few documented cases of *BMP7* related MAC, but all are maternally inherited, with two being loss of function alleles and another a nonsynonymous variant (WYATT *et al.* 2010). With regards to the non-synonymous *Growth and Differentiation Factor 3 & 6* (*GDF3, GDF6)* alleles, 1/3 of the 25 cases are from inheritance of a heterozygous allele from an unaffected parent, while the remaining 2/3 of cases are unknown (ASAI-COAKWELL *et al.* 2007; ASAI-COAKWELL *et al.* 2009; YE *et al.* 2010; WILLIAMSON AND FITZPATRICK 2014). Severities of MAC phenotypes range from unilateral to bilateral, and knockdown of murine or zebrafish *GDF3* and *GDF6* orthologues results in similar MAC and skeletal phenotypes (ASAI-COAKWELL *et al.* 2007; ASAI-COAKWELL *et al.* 2009; FRENCH *et al.* 2009; YE *et al.* 2010). Of note, *Bmp4* and *gdf6a* have also been found to have a central role in patterning of the developing eye, suggesting there is a complex interplay during ocular development between retinal growth, morphogenesis and patterning (BEHESTI *et al.* 2006; FRENCH *et al.* 2009; GOSSE AND BAIER 2009).

The purpose of this study is to further ascertain the genetic and environmental etiology of MAC. I hypothesize that the microphthalmia resulting from *GDF6* coding anomalies is due to a role in the regulation of the cell cycle by BMPs, and aberrant expression of downstream effectors required for ocular growth and patterning. Furthermore, I propose that a homeostatic imbalance of retinoic acid, whether due to environmental or genetic factors, can result in coloboma, and that members of the forkhead box transcription factor have a central role in ocular fissure

formation. To address these hypotheses, I will utilize zebrafish as a model organism for human ocular development.

Zebrafish ocular development and zebrafish as a model organism

Ocular development is well conserved throughout vertebrates, with zebrafish, or *Danio rerio*, as a powerful model organism due to a number of advantageous features. These teleost (ray-finned) fish give large clutches of embryos (~200-300) with rapid and transparent development, have a relatively short life cycle and reach sexual maturity within three months. External development also gives the advantage of environmental manipulation, with the ability of many solutions to diffuse into the embryo via addition to the media. Genetic manipulation of these embryos is relatively easy due to a host of available knock-in and knockout technologies (KARI *et al.* 2007; CERMAK *et al.* 2011; LAWSON AND WOLFE 2011), and the zebrafish genome has been sequenced, with a number of online resources available. Zebrafish are also an excellent model of human disease, as comparison to the human genome indicates that approximately 70% of human genes have at least one zebrafish orthologue, and a conservation of many vertebrate gene networks for over ~450 million years (HOWE *et al.* 2013).

Ocular development begins with expression of *rx3, pax6*, *six3* and *six6,* whose combined expression specifies the retinal anlage and optic primordia, a solid mass of neuroectodermal cells at the anterior neural plate (MATHERS *et al.* 1997; NORNES *et al.* 1998; SEO *et al.* 1998). These cells will evaginate off the neural keel at approximately 7 somites [12 hours post fertilization (hpf)] and make contact with the overlying non-neural ectoderm region that is competent to form the lens (Figure 1-1) (SCHMITT AND DOWLING 1994; DAHM *et al.* 2007). After induction of lens formation at approximately 20 hpf, the optic vesicles then invaginate into a bi-layered optic cup, and at 24 hpf the inner layer gives rise to the neural retina, and the outer layer forms the retinal pigmented epithelium (RPE) (SCHMITT AND DOWLING 1994; DAHM *et al.* 2007). A

consequence of optic vesicle invagination is the formation of a transient fissure at the inferior portion of the eye from ~24 – 36 hpf (Figure 1-1). This fissure is required for entry and exit of neural crest cells (NCCs) and for passage of ocular vasculature and ganglion cell axons (SCHMITT AND DOWLING 1994; CHANG *et al.* 2006). NCCs are multipotent cells distinct to vertebrate development that form a number of specialized structures such as melanocytes, ganglia and parts of the craniofacial skeleton, with developmental anomalies resulting in neurocristopathies such as Hirschsprung's disease and neuroblastoma (GAMMILL AND BRONNER-FRASER 2003; MEULEMANS AND BRONNER-FRASER 2004; BRONNER AND LEDOUARIN 2012; RODRIGUES *et al.* 2012). Migrating in a spatiotemporally controlled fashion, cranial neural crest cells (CNCs) from the developing diencephalon give rise to a specialized subtype, periocular mesenchyme (POM) cells, which are required to form a number of ocular structures (ZACHARIAS AND GAGE 2010; BOHNSACK AND KAHANA 2013; OJEDA *et al.* 2013). During development, POM cells surround the eye and enter through the inferior fissure, with evidence that this entry also has a role in fissure biology, as anomalies in POM migration and differentiation result in coloboma and anterior segment dysgenesis (MATT *et al.* 2005; MCMAHON *et al.* 2009; ZACHARIAS AND GAGE 2010; GROCOTT *et al.* 2011; WEISS *et al.* 2012). Concurrent with ocular fissure opening is the course of ocular rotation and the beginning of retinal neurogenesis (SCHMITT AND DOWLING 1994). Derived from a single-cell population of multipotent retinal progenitor cells (RPCs), neural retinal cells are produced in an orderly fashion beginning at ~28 hpf, with a wave of neurogenesis commencing from a ventronasal location to the nasal, dorsal and temporal quadrants of the eye (RAYMOND *et al.* 1995; SCHMITT AND DOWLING 1996). First born are retinal ganglion cells, then cells of the inner nuclear layer such as bipolar, horizontal and amacrine cells, followed by cone cells, with the continual addition of rod cells throughout ocular development (RAYMOND *et al.* 1995; HU AND EASTER 1999). This population of RPCs is located between the neural retina and ciliary epithelium in an area called the ciliary marginal zone (CMZ) (RAYMOND *et al.* 2006). A unique feature of the zebrafish eye is continued growth throughout the life of the animal, with a

source of retinal neurons provided by the cells of the CMZ. However, much remains to be discerned with regards to the genes that maintain this population and the resulting microphthalmia upon mutation (NUCKELS *et al.* 2009).

Retinal patterning in zebrafish

Vertebrate ocular development includes not only tissue morphogenesis and growth, but also the innervation of the retinal ganglion cells to the visual processing center in the brain. The visual processing center in zebrafish is the optic tectum, while in mammals it is the superior colliculus and the lateral geniculate nucleus. Ocular development is dependent upon the dorsal-ventral and nasal-temporal positional identity of retinal cells, provided by expression of spatially restricted genes, which begins after evagination of the optic vesicles. The consequence of retinal patterning is the induction of expression of the Eph receptors (Eph), which are receptor tyrosine kinases, and the ligand Ephrin (Efn). This binding of Efn ligands to Eph receptors results in either attraction or repulsion between migrating retinal ganglion cell axons and target tissues (SPERRY 1963; MURAI AND PASQUALE 2003), which facilitates axonal migration through rearrangements of the cytoskeleton, and changes in cell adhesion that result in growth cone spread or collapse (WOO *et al.* 2009). For specification of the nasal eye, a combinatorial signal of the Fibroblast growth factors (FGFs) FGF8, FGF3 and FGF24 is required for induction of the nasal transcription factor, *forkhead box G1 (foxg1*), which then induces expression of *ephrinA* ligands (PICKER AND BRAND 2005; PICKER *et al.* 2009). Counter to this, in the temporal retina, is *forkhead box D1* (*foxd1*), which is required for expression of *ephA* receptors (TAKAHASHI *et al.* 2009; CARRERES *et al.* 2011). These nasal and temporal expression patterns are antagonistic to each other, as are dorsal-ventral transcription factors. In the dorsal retina, there are two phases of patterning, initiation and maintenance.

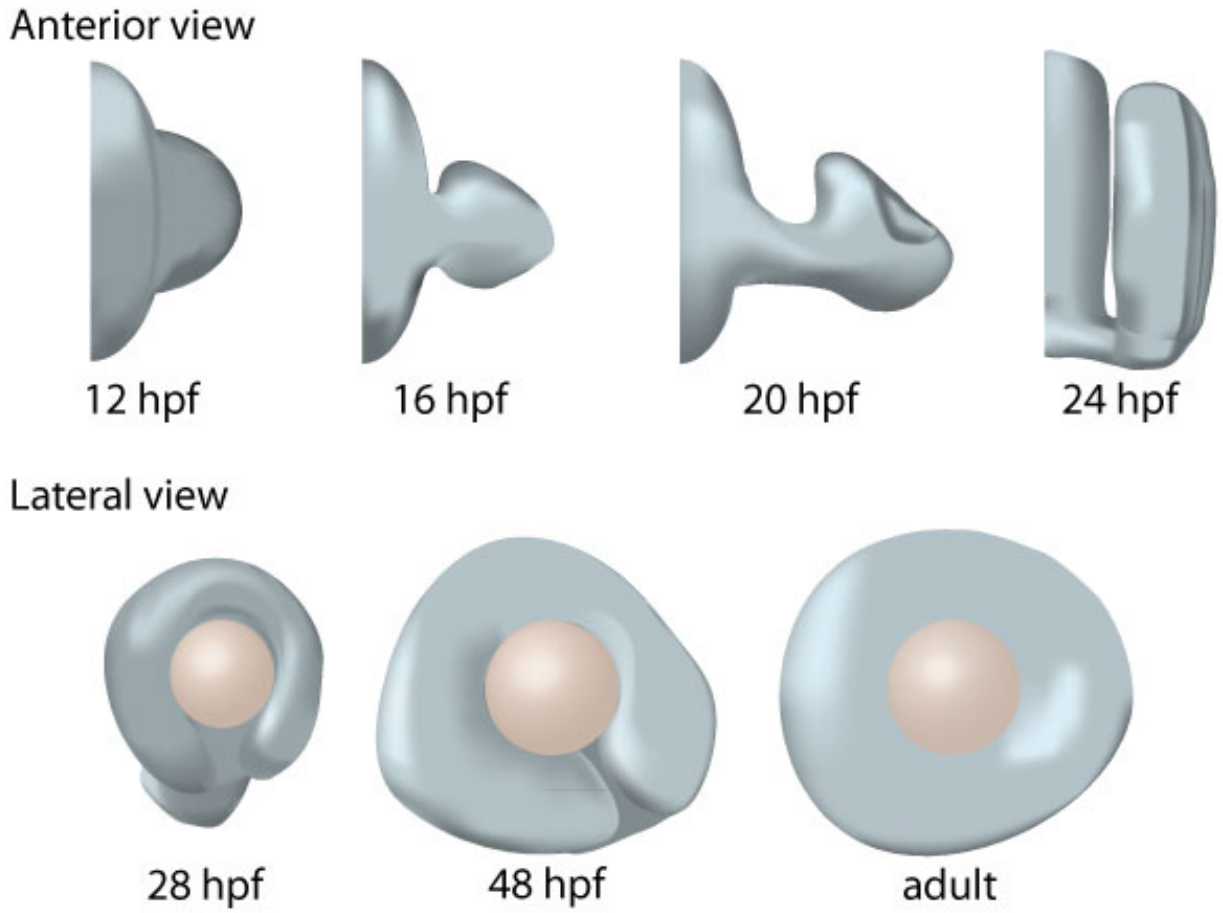

Figure 1-1: Zebrafish ocular development.

At ~12 hpf (7 somites) the optic primordia cells evaginate from the neural keel until they make contact with the overlying non-neural ectoderm where they will induce formation of the lens at ~20 hpf. The optic vesicle then invaginates to form a bi-layered optic cup, with the open choroidal fissure at the inferior portion of the eye from ~ 24 – 48 hpf. Please note that Caroline Cheng, a PhD student in the lab of Dr. Andrew Waskiewicz, owns the copyrights to this figure.

Required for initiation are the bone morphogenetic proteins (BMPs) BMP2, BMP4, and growth and differentiation factor 6a (Gdf6a) (FRENCH *et al.* 2009; GOSSE AND BAIER 2009; KRUSE-BEND *et al.* 2012), with the Wnt-β catenin pathway and Secreted frizzled-related proteins (SFRPs) facilitating maintenance (VEIEN *et al.* 2008; HOLLY *et al.* 2014). The dorsal eye expresses the T-box transcription factor *tbx5,* the retinoic acid (RA) synthesis enzyme *aldehyde dehydrogenase 1a2* (*aldh1a2),* the BMP pseudoreceptor *BMP and activin membrane-bound inhibitor* (*bambi*), and the ephrin ligand *efnb2a* (BEHESTI *et al.* 2006; FRENCH *et al.* 2009). In the ventral eye RA is required for tissue morphogenesis and SHH for cellular identity, which induce the expression of *aldehyde dehydrogenase 1a3* (*aldh1a3)* and *ventral homeobox 2* (*vax2),* whose expression is antagonistic to that of *tbx5* and is required for the expression of the *eph* receptors *ephb2* and *ephb3* (MARSH-ARMSTRONG *et al.* 1994; EKKER *et al.* 1995; SASAGAWA *et al.* 2002; FRENCH *et al.* 2009).

Bone morphogenetic protein signaling

Bone Morphogenetic Proteins (BMPs) and Growth and Differentiation Factors (GDFs) are members of the Transforming Growth Factor-β (TGFβ) family of secreted signaling molecules that facilitate control of transcription through binding of transmembrane receptors (NOHE *et al.* 2004; SIEBER *et al.* 2009). After cleavage of the BMP propeptide to active ligand form, BMP ligands homodimerize, and then bind to serine/threonine kinase BMP type I and type II transmembrane receptors for activation of a signal transduction pathway (NOHE *et al.* 2004; SIEBER *et al.* 2009). These receptors heterodimerize, and attract another receptor heterodimer, forming a heterotetrameric complex (NOHE *et al.* 2004). Signal transduction is continued through the Smad family of proteins of which there are three members; there are receptor-activated Smads (R-Smads1/5/8), inhibitor Smads (I-Smads6/7) and a common-mediator Smad (co-Smad4) (NOHE *et al.* 2004; SIEBER *et al.* 2009). The BMP Type I receptor phosphorylates Smad1/5/8, which then forms a complex with Smad4 and is able to enter the nucleus to regulate

transcription of genes by binding to BMP responsive elements on target DNA (NOHE *et al.* 2004; SIEBER *et al.* 2009). BMP signaling is regulated by a number of factors. Antagonists such as Noggin, Chordin, Gremlin and Dan can bind BMP ligands in the extracellular matrix. There are pseudoreceptors such as Bambi that do not have an intracellular kinase domain and block formation of signaling complexes. Intracellularly, Smad6/7 can prevent formation and phosphorylation of the nuclear translocation complex of Smad1/5/8 and Smad4, and target BMP receptors for degradation (HATA *et al.* 1998; ONICHTCHOUK *et al.* 1999; NOHE *et al.* 2004).

The BMPs are critical for a number of developmental processes. In vertebrates, BMPs establish the first embryonic dorsal-ventral patterning gradient, are critical for axis formation, cell fate, neural and somite patterning, skeletal and limb development, and organogenesis for the kidney, tooth, lung and gut (HOGAN 1996). BMPs also have well-recognized roles in ocular development, such as the regulation of ocular cell cycle with coding anomalies in *GDF3* and *GDF6* resulting in MAC (ASAI-COAKWELL *et al.* 2007; ASAI-COAKWELL *et al.* 2009; FRENCH *et al.* 2009; YE *et al.* 2010), and a requirement for *gdf6a* in the initiation and maintenance of dorsal ocular patterning (FRENCH *et al.* 2009; GOSSE AND BAIER 2009). As well, model organisms have ocular anomalies resulting from mutations in BMP antagonists (HUILLARD *et al.* 2005; PAULSEN *et al.* 2011; WEBB *et al.* 2012).

Forkhead box transcription factors

The *forkhead box* genes, or *FOX* genes, are a group of transcription factors with central roles in the developmental and adult life of a vast number of species, from fungi to animals (BENAYOUN *et al.* 2011). The first FOX gene was described 25 years ago, in a *Drosophila* mutant with an irregular spiked-head, a consequence of a loss of the homeotic gene *fork head* (WEIGEL et al. 1989*)*. Classified as a transcription factor after comparison to mammalian *hepatocyte nuclear factor 3* (*HNF3*) (WEIGEL AND JACKLE 1990), the FOX transcription factors all share a 110-amino-acid DNA binding domain, composed of a core of 3 α-helices (H1-3), three β-strands, and

two loops, or wings (W1-2), which are uniquely configured and earn FOX transcription factors the name "winged" transcription factors (Figure 1-2 A) (CLARK *et al.* 1993; CARLSSON AND MAHLAPUU 2002; BENAYOUN *et al.* 2011). Binding of DNA is facilitated by α-helix 3, which recognizes the FOX DNA consensus sequence [5'-(G/A)(T/C)(A/C)AA(C/T)A-3'] in the major groove, with binding specificity and affinity provided by the wings that interact with the minor groove, and by the bases surrounding the core sequence (PIERROU *et al.* 1994; CIRILLO AND ZARET 2007) (Figure 1-2B). Typically, forkhead transcription factors bind as monomers, but binding as homodimers (TSAI *et al.* 2006) and even heterodimers has also been reported (SEOANE *et al.* 2004). This promiscuity in binding partners, along with posttranslational modifications stimulated by environmental signals, results in a strong diversity of DNA target selection by the FOX proteins (CIRILLO AND ZARET 2007). In addition to transcription factors, FOXs have been shown to be cell cycle regulators and effectors of the Shh, Wnt/β-catenin and TGF- β signal transduction pathways, which may account for their extensive roles in development (CIRILLO AND ZARET 2007; MYATT AND LAM 2007). In particular, precise FOX gene dosage appears to be critical for correct ocular development, with most mutations inherited in an autosomal dominant fashion. Duplications or deletions in the *FOXC1* locus result in anterior segment anomalies such as glaucoma, iris hypoplasia and Axenfeld-Rieger in patients, murine and zebrafish models, with a requirement in ocular blood vessel formation and maintenance (NISHIMURA *et al.* 1998; LEHMANN *et al.* 2000; SKARIE AND LINK 2009; SEO *et al.* 2012). Haploinsufficiency of a closely related gene, *FOXC2*, also causes anterior segment anomalies in both humans and mice (FANG *et al.* 2000; SMITH *et al.* 2000). Improper eyelid development results with null or hypomorphic *FOXL2* alleles (CRISPONI *et al.* 2001), and mutations in *FOXE3* result in atypical lens development (BROWNELL *et al.* 2000; SEMINA *et al.* 2001). Lastly, the action of *Foxg1* and *Foxd1* are required for formation of the retinotectal map by their respective expression in the nasal and temporal retina (YUASA *et al.* 1996; LEHMANN *et al.* 2000).

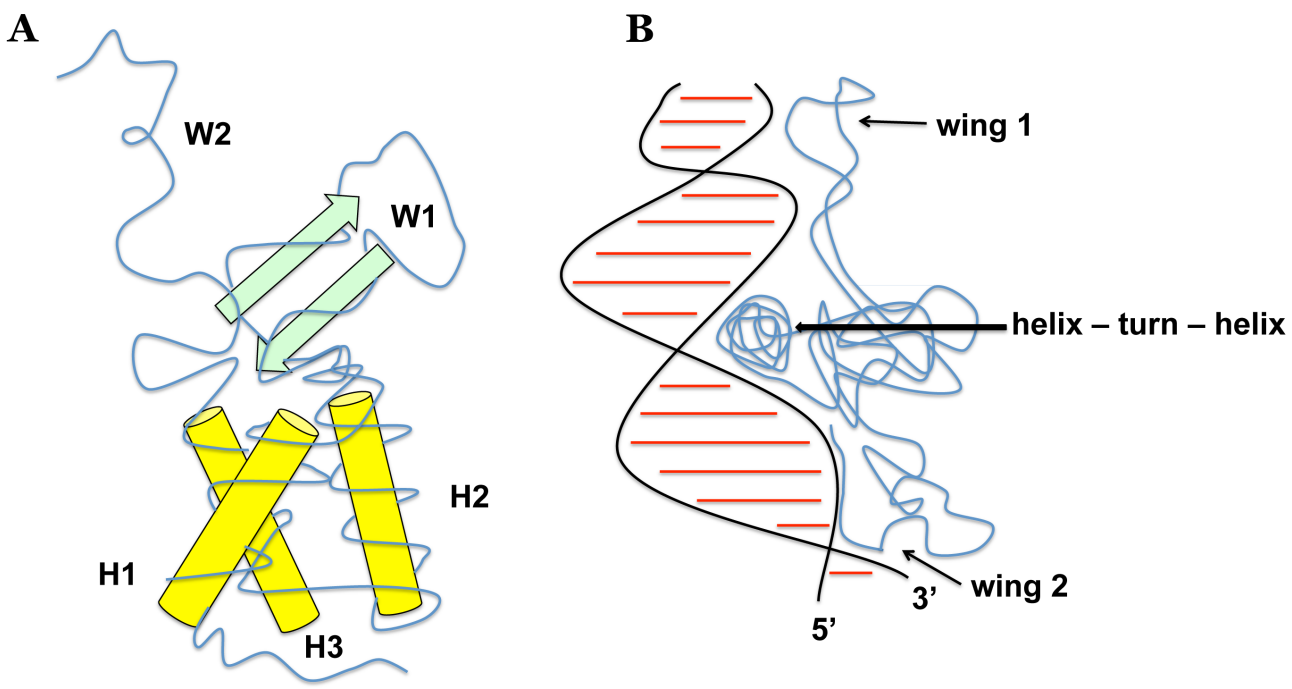

Figure 1-2: Theoretical depiction of the structure of a forkhead box protein alone and bound to DNA.

FOX proteins are composed of three α-helices (H1, H2, H3), with H3 being the recognition helix that makes contact with the major groove of DNA, and two wings (W1, W2), that interact with the minor groove of DNA, with W1 composed of two antiparallel β-strands (A). The α-helices bind to the major groove of DNA, with H3 acting as the recognition helix. Wing 1 and wing 2 facilitate the DNA binding of the forkhead protein (B).

Retinoic Acid

Retinoic acid (RA) is a morphogen critical for embryonic development and adult processes. The concentration of this metabolite is of particular importance, as both excesses and deficiencies have harmful consequences. Vitamin A (retinol) is absorbed into the cell from the blood and then bound to cellular retinol-binding protein (CRBP) (Figure 1-3). Retinol is metabolized by retinol dehydrogenases (retinol dehydrogenase 10/rdh10) to retinal/retinaldehyde, and then to retinoic acid by retinaldehyde dehydrogenases (aldehyde dehydrogenase 1 family, member A2/aldh1a2, aldehyde dehydrogenase 1 family, member A3/aldh1a3) (Figure 1-3) (MADEN 2002). Recently, it has been shown that cytochrome P450 1B1 (cyp1b1) is able to synthesize RA from retinol independently of these steps (CHAMBERS *et al.* 2007). In the cytoplasm, free RA is bound by cellular RA-binding protein (CRABP), but is released for entry into the nucleus, where it binds to retinoic acid receptors (RARs) and retinoid X receptors (RXRs), which then heterodimerize and bind the RA-responsive element (RARE) on DNA for regulation of transcription (Figure 1-3) (MADEN 2002; NIEDERREITHER AND DOLLE 2008). The cytochrome P450 26 A1 and B1 (Cyp26A1 & Cyp26B1) enzymes are responsible for the breakdown of RA into metabolites such as 4-hydroxy-RA and 4-oxo RA, which are further broken down and eliminated (Figure 1-3) (MADEN 2002; NIEDERREITHER AND DOLLE 2008).

With regards to development, RA is an indispensible morphogen with countless functions. A short list includes roles in neural tube, hindbrain development and rhombomere identity, body axis patterning, neuronal cell differentiation, along with limb, heart, pancreas, kidney, lung, and inner ear development (MADEN 2002; NIEDERREITHER AND DOLLE 2008). Studies have shown that gestational deficiencies of RA can result in characteristic central nervous system malformations, but an excess of RA during development is also teratogenic (MADEN 2002; NIEDERREITHER AND DOLLE 2008).

RA has central roles in ocular development and in adult eye function. Adult rats deprived of Vitamin A go blind (WOLBACH AND HOWE 1925), likely due to the requirement of Vitamin A for the formation of rhodopsin and iodopsin, photosensitive pigments used by rods and cones, respectively (DOWLING AND WALD 1960). During mammalian development, if Vitamin A deficient diets are fed to pigs and rats this results in piglets with anophthalmia and pups with coloboma (WILSON *et al.* 1953; MADEN 2002), while in avian species the ventral optic stalk and ventral retina does not form (MADEN *et al.* 2007). These phenotypes also extend to teleost fish; in zebrafish, inhibition of RA synthesis results in hemianopsia and microphthalmia (MARSH-ARMSTRONG *et al.* 1994; LE *et al.* 2012), whereas addition of ectopic RA stimulates proliferation of cells of the ventral retina and subsequent retinal duplication (HYATT *et al.* 1992). Human cases of this phenomenon have also been documented. In particular, Asian countries with rice-dependent diets prone to Vitamin A deficiency have a higher prevalence of ocular congenital anomalies (HORNBY *et al.* 2000). Research over the last decade has focused on the biological function of RA in ocular development. In mouse, RA was thought to have a role in dorsoventral ocular patterning (WAGNER *et al.* 2000), but recent findings have shed doubt on this notion (MATT *et al.* 2005; MOLOTKOV *et al.* 2006). Instead, RA is required for optic vesicle invagination, growth of extra ocular muscle, and for anterior segment formation (MIC *et al.* 2004; MOLOTKOV *et al.* 2006; DUESTER 2008; MATT *et al.* 2008). Additionally, RA is required for growth of the ventral retina and for remodeling migrating POM cells by stimulating apoptosis (MATT *et al.* 2005). In chick, RA is required for visual topographic mapping by regulating the expression of axonal guidance molecules (SEN *et al.* 2005), and in zebrafish, RA promotes ventral ocular characteristics, has a role in POM migration (HYATT *et al.* 1996b; LUPO *et al.* 2011; BOHNSACK AND KAHANA 2013) and in photoreceptor development (HYATT *et al.* 1996a; PRABHUDESAI *et al.* 2005; STEVENS *et al.* 2011).

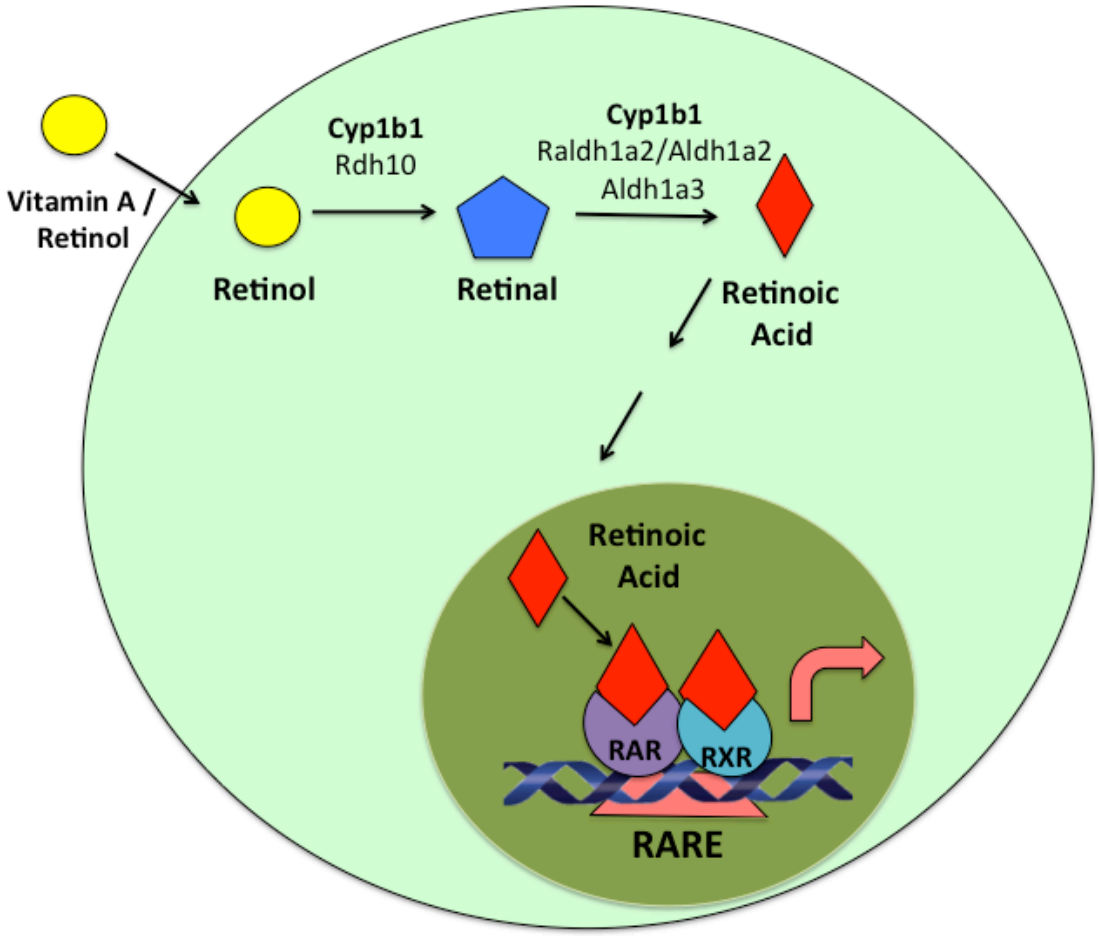

Figure 1-3: The retinoic acid metabolic pathway.

Retinol enters the cell from the blood and is metabolized from retinol to retinal by Retinol dehydrogenase 10 (Rdh10) and Cytochrome P450 1B1 (Cyp1b1), and then from retinal to retinoic acid by the Retinaldehyde dehydrogenases 1a2 and 1a3 (Raldh1a2/Aldh1a2, Aldh1a3) and Cyp1b1. Retinoic acid enters the nucleus and binds to retinoic acid receptor (RAR) and retinoid X receptor (RXR), which heterodimerize and bind to target DNA at the retinoic acid responsive element (RARE) to control transcription. Please note that Tara Stach created this figure with the exception of the DNA double helix, for which Caroline Cheng owns the copyrights.

Purpose of this study

The purpose of this study is to further ascertain the genetic and environmental etiology of MAC, with the ultimate goal of developing preventative and more efficacious therapeutics. I hypothesize that the microphthalmia resulting from *GDF6* coding anomalies is caused by BMPs' role in the regulation of the cell cycle, and aberrant expression of downstream effectors required for ocular growth and patterning. Furthermore, I propose that a homeostatic imbalance of retinoic acid, whether due to environmental or genetic factors, can result in coloboma, and that members of the forkhead box transcription factor family have a central role in ocular fissure formation. In chapter 3, I will identify the mechanism by which the loss of *gdf6a* results in microphthalmia, and a novel role for *foxi1* and *foxi2* in polarization of the ciliary marginal zone. In chapter 4, I will further describe the ocular developmental roles of *foxi1* and *foxi2*, and the discrepancies in phenotypes that result from different knockdown technologies. In chapter 5, I describe potentially pathogenic *CYP1B1* mutations present in a superior coloboma proband, which model the requirement of retinoic acid in ocular fissure closure, and the role of Foxg1 and Foxd1 in dictating superior fissure formation. Finally, in chapter 6, I summarize my findings and how they have advanced ocular research.

Chapter 2

Materials and Methods

A portion of this chapter has been modified from the publication:

*French CR, **Stach TR**, March LD, Lehmann OJ, Waskiewicz AJ. Apoptotic and Proliferative Defects Characterize Ocular Development in a Microphthalmic BMP Model. Invest Ophthalmol Vis Sci. 2013 Jul 10;54(7):4636-47*

2.1: Materials and methods pertaining to Chapter 3: Apoptotic and Proliferative Defects Characterize Ocular Development in a Microphthalmic BMP Model

Zebrafish husbandry, morpholino injections and in situ hybridization

Zebrafish were cared for according to standard protocols, and embryos grown in embryo media at either 25.5°C, 28.5°C, or 33°C to be appropriately staged (KIMMEL *et al.* 1995). Zebrafish embryos grown past 24 hours post fertilization (hpf) were treated with 0.003% 1-phenyl 2-thiourea (PTU; Sigma-Aldrich, St. Louis, MO, USA) to prevent pigment formation. The AB strain of wild-type (WT) fish and the *gdf6a*^{s327} mutant line (GOSSE AND BAIER 2009) were utilized. The latter, hereafter described as *gdf6a*$^{-/-}$, encodes a S55X truncation producing a 54 amino acid peptide lacking the mature domain. For inhibition of *foxi2,* 4 ng of a translation blocking morpholino (MO) (TCGATGGTGTTCATATCTCCAGTGC) was injected into 1-2 cell stage embryos. *In situ* hybridization (ISH) was performed as previously described (see page 29 of this thesis for full protocol) (GONGAL AND WASKIEWICZ 2008; THISSE AND THISSE 2008), with embryos fixed overnight at 4°C in 4% paraformaldehyde (PFA) and permeabilized by incubation in 10 μg/ml Proteinase K for 20 minutes. Animal care protocols were approved by the University of Alberta Biosciences Animal Care Committee.

Microarray Analysis

Microarrays were performed using Agilent's 4X44K whole genome chips (version 2). Four biological replicates were performed, with each array using RNA isolated from separate matings. RNA was isolated from 30 phenotypically wild type (WT) and 30 *gdf6a*$^{-/-}$ eyes at 2 dpf using the RNAqueous kit (Ambion) and then amplified and labeled [low input linear amplification kit (Agilent)]. Labeled RNA was hybridized for 17 hours at 65°C and then processed as per the manufacturer's protocol (Agilent), scanned on a GenePix 4000 scanner prior to data extraction using Agilent's feature extraction software. Dr. Curtis French at the University of Alberta performed all steps.

Immunohistochemistry

For analysis of apoptosis, embryos fixed in 4% PFA were permeabilized with ice-cold acetone (7 minutes), washed in water (5 minutes), prior to four 5 minute washes in phosphate-buffered saline with 0.5 % Tween-20 (PBST). For analysis of cell proliferation, fixed embryos were permeabilized using Proteinase K (10 μg/ml) [20 minutes (2 days post fertilization (dpf)) or 45 minutes (4 dpf larvae)], re-fixed (20 minutes in 4% PFA), washed four times in PBST (5 minutes each), and then treated with 95°C 10 mM citric acid buffer (10 minutes). Slides containing 15 μM sections were treated with 95°C citric acid buffer, but were not permeabilized. Embryos and slides were blocked for 1 hour at room temperature in 5% normal goat serum and 2% BSA. Primary antibodies used were rabbit anti-activated Caspase 3 (1/1000, BD Biosciences), and rabbit anti-phosphohistone H3 (1/1000, BD Biosciences). Embryos and slides were incubated in secondary antibody (goat anti-rabbit AlexaFluor 488, 1/1000, goat anti-rabbit Alexa Fluor 568; Molecular Probes) for 2 hours at room temperature. All embryos were washed for 5 minutes in PBST, then 4 times for 10 minutes in PBST after both primary and secondary antibody incubations. Hoechst 33258 nuclear stain (1/1000, Molecular Probes) was added to the second 10-minute wash after secondary antibody incubation. Embryos and slides were mounted in Prolong Gold (Molecular Probes) for visualization.

Genotyping

The offspring of a *gdf6a*$^{+/-}$ heterozygous incross were genotyped by high-resolution melt (HRM) analysis performed on genomic DNA, extracted in 10 ml of 50 mM NaOH (95°C, 10 minutes, neutralized with 1 ml Tris-HCl, pH 8.0). PCR was performed using primers optimized for HRM (GCGTTTGATGGACAAAGGTC; CCGGGTCCTTAAAATCATCC), MeltDoctor HRM Master Mix (Applied Biosystems) and a ABI 7500 HT Fast RT PCR machine or Qiagen Rotor Gene Q qPCR machine (1 cycle, 95°C (10 minutes); 40 cycles, 95°C (15s) & 60°C (20s), 1 cycle, 95°C (15s), 60°C (1 min), 95°C (15s) & 60°C (15s). Results were analyzed via HRM 2.0 Software (ABI) or Qiagen

software v2.02 and variants were initially confirmed by Sanger sequencing. Quantification of average eye size was performed using arbitrary units in Image J, with *gdf6a*$^{+/-}$ control treated eyes quantified as 100% eye size.

Pharmacological Treatment

Embryos were treated from 5 hpf to 31 hpf with 0.1 mM P7C3, previously shown to protect newborn neurons from apoptosis, hypothesized to be through the maintenance of mitochondrial membrane integrity (Asinex) (PIEPER *et al.* 2010) or DMSO as a vehicle control. 28 hpf embryos were fixed and whole-mount immunofluorescence was performed using anti-active Caspase 3 antibody (BD Pharmingen) with the nuclear counterstain Hoechst 33258. Dissected eyes were visualized using confocal microscopy (Zeiss LSM 700 on Axio Observer.Z1). All photographed eyes were genotyped by PCR and sequencing. For quantification of eye size, embryos treated with P7C3 from 5 hpf to 31 hpf were transferred into regular embryo media and grown to 3 dpf. Embryos were photographed and individually genotyped (as described above). Eye area was quantified using ImageJ64 processing software. Student *t*-tests were performed with Bonferonni correction for multiple comparisons.

2.2: Materials & methods pertaining to Chapters 4 & 5

Zebrafish maintenance, strains, genotyping and morpholinos

Zebrafish were cared for as outlined by standard protocols (WESTERFIELD 1993), in accordance with the Canadian Council for Animal Care guidelines and approved by the University of Alberta Animal Care and Use Committee for Biosciences. All embryos were grown in embryo media (EM) (15 mM NaCl, 500 nM KCl, 1 mM $CaCl_2$, 150 nM KH_2PO_4, 1 mM $MgSO_4$, 715 nM $NaHCO_3$) with penicillin-streptomycin solution (10 000 units penicillin, 10 mg/ml streptomycin, diluted 1:100 in EM, Sigma-Aldrich) at either 25.5°C, 28.5°C, or 33°C to be appropriately staged (KIMMEL *et al.* 1995). If embryos were to be raised past 24 hpf, EM supplemented with 0.006%

N-phenylthiourea (PTU) (Sigma-Aldrich) was added to embryos, and the solution was changed every 12 hours.

Morpholino oligonucleotides (MO) were introduced as a rapid and relatively simple technique for knockdown of gene expression in zebrafish (NASEVICIUS AND EKKER 2000). All MOs described here are translation blocking, and were designed and ordered from Gene Tools (Table 2-2). MOs were diluted to a 20 mg/ml stock solution using sterile water, and then diluted to a working concentration in Danieau buffer (58 mM NaCl, 0.7 mM KCl, 0.4 mM $MgSO_4$, 0.6 mM $Ca(NO_3)_2$, 5 mM HEPES [4-(2-hydroxethyl)piperazine-1-ethanesulfonic acid], pH 7.6) and stored at 4°C. MOs were heated to 65°C for 10 minutes and cooled to room temperature, then injected into 1-4 cell embryos using 1.2 mm thin-wall borosilicate tubing (Sutter Instruments). Needles were pulled using a Model P-87 Flaming/Brown Micropipette Puller (Sutter Instruments), and injection was done using an ASI MPPI-2 Pressure Injector (Applied Scientific Instrumentation) with a pressure of 27 psi. Pulse duration was 0.5 – 3 ms, and dosage was estimated by bolus size delivered.

The mutant *foxi1* allele (*foxi1*^{hi3747Tg}), also known as *foo*, was identified from insertional mutagenesis screens (AMSTERDAM *et al.* 1999; GOLLING *et al.* 2002; AMSTERDAM *et al.* 2004), and was obtained from the Zebrafish International Resource Center (ZIRC). The *hi3747Tg* allele is a mutagenic proviral integration at the 5' end of the gene that results in protein truncation before the forkhead box DNA binding domain. Homozygous mutant embryos and heterozygote adults were identified via pair-wise crossing and analysis of Mendelian ratios for irregular otic vesicle phenotypes, and by PCR amplification of the retroviral containing region, respectively (Figure 2-1 & Table 2-1). Before obtaining the *foxi1*^{hi3747Tg} mutant line, 2 ng of *foxi1* translation blocking morpholino (TAATCCGCTCTCCCTCCAGAAACAT) was co-injected with 1 ng of translation-blocking *p53* MO (GCGCCATTGCTTTGCAAGAATTG), or 1 ng of *p53* MO was injected alone as a WT comparison, as knockdown of *p53* has been previously shown to reduce severity of non-specific MO effects (ROBU *et al.* 2007).

For knockdown of *foxi2* expression, 4 ng of translation blocking MO (TCGATGGTGTTCATATCTCCAGTGC) was injected. The AB strain of wild-type (WT) fish was used for all *foxi1* and *foxi2* injections.

The mutant *foxg1b* allele, *sa2593* (*foxg1b*^{sa2593}), was identified from a large-scale mutagenesis screen performed by the Sanger Institute (KETTLEBOROUGH *et al.* 2013). The mutation is a G-to-A substitution at position 590 in the *foxg1b* open reading frame (ORF), which results in a premature stop codon and truncated protein (KETTLEBOROUGH *et al.* 2013). Adult fish and embryos were genotyped using a BsrI (New England Biolabs) digestion of a 243 base pair (bp) *foxg1b* PCR product (Table 2-1) (Figure 2-2). For this reaction, single embryo genomic DNA was extracted in 10 µl of 50 mM NaOH (95°C, 20 minutes, neutralized with 2 µl Tris-HCl, pH 8.0) and diluted 1/5.

For assessment of ocular blood vessel phenotypes, *foxg1b*^{sa2593} fish were outcrossed to the *Tg*(*flk1:EGFP*)^{s843} reporter line (JIN *et al.* 2005), and carriers of the enhanced green fluorescent protein (EGFP) construct were identified either by visual screening under an Olympus stereomicroscope or by PCR amplification of EGFP (Table 2-1). Before obtaining the *foxg1b*^{sa2593} line, 4 ng of translation-blocking *foxg1b* MO (ACTCTGGTCTCCCATGCCGGGTGAT) were co-injected with 2 ng of translation-blocking *p53* MO, along with 4 ng of the previously described (DUGGAN *et al.* 2008) translation-blocking *foxg1a* MO (TCCCATATCCAACATCACAAGTAAG). Four ng of the *foxg1a* MO were either injected alone into *foxg1b*^{sa2593} heterozygous cross embryos, or with *foxg1b* and *p53* MO into the *Tg*(*rx3*:*GFP)* reporter line (REMBOLD *et al.* 2006).

To knockdown the expression of *foxd1,* 5 ng of translation blocking MO (TCATGGCTCTCTCGGGTTTCCCGAT) were injected into WT embryos.

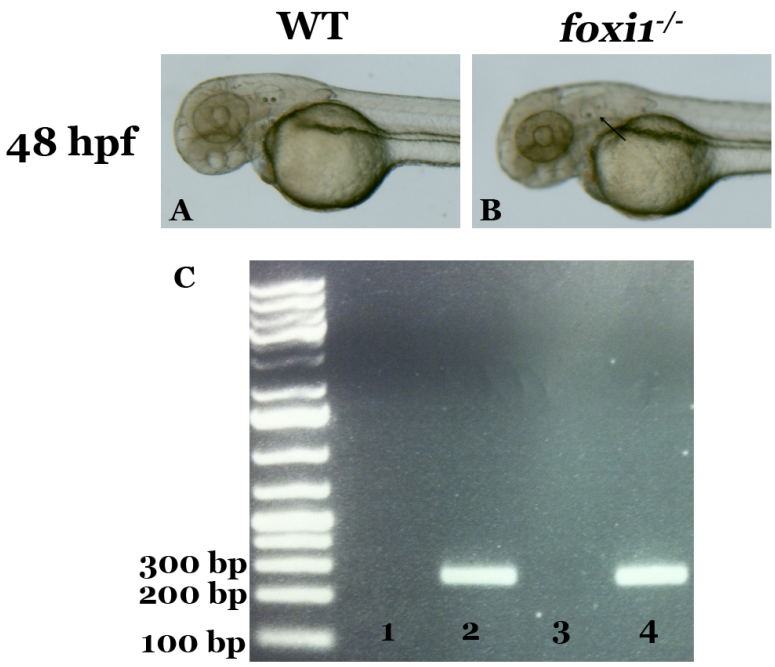

Figure 2-1: *foo* mutant fish, identified by otic vesicle phenotypes and PCR amplification of the retroviral insert.

As compared to WT fish (A), *foxi1*^{hi3747Tg} larvae at 48 hpf have split and aberrantly developed otic vesicles (black arrows) (B). Genotyping of *foxi1*$^{hi3747Tg/-}$ adults by PCR amplification of the integrated retrovirus and surrounding genomic DNA results in a 256 bp band (C. 2 & 4), while WT sibling DNA does not result in a PCR product (C. 1 & 3).

Table 2-1: Primer sequences for zebrafish genotyping

Gene	Forward Primer (5'-3')	Reverse Primer (5'-3')	Size (bp)	Tm (°C)
foxi1^{hi3747Tg}	CTGACCTTGATCTGAACTTCTCTATTC	CCATGTTTCTGGAGGGAGAGC	256	60.0
*foxg1b**	TTCCAGCGATGACGTGTTTAT	AGTAAAGTTCCGTACGTGTGTCCT	243	62.0
*EGFP**	AGCTGACCCTGAAGTTCATCTG	CATGATATAGACGTTGTGGCTGTT	338	60.0

*Primer construction by author

Table 2-2: Morpholinos utilized. All morpholinos are translation blocking, and were designed and obtained from Gene Tools

Gene	Sequence (5'-3')	Dose
foxi1	TAATCCGCTCTCCCTCCAGAAACAT	2 ng
foxi2	TCGATGGTGTTCATATCTCCAGTGC	4 ng
foxd1	TCATGGCTCTCTCGGGTTTCCCGAT	5 ng
foxg1a	TCCCATATCCAACATCACAAGTAAG	4 ng
foxg1b	ACTCTGGTCTCCCATGCCGGGTGAT	4 ng
p53	GCGCCATTGCTTTGCAAGAATTG	1 – 2 ng

Table 2-3: Primer sequences for antisense PCR based RNA probes

Gene	Forward primer (5'-3')	Reverse primer (5'-3')	Size (bp)	Tm (°C)
foxd1	AGGCAACTACTGGACGCTAGAC CCTG	GAACAGACCGTGTAAAAATATCACACTC CGAG[1]	1086	59
foxg1a	AAATGGCTTGAGTGTTGACAGA CTCG	GAAGAATGTGACCTGCATGGTGGTGAC[1]	1165	63
*foxg1b**	CGACTTCATTCAGCATCAAGAGC	GAATGTGCCCTGAGAGTAATCCAGC[1]	820	58
*foxg1c**	ACAAGTCGTCATTCAGCATCAGC	GAAAGGTAAGATTCCTCCTGCGACC[1]	995	58
*foxg1d**	TCTCCCGTTGGTTTGTTATCAGT G	GAAAATATTTCCAGCCAGACTGCTGCT[1]	844	65

1) 5' end of reverse primer modified with T3 promoter sequence CATTAACCCTCACTAAAGG

*probe construction by author

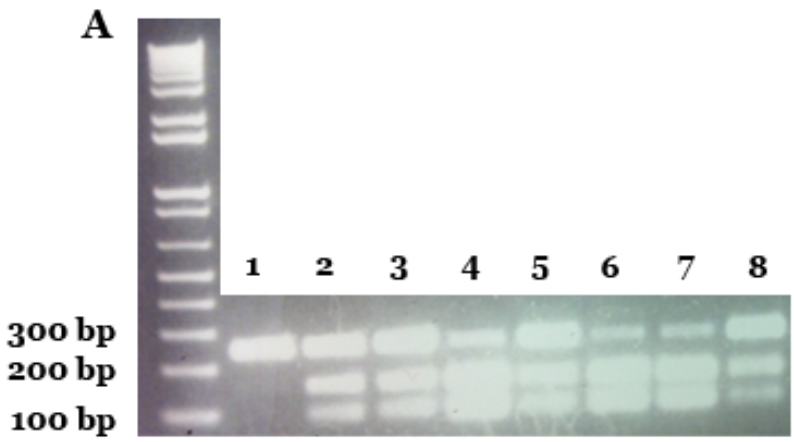

Figure 2-2: Genotyping of *foxg1b*$^{+/-}$ pair-wise cross embryos by BsrI digestion of the amplified *foxg1b* region containing the single nucleotide polymorphism, sa2593, a G-to-A substitution at position 590 of the open reading frame.

BsrI (New England BioLabs) recognizes and cuts at sequence 5′...ACTGGN▼...3′ / 3′...TGAC▲CN...5′. The 243 bp amplified WT *foxi1b*$^{+/+}$ DNA product only undergoes partial digestion after 4 hours incubation, with a faint 243 bp product remaining along with the digested, very bright 150 and 93 bp bands (4, 6 & 7). The 243 bp DNA product amplified from *foxg1b*$^{-/-}$ embryos does not undergo digestion (1), while *foxg1b*$^{+/-}$ DNA undergoes a partial digestion to a 150 and 93 bp product, but there is a greater amount of undigested 243 bp product as compared to *foxg1b*$^{+}$/$^{+}$ DNA (2, 3, 5 & 8).

In situ hybridization

In situ hybridization (ISH) anti-sense RNA probes were created by a PCR or vector based approach, with probe design targeting either the coding sequence or the 3' untranslated region (UTR) of the gene. For a PCR based approach, the probe was synthesized by adding a T7 or T3 binding site onto the 3' end of the reverse primer used to amplify the probe sequence of interest, as previously described(THISSE AND THISSE 2008) (Table 2-3). For a vector-based approach, the amplified sequence of interest was subcloned into Topo4PCR (Invitrogen) and either the T3 or T7 promoter was used for reverse transcription based on the orientation of the sequence (Table 2-3). Purified PCR products or linearized plasmids were then used to transcribe antisense probes, and probes were diluted 1/100 or 1/200 in hybridization solution (50% formamide, 50 μg/ml heparin, 5X SSC [saline sodium citrate buffer], 0.1% Tween-20, 0.092 M citric acid in sterile water). For *in situ* analysis, all washes were performed at room temperature (RT) unless otherwise stated. Embryos were fixed in a 4% paraformaldehyde (PFA) phosphate buffered saline (137 mM NaCl, 2.7 mM KCl, 10 mM Na_2HPO_4, 1.8 mM KH_2PO_4, pH 7.4) (PBS) solution for four hours or overnight at 4°C. Following 5 X 5 minute phosphate buffered saline with 0.1% Tween-20 (PBST) washes and de-chorionation, embryos were permeabilized with Proteinase K (10 μg/ml) in PBST for 2 minutes (22 – 28 hpf embryos) or for 30 minutes (48 hpf embryos). After permeabilizaiton, embryos were re-fixed in 4% PFA for 20 minutes, and washed 5 X 5 minutes with PBST. Prehybridization solution (hybridization solution with 500 μg/ml yeast tRNA) was then added for 1-2 hours at 65°C. Probe was left overnight at 65°C and saved for re-use. ISH washes in a 65°C water bath proceeded as follows: 66% hybridization & 33% 2X SCC solution for 5 minutes, 33% hybridization & 66% 2X SCC solution for 5 minutes, 2X SCC for 5 minutes, 0.2X SSC & 0.1% Tween-20 solution for 20 minutes, 0.1X SSC & 0.1% Tween-20 solution 2X 20 minutes, followed by washes at RT on a shaker: 66% 0.2X SSC & 33% PBST solution for 5 minutes, 33% 0.2X SSC & 66% PBST solution for 5 minutes, PBST for 5 minutes. Blocking solution (2% sheep serum, 2 mg/ml bovine serum albumin [BSA], PBST) was added to

embryos for 1 – 2 hours, and then fresh block with a 1/5000 dilution of the primary antibody, Anti-Digoxigenin-AP, FAB fragments (Sheep IgG, Roche), added for 2 hours, and then embryos were washed 5 X 15 minutes with PBST. For coloration, embryos were washed 5 X 5 minutes in coloration buffer (100 mM Tris-HCl pH 9.5, 50 mM $MgCl_2$, 100 mM NaCl & 0.1% Tween-20 in sterile water), and then coloration solution (0.45 mg/ml 4-nitro blue tetrazolium chloride [NBT] and 0.175 mg/ml 5-bromo-4-chloro-3-indolyl-phosphate [BCIP] [Roche] in coloration buffer) was added to embryos, which were incubated in the dark and periodically checked. When complete, embryos were washed 2 X 15 minutes in stop solution (PBST pH 5.5), 2 X in PBST, and stored at 4°C in the dark. Whole images of embryos on the yolk were photographed with an Olympus SZX12 stereomicroscope with QCapture Suite PLUS Software v3.3.1.10 and a Micropublisher 5.0 RTV camera (QImaging). Embryos were manually deyolked, dissected, and photographed with a Zeiss AxioImager.Z1 compound microscope (Zeiss Plan-APOCHROMAT 20x/0.8 lens), using an Axiocam HRm digital camera (Zeiss) and Axiovision SE64 Rel.4.8 software for RGB color photos.

Whole mount immunofluorescence

Anti-laminin

All washes were performed at RT on a nutator, unless otherwise stated. Embryos were fixed in 4% PFA for four hours or overnight at 4°C, and then washed 4 X 5 minutes in PBST and dechorionated. For permeabilizaiton, embryos were bathed in a Proteinase K (10 μg/ml) PBST solution (2 minutes for 22 hpf, 30 minutes for 48 hpf), and then washed 4 X 5 minutes in PBST and 1 X 5 minutes in 0.1% Tween-20 solution in sterile water. Ice-cold acetone (-20°C) was added to embryos, which were placed at -20°C for 7 minutes. After permeabilizaiton, embryos were washed 2 X with 0.1% Tween-20 in sterile water, and 4 X 5 minutes in PBST. Blocking solution (5% goat serum in PBST) was then added for a minimum of one hour. Embryos were incubated in primary antibody (rabbit anti-laminin L9393, Sigma-Aldrich), diluted 1/500 in

blocking solution, overnight at 4°C. Embryos were washed 5 X 15 minutes with PBST, and then incubated overnight at 4°C in secondary antibody, AlexaFluor® 568 goat anti-rabbit (Life Technologies Inc.) 1/1000 in blocking solution in the dark. The following day, embryos were washed 5 X 15 minutes in PBST, manually dissected, with eyes mounted on glass slides in Aqua-Poly/Mount (Polysciences, Inc.) and allowed to solidify at 4°C overnight, or whole embryos were oriented in UltraPure™ low-melting point agarose (Invitrogen) on a depression slide, or on 35 mm petri dishes and imaged using a Zeiss W N-ACHROPLAN 20X/0.5 dipping lens or a Zeiss Plan-APOCHROMAT 20x/0.8 lens. Embryos were imaged using a LSM 700 compact confocal microscope (Zeiss) with ZEN 2010 v6.0 Software.

Anti-activated Caspase 3

For analysis of apoptosis, embryos were fixed in 4% PFA for 4 hours at RT or overnight at 4°C. All washes were performed at RT on a nutator unless otherwise stated. Embryos were washed out of fix 3 X 20 minutes in PBS, 1 X 5 minutes in 0.1% Tween-20 in sterile water, and then permeabilized in ice-cold acetone chilled to -20°C, for 7 minutes at 4°C on a nutator, followed by a 1 X 5 minute wash in 0.1% Tween-20 sterile water and 1 X 5 minutes in PBS to remove any residual acetone. Embryos were blocked for 90 minutes in a PBS, 1% DMSO, 1% Triton, 1% Tween-20 (PBSDTT), 4% goat serum solution, before incubation in the primary antibody, rabbit anti-activated Caspase 3 (BD Biosciences), 1/400 in block for 2 hours at RT or overnight at 4°C. Embryos were rinsed 2X and washed 2 X 20 minutes in PBSDTT before incubation in secondary antibody, goat anti-rabbit AlexaFluor® 488 (Molecular Probes), 1/1000 in block in the dark for 2 hours. Embryos were rinsed 2X and washed 4 X 15 minutes in PBSDTT before visualization on the yolk as described above.

Anti-phosphohistone H3

For analysis of proliferation, embryos were fixed in 4% PFA for 4 hours at RT or overnight at 4°C. All washes were performed at RT on a nutator unless otherwise stated. Embryos were

washed 5 X 5 minutes in PBST, permeabilized with Proteinase K (10 μg/ml) in PBST (2 minutes for 24 hpf), re-fixed for 20 minutes in 4% PFA, and again washed 5 X 15 minutes in PBST. Embryos were incubated for 20 minutes at 95°C in 10 mM citric acid buffer (or 10 mM sodium citrate buffer) and blocked for at least 1 hour in a 3% BSA PBST solution. Primary antibody, rabbit anti-phosphohistone H3 (BD Biosciences), was diluted 1/1000 in blocking solution and left on for 2 hours, and then removed with 5 X 15 minute PBST washes. Secondary antibody, goat anti-rabbit AlexaFluor® 488 (Molecular Probes), was also diluted 1/1000 in blocking solution and left for 2 hours in the dark before 5 X 15 minute PBST washes. Images were taken on the yolk in PBST as described above.

Pharmacological treatment

Live embryos were dechorionated at ~75% epiboly using 1 mg/ml of Pronase E (Sigma-Aldrich), with gentle agitation for 3-5 minutes. When chorions began to crumple, embryos were washed 5X with EM, and then placed on agarose-coated plates (1.2% agarose melted in EM). 100 mg of all trans retinol (Vitamin A, Sigma-Aldrich) was dissolved to a 1 M stock solution using 100% ethanol, diluted to a 100 μM working stock with 100% ethanol, and embryos were treated with 0.6 μM all trans retinol diluted in EM. Control treatment was the same concentration of 100% ethanol diluted in EM. Old solution was removed and fresh solution added two times per day. 48 hpf all trans retinol embryos were photographed on the yolk as described above, and student's t-test was performed with Bonferonni correction for multiple comparisons.

Mutagenesis

CYP1B1 constructs were a kind gift from the lab of Dr. Michael Walter, and all WT *CYP1B1* constructs were initially shuttled and cultured by Dr. Curtis French (Table 2-4). Mutagenesis was performed according to the QuikChange Lightning Site-Directed Mutagenesis Kit® (Agilent Technologies), with modifications outlined here. Using the provided WT *CYP1B1* pDONR221, pcDNA-3.2/V5-DEST and pcDNA-DEST47 vectors provided (Table 2-4), mutagenesis to R368H

CYP1B1 (c.1103G>A) proceeded as follows. To a final volume of 50 µl, 3 separate reactions that differed by WT vector concentration (25, 50 & 100 ng) were performed to determine which was most effective. Each reaction was composed of 5 µl of the provided 10X reaction buffer, 125 ng each of the R368H forward (GGTCGTGGGGAGGGACCATCTGCCTTGTATGGGTGACCAGCCC) and reverse (GGGCTGGTCACCCATACAAGGCAGATGGTCCCTCCCCACGACC) (Table 2-5) HPLC purified primers, 1 µl of the provided dNTP mix, 1.5 ul of the provided Quiksolution reagent, the required volume of vector DNA, and sterile water to 50 µl. 1 µl of Quikchange lighting enzyme was added, and the reaction was placed in a thermocycler and cycled as follows: 1X at 95°C for 2 minutes, 18X at 95°C for 20 seconds, 60°C for 10 seconds, 68°C for 4 minutes, 1X at 68°C for 5 minutes. Amplification products were then digested with 2 µl of *Dpn* I, which was gently mixed in by pipetting, the reaction mixture was spun down, and then incubated for 5 minutes at 37°C in the thermocycler. 5 µl of the reaction volume was used to transform 25 µl of One Shot® TOP10 Chemically Competent *E. coli* (Invitrogen) and volumes of 10, 50 and 100 µl of each reaction were plated on the appropriate antibiotic (Table 2-4) and grown overnight at 37°C. Isolated colonies were chosen the next day for overnight culturing, mini preps (QIAprep Spin Miniprep Kit, Qiagen) and sequencing to confirm successful mutagenesis. Cultures found to carry the R368H *CYP1B1* mutation were then midi-prepped (Qiagen Plasmid *Plus* Midi Kit, Qiagen). This reaction was also performed on the WT *CYP1B1* pcDNA-DEST47 vector (Table 2-4). As the A287X *CYP1B1* (c.859delG) mutation results in a premature stop codon that would interfere with production of a V5 or GFP tag, additional steps were taken in the construction of these vectors to produce a 933 bp sequence, versus the complete 1632 bp sequence. The QuikChange® Mutagenesis kit was used as above with A287X *CYP1B1* forward (CCTTCGGCCCGGGCCGCCCC) and reverse (GGGGCGGCCCGGGCCGAAGG) (Table 2-5) HPLC purified primers, using the WT *CYP1B1* pDONR221 vector (Table 2-4).

Table 2-4: CYP1B1 vectors

Gene	Vector	Antibiotic	ORF
WT *CYP1B1*	pDONR221	Kanamycin	No stop codon
WT *CYP1B1*	pcDNA-DEST47	Ampicillin	No stop codon
WT *CYP1B1*	pcDNA-3.2/V5-DEST	Ampicillin	No stop codon
WT *CYP1B1*	pcDNA-3.2/V5-DEST	Ampicillin	Stop codon
WT *CYP1B1*	pCS2+	Ampicillin	Stop codon
R368H *CYP1B1*	pDONR221	Kanamycin	No stop codon
R368H *CYP1B1*	pcDNA-3.2/V5-DEST	Ampicillin	No stop codon
R368H *CYP1B1*	pcDNA-DEST47	Ampicillin	No stop codon
R368H *CYP1B1*	pCS2+	Ampicillin	Stop codon
A287X *CYP1B1 (*full sequence)	pDONR221	Kanamycin	Stop codon resulting from mutation
A287X *CYP1B1* (933 bp)	pDONR221	Kanamycin	No stop codon
A287X *CYP1B1* (933 bp)	pcDNA-DEST47	Ampicillin	No stop codon
A287X *CYP1B1* (933 bp)	pcDNA-3.2/V5-DEST	Ampicillin	No stop codon
A287X *CYP1B1* (933 bp)	pCS2+	Ampicillin	Stop codon

Table 2-5: Primers used for CYP1B1 mutagenesis

Gene	Forward primer (5' – 3')	Reverse primer (5' – 3')	Tm (°C)
A287X *CYP1B1**	CCTTCGGCCCGGGCCGCCCC	GGGGCGGCCCGGGCCGAAGG	84.7
R368H *CYP1B1**	GGTCGTGGGGAGGGACCAT CTGCCTTGTATGGGTGACCAGCCC	GGGCTGGTCACCCATACAAGGCAG ATGGTCCCTCCCCACGACC	73.5
A287X *CYP1B1* attB	GGGGACAAAGTTGTACAAAAAAG CAGGCTTAGCCACCATGGGCACC AGCCTCAGCCC	GGGGACCACTTTGTACAAGAAAGCTG GGTATGTCGCGGGGGGCGGCCCGGG	

*HPLC purified
All primers were designed by the author

After sequencing to confirm correct mutagenesis to A287X *CYP1B1* pDONR221, plasmid DNA was amplified with attB forward (GGGGACAAAGTTGTACAAAAAAGCAGGCTTAGCCACCATGGGCACCAGCCTCAGCCC) and reverse (GGGGACCACTTTGTACAAGAAAGCTGGGTATGTCGCGGGGGGCGGCCCGGG) primers using Pfx50™ DNA Polymerase (Invitrogen) to create a 933 bp attB-PCR product for subsequent Gateway® cloning (Invitrogen). The PCR product was gel purified (QIAquick Gel Extraction kit, Qiagen) and used as directed in the Gateway® BP reaction to create an A287X *CYP1B1* entry clone (Table 2-4). Transformants were cultured, mini-prepped and sequenced. Vectors containing the correct 933 bp A287X *CYP1B1* sequence were then used as directed in the Gateway® LR reaction with the desired destination vector (pcDNA-DEST47 & pcDNA-3.2/V5-DEST) to create A287X *CYP1B1* pcDNA-DEST47 and A287X *CYP1B1* pcDNA-3.2/V5-DEST vectors (Table 2-4). Vectors containing the correct sequence were midi-prepped.

The WT *CYP1B1* pDONR221 vector was shuttled into the pCS2+ vector (Dr. Jakub Famulski), and then mutagenesis, as described above, was done on WT *CYP1B1* pCS2+ vectors to create A287X pCS2+ and R368H pCS2+ constructs.

Western Blots

Transfection & cell harvesting

For *CYP1B1* western blots, four 100X20 mm plates (Cell Star® cell culture dishes, Greiner Bio-One) of COS-7 (CV-1 in Origin, carrying SV40, 7) cells were transfected with the respective 4 µg of midi-prepped pcDNA-3.2/V5-DEST vector DNA (WT *CYP1B1,* R368H *CYP1B1,* A287X *CYP1B1* & untransfected control) diluted in Gibco® 1X Dulbecco's Modified Eagle Medium [DMEM, high glucose, high pyruvate (4.5g/L D-Glucose, L-Glutamine, 110 mg/L sodium pyruvate)]. To prepare vector DNA for transformation, 400 µl of DMEM warmed to 37°C was added to plasmid DNA, and a 3:1 volume ratio of FuGene® HD Transfection Reagent to DNA

(Promega) was added to the center of the microcentrifuge tube and mixed by gentle pipetting. After 30 minutes at RT, the entire contents were mixed again and added to Cos-7 cells in a spiral pattern. Cells were placed in a CO_2 chamber at 37°C and allowed to grow overnight. The next day, cell media was removed by aspiration and cells were washed 2X with 5 ml of chilled 1X PBS. A working stock solution of 0.1 M phenylmethylsulfonyl floride (PMSF, Roche) was diluted to 0.001 M in cold 1X PBS, and 1 mL was added to the cells, one plate at a time, and cells were lifted (Costar cell lifter, Corning™, Fisher Scientific) and transferred to pre-chilled microcentrifuge tubes.

Protein Extraction, Resolution & Electrotransfer

Cells were spun for 5 minutes, at 3000 rpm at 4°C, the supernatant was removed, and 200 µl of chilled lysis buffer [radio-immunoprecipitation assay buffer (RIPA buffer, 150 nM sodium chloride, 1.0% Triton X-100, 0.5% sodium deoxycholate, 0.1% SDS, 50 mM Tris-HCl, pH 8.0), 0.001 M PMSF, & protease inhibitor cocktail (PIC, Sigma-Aldrich), diluted 1/50] was used to resuspend cells, which were left on a nutator for 1 hour at 4°C. Cells were sonicated with a Fisher Sonic Dismembrator Model 60 (Fisher Scientific) for 10 seconds, and then spun for 5 minutes at 13000 rpm at 4°C. For quantification of harvested protein, the concentration of samples was determined by comparison and correction, using standards established on a NanoDrop Lite Spectrophotometer (Thermo Scientific) and a BSA scale (10, 5, 2.5, 1.25, 0.625 & 0.3125 mg/ml). Using a Mini Trans-Blot® Cell apparatus (BioRad), 100 µg of each protein sample was ran, in parallel, on a 12% sodium dodecyl sulfate-polyacrylamide gel electrophoresis (SDS-PAGE) separating gel [30% Acrylamide/bis solution 37:5:1 (Bio Rad), 4X SDS-PAGE separating gel buffer, pH 8.8 (1.5 M Tris-HCl, pH 8.8 & 0.4% SDS), 10% ammonium persulfate (APS, Bio-Rad), tetramethylethlenediamine (TEMED, Thermo Scientific) & sterile water] after loading into a stacking gel [Acrylamide/bis 37:5:1, 4X stacking gel buffer pH 6.8 (0.5 M Tris-HCl, pH 8.8 & 10% SDS), 10% APS, TEMED & sterile water] and bathed in 1x SDS-PAGE running gel buffer

(10X SDS-PAGE running gel buffer: 0.25 M Tris, 1.92 M glycine, 10% SDS) . Samples were run for 30 minutes at 50 amps, or until the lowest band of the protein ladder (Precision Plus Protein™ Standards, Dual Color, BioRad) reached the bottom of the gel caster. Using a Mini Trans-Blot® Cell apparatus (Bio Rad), protein was transferred onto a nitrocellulose membrane, 0.45 µM (BioRad), in 1X SDS-PAGE transfer buffer (10X SDS-PAGE transfer buffer: 0.25 M Tris, 1.92 M glycine, 10% SDS & sterile water, diluted to 1X using a 1/10 volume of methanol, and sterile water) at 30 V, overnight at 4°C.

Protein visualization – V5 tagged protein

After protein transfer was complete, the nitrocellulose membrane was blocked for 1 hour at RT on a shaker in a 5% milk and Tris-buffered saline with Tween-20 (TBST, 1 M Tris-HCl, pH 8.0, 5M NaCl, 0.05% Tween-20, sterile water) solution. The membrane was then incubated in primary antibody, V5 mouse monoclonal (Invitrogen), 1/5000 in blocking solution and 0.02% sodium azide (NaN_3), for 2 hours at RT or overnight at 4°C on a shaker, and primary antibody was saved and stored at -20°C for re-use. The membrane was given 2X TBST rinses, followed by 3 X 1 5 minute TBST washes at RT on a shaker, and then incubated in secondary antibody, peroxidase-conjugated AffiniPure Goat Anti-mouse IgG (H+L) (Jackson ImmunoResearch Laboratories, Inc.), 1/5000 in blocking solution, for 1 hour at RT on a shaker. The membrane was given 2X rinses and 3 X 15 minute TBST washes, followed by 2X rinses and 1 X 15 minute TBS (TBST without 0.05% Tween-20) wash. Once complete, the membrane was dried and then soaked for 5 minutes in Pierce ECL Western Blotting Substrate (Thermo Scientific), dried, wrapped and placed in an Autoradiography cassette (Fisher Biotech) and medical x-ray film (Fujifilm) was allowed to develop for 20 minutes before it was processed (Protec Ecomax X-ray film processor). The western blot described in this thesis has n=2 biological replicates. In the first biological replicate there was one technical replicate, and in the second biological replicate

there were two technical replicates, performed together simultaneously using protein collected from the same COS7 cells.

α-tubulin

For all western blots, α-tubulin was used as a loading control, and all washes were done at RT on a shaker unless otherwise stated. After completion of detection of the V5 tagged protein, the nitrocellulose membrane was rinsed 1X in TBST, and then the primary antibody was removed using 0.2 M sodium hydroxide (NaOH) for 20 minutes. The membrane was blocked for 1 hour in 5% milk and TBST, given 2X quick TBST washes, and incubated in primary antibody, bovine alpha-tubulin mouse mAb (Invitrogen), 1/10000 with 0.02% NaN_3 in blocking solution for 90 minutes. The membrane was given 2X TBST rinses, and 3 X 15 minute TBST washes, and incubated in secondary antibody, peroxidase-conjugated AffiniPure Goat Anti-mouse IgG (H+L) (Jackson ImmunoResearch Laboratories, Inc.), 1/5000 in blocking solution for 1 hour. The membrane was rinsed 2X and washed 3 X 15 minutes in TBST, rinsed 2X and washed 1 X 15 minutes in TBS, and then developed as described above.

Reporter gene assays

To measure cytochrome P450 (CYP) activity directly, a modified protocol using both the P450-Glo™ CYP1B1 Assay (Promega), and Dual-Luciferase® Reporter Assay (Promega) was employed, which was adapted from a previously described method (BAGIYEVA *et al.* 2007). Performed once in biological replicates of six individual transfections per construct, cultured Cos-7 cells (24 well cell culture plate, Cellstar®, Greiner Bio-One) were transfected with the respective GFP tagged constructs (WT, R368H & A287X *CYP1B1* pcDNA-DEST47), or an empty pCS2+ vector as a control. Each well was transfected with 500 ng of construct DNA, a 3:1 µl/µg ratio of X-tremeGene 9 DNA Transfection Reagent (Roche) to DNA, and 5 ng of *Renilla* Luciferase reporter vector (Promega) as a transfection control, in a 100 µl volume of DMEM (as described above), and placed in a 37°C CO_2 chamber. After 48 hours of growth, cell media was removed and 0.1

mM of Luciferin-CEE (Promega) in fresh DMEM was added to each well, and cells were returned to the 37°C CO_2 incubator and left for three hours. To detect D-luciferin (modified beetle luciferin) produced by each construct, which is a direct read-out of CYP1B1 enzymatic activity, 100 µl of reconstituted Luciferin Detection Reagent (Promega) and 50 µl of individual cell culture media were added to a cuvette (12 X 50 mm disposable cuvettes, Promega), vortexed, and inserted into a luminometer (Turner BioSystems Luminometer Model TD-20/20). For detection of constitutively active Renilla luciferase, which acts as a transfection efficiency control, 100 µl of Stop & Glo® Reagent (Promega) were added to the cuvette, vortexed, and read on the same luminometer. The six biological replicate values for each construct were averaged and corrected for according to transfection efficiency, using the empty pCS2+ Renilla luciferase value as a representation of 100% transfection efficiency.

Chapter 3

Apoptotic and Proliferative Defects Characterize Ocular Development in a Microphthalmic BMP Model

This chapter has been modified from the publication:

*French CR, **Stach TR**, March LD, Lehmann OJ, Waskiewicz AJ. Apoptotic and Proliferative Defects Characterize Ocular Development in a Microphthalmic BMP Model. Invest Ophthalmol Vis Sci. 2013 Jul 10;54(7):4636-47*

C.R. French and myself are co-first authors of this paper. C.R. French is responsible for Figures 1, 2, 4, the majority of 5, 6, Supplementary Figure 1, and performing all steps of the Microarray. I am responsible for Figures 7 and 8, panels M – T in Figure 5, and aiding L.D. March with preliminary experiments leading to Figure 3, of which she is responsible. This manuscript was written and assembled by myself, with aid in figure assembly and manuscript edits from C.R. French and L.D. March. A.J. Waskiewicz was the supervisory author and was involved with concept formation, manuscript composition and edits. O.J. Lehmann provided manuscript edits and was the co-supervisor of this project.

3.1: Introduction

Microphthalmia, the presence of a small eye, and anophthalmia, the complete lack of ocular tissue, represent part of a phenotypic spectrum of congenital anomalies present in up to 11% of blind children (MORRISON *et al.* 2002; VERMA AND FITZPATRICK 2007; PARKER *et al.* 2010). Their complex etiology includes both environmental and genetic factors (KALLEN *et al.* 1996; VERMA AND FITZPATRICK 2007), with the latter encompassing coding mutations, copy number variations and position effects induced by chromosomal translocations. Integrative studies of eye development in zebrafish, chick, mouse and fly models have identified numerous genes essential for eye formation in which mutations contribute to microphthalmia and anophthalmia. The coordinated action of inductive signals, tissue interactions, and morphogenic movements are a prerequisite for normal ocular development and vision.

Initially, homeodomain transcription factors such as *Rax, Six3, Pax6* and *Otx2* specify the presumptive ocular field that evaginates from the diencephalon to form the optic vesicle (FUHRMANN 2010; BARDAKJIAN AND SCHNEIDER 2011; SHAHAM *et al.* 2012). Heterozygous *OTX2* and *RAX* mutations in human, mouse (*Rx)*, and zebrafish (*rx3*) result in anophthalmia or bilateral microphthalmia, with *rx3* mutants exhibiting defects in cellular movement and proliferation (RAGGE *et al.* 2005; FUHRMANN 2010; SCHILTER *et al.* 2011). Once the optic vesicles contact the surface ectoderm, *Six3, Pax6* and *Sox2* play critical roles first in lens placode formation and induction, and subsequently in lens development (LIU *et al.* 2006; SMITH *et al.* 2009; FUHRMANN 2010). The importance of lens induction is illustrated by reduced levels of mouse *Six3, Pax6* or *Sox2* resulting in microphthalmia or anophthalmia (VAN RAAMSDONK AND TILGHMAN 2000; VERMA AND FITZPATRICK 2007; SMITH *et al.* 2009; SHAHAM *et al.* 2012). In mammals, *Pax6*, *Sox2* and *Otx2* contribute to the specification of the optic vesicle, whose inner layer becomes the neural retina, and requires *Pax6* and *Sox2* expression for accurate progenitor cell specification (WEN *et al.* 2008; MATSUSHIMA *et al.* 2011). Mouse and chick analyses similarly

demonstrate the requirement of *Mitf* and *Otx2* for retinal pigment epithelium (RPE) specification, which is essential for normal ocular growth (MARTINEZ-MORALES *et al.* 2003; WESTENSKOW *et al.* 2009; FUHRMANN 2010).

Central to the determination of eye size is the control of retinal progenitor cell proliferation and survival. Genes regulating both processes cause microphthalmia in patients and model organisms when mutated (WU *et al.* 2003; STEINGRIMSSON *et al.* 2004; DHOMEN *et al.* 2006; THIEL 2013). Subsequent to cell cycle exit and differentiation of retinal neurons, the zebrafish eye continues to grow via the addition of new retinal neurons. A population of progenitor cells is maintained for this purpose at the interface between neural retina and ciliary epithelium, a region called the ciliary marginal zone (CMZ)(RAYMOND *et al.* 2006). Thus in zebrafish, mutation of genes that maintain this cell population may also result in microphthalmia (NUCKELS *et al.* 2009), yet little is known concerning the molecular regulation of cell proliferation in the CMZ.

The Bone Morphogenetic Proteins (BMPs) and Growth and Differentiation Factors (GDFs) have well-recognized ocular developmental roles. BMP's regulate both apoptosis and proliferation in the eye, with mutation or copy number variation of 3 BMPs (*GDF3, GDF6* and *BMP4*) associated with microphthalmia, anophthalmia or coloboma (MAC) in patients. The contribution of this gene family is extended by the large number of paralogs implicated in eye development through model organism analysis (e.g. *bmp2, bmp7* and *gdf11*) (TROUSSE *et al.* 2001; ASAI-COAKWELL *et al.* 2007; BAKRANIA *et al.* 2008; ASAI-COAKWELL *et al.* 2009; GONZALEZ-RODRIGUEZ *et al.* 2010; YE *et al.* 2010; REIS *et al.* 2011). Similarly, perturbed function of multiple BMP antagonists including *gremlin*, *chordin-like 1* and *Bambi,* induce ocular anomalies in model organisms and for some (*CHRDL1)*, comparable and severe patient anterior segment phenotypes have been defined (HUILLARD *et al.* 2005; PAULSEN *et al.* 2011; WEBB *et al.* 2012). We previously

demonstrated *gdf6a*$^{-/-}$ mutant zebrafish lack Smad 1/5/8 phosphorylation in the developing retina, and we and others demonstrated that *gdf6a* lies at the top of the hierarchy of genes controlling the patterning of the dorsal-ventral axis of the developing retina (FRENCH *et al.* 2009; GOSSE AND BAIER 2009). In addition to this fundamental role in retinal patterning, *gdf6a* mutants display bilateral microphthalmia (HANEL AND HENSEY 2006; FRENCH *et al.* 2009; GOSSE AND BAIER 2009; DEN HOLLANDER *et al.* 2010).

Since the cellular mechanisms that underlie this microphthalmic phenotype have yet to be elucidated, we hypothesized that aberrant regulation of cell cycle and apoptosis might contribute to the microphthalmic phenotype, and examined both during *gdf6a*$^{-/-}$ ocular development in zebrafish. We demonstrate that *gdf6a*$^{-/-}$ eyes are microphthalmic at early developmental stages due to reduced retinal progenitor cell number. We show that rescue of elevated ocular apoptosis during development does not restore normal eye size in *gdf6a*$^{-/-}$ larvae. Microarray analysis revealed aberrant expression of genes with roles in cellular proliferation in the CMZ, which included members of the *forkhead box* (*fox*) family of transcription factors. Notably, several of these genes have fundamental roles in development, cell cycle control and contribute to ocular disorders (MYATT AND LAM 2007; HANNENHALLI AND KAESTNER 2009). We find a significant reduction in CMZ proliferation in *gdf6a*$^{-/-}$ larvae, with a requirement of *foxi1* and *foxi2* in mediating dorsal-ventral polarity of the CMZ and in Gdf6a-mediated eye size determination.

3.2: Results

Loss of *gdf6a* expression results in microphthalmia

The zebrafish *gdf6a*$^{-/-}$ line studied contains a c.164C>A mutation that creates a premature stop codon, resulting in premature truncation of the protein, with loss of the mature domain of the protein (GOSSE AND BAIER 2009). Homozygous mutant embryos display bilateral microphthalmia, and in comparison to wild type (WT) or heterozygotes, the eye is noticeably

smaller at 2 dpf (Figure 3-1 A-B), with microphthalmia more pronounced by 4 dpf (Figure 3-1 C-D). Previous studies demonstrated *gdf6a's* expression adjacent to the developing eye field at the 3 somite stage, and from the 10 somite stage onwards in the dorsal retina and dorsal epidermis (FRENCH *et al.* 2009; GOSSE AND BAIER 2009), indicating that specification of retinal progenitor cells may influence eye size. From 2-4 dpf, *gdf6a* is expressed within the dorsal CMZ (Figure 3-1 E-H), highlighting a potential role for defective cell proliferation in the determination of *gdf6a*$^{-/-}$ eye size.

Reduced number of retinal progenitor cells in *gdf6a*$^{-/-}$ embryos at 24 hpf

As eye size is noticeably smaller in *gdf6a*$^{-/-}$ embryos by 24 hpf, we conducted an analysis of the number of retinal progenitor cells and proliferation at this time point. Although the expression of a subset of genes that control proliferation is reduced in homozygous mutants [(*myca*, Figure 3-2 A, B) and (*mych,* Figure 3-2 C, D)], both the number and percent of proliferating cells at this time point is unchanged (Figure 3-2 E-H). Thus it unlikely that early small eye phenotypes are due to a proliferation defect. However, the number of progenitor cells is clearly reduced in *gdf6a*$^{-/-}$ eyes (111.7±8.0) when compared to wild type siblings [(125±7.7, p=0.00017, *t*-test, (Figure 3-2 G)], indicating that processes occurring prior to 24 hpf influence eye size in *gdf6a*$^{-/-}$ embryos.

Inhibition of the increased rates of apoptosis in the *gdf6a*$^{-/-}$ eye does not rescue eye size

Previous characterization of *gdf6a*$^{-/-}$ embryos (DEN HOLLANDER *et al.* 2010) and our findings (Figure 3-3) show high rates of apoptosis throughout the developing eye. To determine if this contributes to microphthalmia, as previously suggested (DEN HOLLANDER *et al.* 2010), *gdf6a*$^{-/-}$ embryos were treated with either P7C3, a pharmacological agent that inhibits apoptosis (PIEPER *et al.* 2010), or DMSO control. Analysis of ocular activated Caspase-3 staining at 28 hpf indicates that heterozygous embryos have low levels of apoptosis when incubated with either P7C3 or DMSO (Figure 3-3 A, C). High levels of apoptosis are observed in control DMSO treated

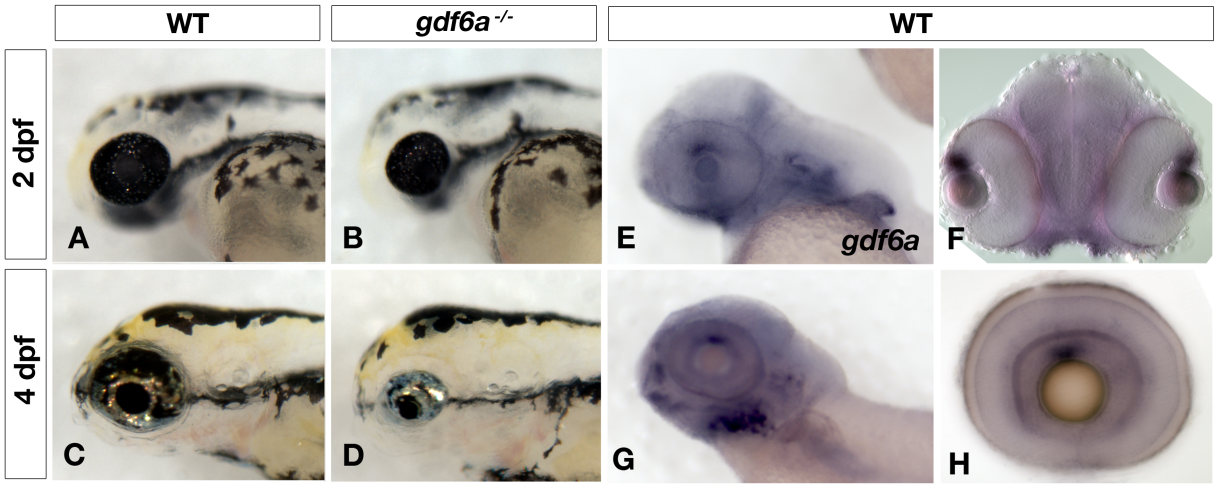

Figure 3-1: Analysis of *gdf6a* expression and ocular size.

At 2dpf *gdf6a*$^{-/-}$ embryos exhibit microphthalmia (A, B) that is more evident by 4dpf (C, D). At 2dpf, *gdf6a*'s ocular expression is confined to a small area of the dorsal retina (E), and in cross-section this domain includes the dorsal ciliary marginal zone (CMZ) and ganglion cell layer (F). Expression remains in the dorsal retina (G), with low levels of expression detected throughout the ganglion cell layer and CMZ at 4 dpf (H). Live pictures were taken at 90X, *in situ* pictures were taken at 200X.

gdf6a$^{-/-}$ embryos [mean number of foci (μ)=76, n=34], which is significantly decreased when treated with P7C3 [(μ) =16, n=33, ($p < 0.00001$, *t*-test) (Figure 3-3 B, D). This rescue of apoptosis in *gdf6a*$^{-/-}$ did not result in any significant rescue of eye size at 3 dpf, as P7C3 treated *gdf6a*$^{-/-}$ eyes were still significantly smaller than their control treated heterozygous siblings (50.3% of eye size, *t*-test $p < 0.1 \times 10^{-8}$) or P7C3 treated heterozygous siblings (62% of eye size, $p < 0.001$, *t*-test) (Figure 3-3 E). These data demonstrate that *gdf6a*$^{-/-}$ induced apoptosis is not a major contributor to the microphthalmia phenotype as partial rescue does not measurably affect ocular size. Incubation of embryos in P7C3 may affect other aspects of retinal development in addition to apoptosis, as evidenced by the subtle change in eye size of treated heterozygous eyes (Figure 3-3 E).

Genes with roles in cell cycle progression have reduced expression in *gdf6a*$^{-/-}$ eyes

To investigate whether later developmental events contribute to microphthalmia in *gdf6a* mutants, we assessed transcriptome changes at 2 dpf via microarray analysis. Using cut-offs of greater than or equal to 1.75 fold change in expression, 226 transcripts are down-regulated and 90 transcripts are up-regulated in *gdf6a*$^{-/-}$ embryos. Notably, the microarray results reveal significant alteration in expression of genes with roles in cell differentiation and patterning, including *atonal homolog 7*, *t-box 2b* and *t-box 4, forkhead box N4,* and *H6 family homeobox 1*, with the findings validated by *in situ* hybridization (Figure 3-4, Supplementary Figure 3-1 A-J). To identify *gdf6a*-dependent transcripts that play a role in proliferation, we focused on genes with ocular expression in the CMZ. Many genes responsible for regulation of cell cycle are down regulated in *gdf6a*$^{-/-}$ embryos (Figure 3-5), suggesting that they contribute to the microphthalmia phenotype. Indeed, *in situ* hybridization demonstrates the expression of six genes reduced or eliminated specifically in the CMZ of *gdf6a*$^{-/-}$ eyes, but minimally changed or unaffected in other areas of the embryo. This is compatible with a *gdf6a* specific role in control of ocular cell cycle. Altered genes include *carbamoyl-phosphate synthetase 2, aspartate*

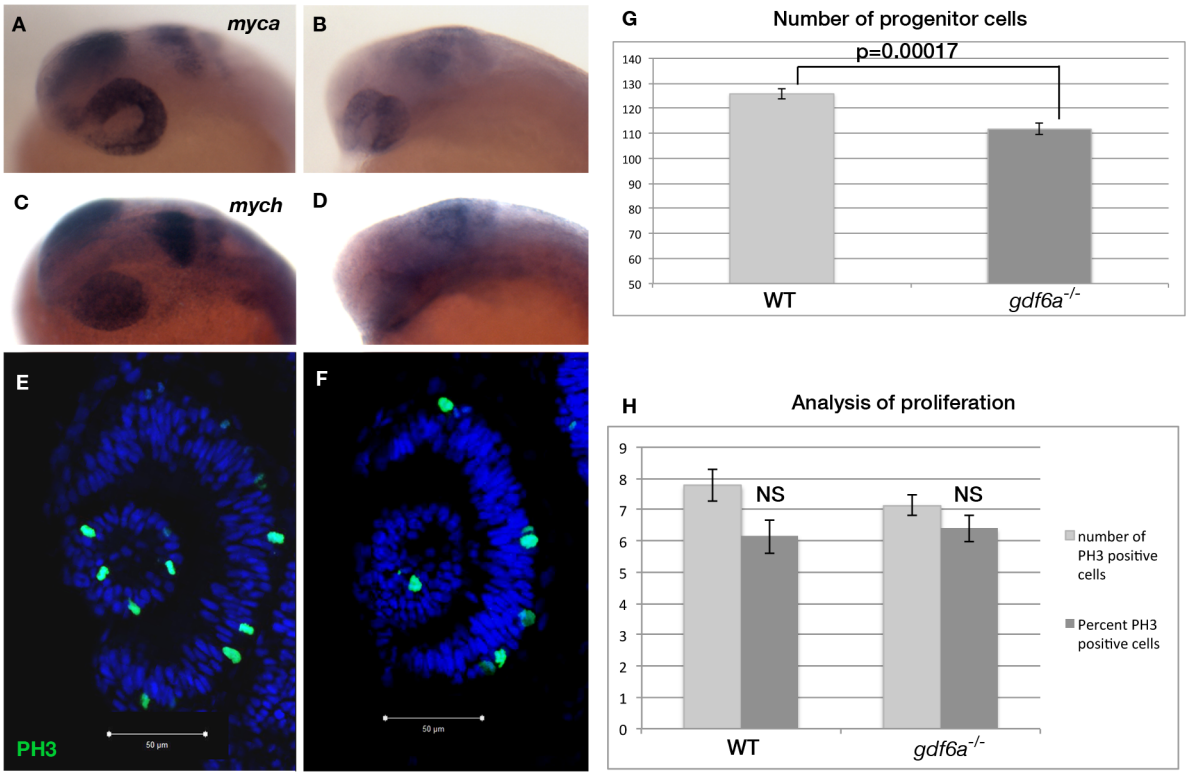

Figure 3-2: Reduced number of retinal progenitors contribute to microphthalmia in *gdf6a*$^{-/-}$ embryos.

While a difference in the expression of cell cycle regulators such as *myca* (A, B) and *mych* (C, D) is observed in *gdf6a* mutants at 24 hpf, no defects in the number or percentage of proliferating cells is observed (E and F). These data are quantified in (H). However, by this time there is a clear reduction in the number of retinal progenitor cells in *gdf6a* mutant eyes (p=0.00017, *t*-test) (G), indicating that reduced cell number contributes to the observed microphthalmia at early stages of development. Graphical data are presented as mean ± standard error. *In situ* pictures taken at 200X.

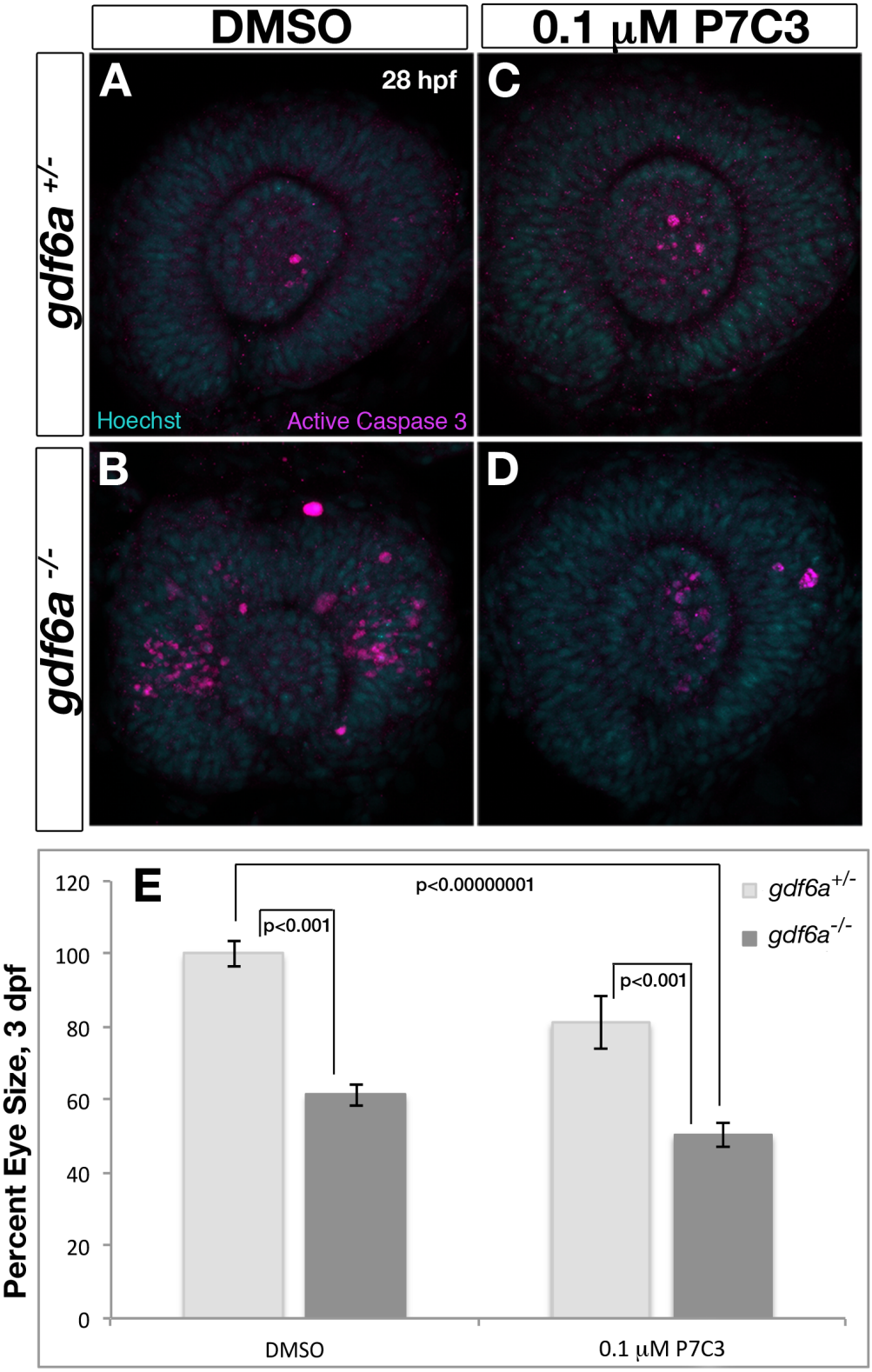
DMSO
0.1 μM P7C3
A
28 hpf
C
gdf6a +/-
Hoechst
Active Caspase 3
B
D
gdf6a -/-
E
p<0.00000001
p<0.001
p<0.001
gdf6a+/-
gdf6a-/-
Percent Eye Size, 3 dpf
120
100
80
60
40
20
0
DMSO
0.1 μM P7C3

Figure 3-3: Inhibition of apoptosis in *gdf6a*$^{-/-}$ eyes does not rescue microphthalmia.

In contrast to the low levels of ocular apoptosis observed in *gdf6a*$^{+/-}$ embryos treated with DMSO (A) or the apoptosis inhibitor P7C3 (C), *gdf6a-/-* embryos exhibit high levels of retinal apoptosis (B). Treatment of *gdf6a*$^{-/-}$ embryos with P7C3 results in significant reduction in the number of cells undergoing apoptosis in the eye at 28 hpf ($p<0.00001$, *t*-test) (D). At 3 dpf, no rescue of eye size is observed, as P7C3 treated *gdf6a-/-* eyes remain significantly smaller than both DMSO treated ($p<0.00000001$, *t*-test) or P7C3 treated ($p<0.001$, *t*-test) heterozygous siblings. Graphical data are presented as mean ± standard error. Confocal pictures taken at 400X.

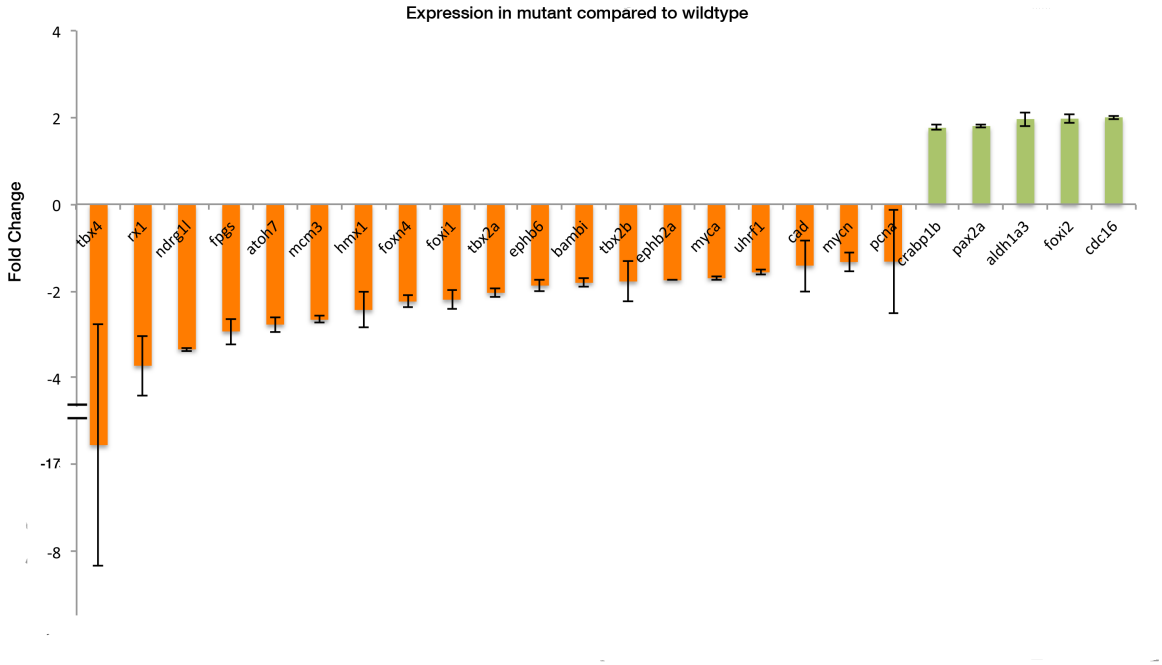

Figure 3-4. Summary of genes in which expression is maximally dysregulated in *gdf6a*$^{-/-}$ mutants.

Graphical representation of microarray data illustrating the fold changes in expression in 24 genes that are up (green) or down-regulated (orange) in *gdf6a*$^{-/-}$ mutants. Note the down-regulation of genes with roles in the cell cycle, such as *fpgs*, *mcm3, myca*, *mycn* and *pcna*, along with alterations in three forkhead box transcription factors, *foxn4*, *foxi1* and *foxi2***.** Data are presented as mean ± standard error.

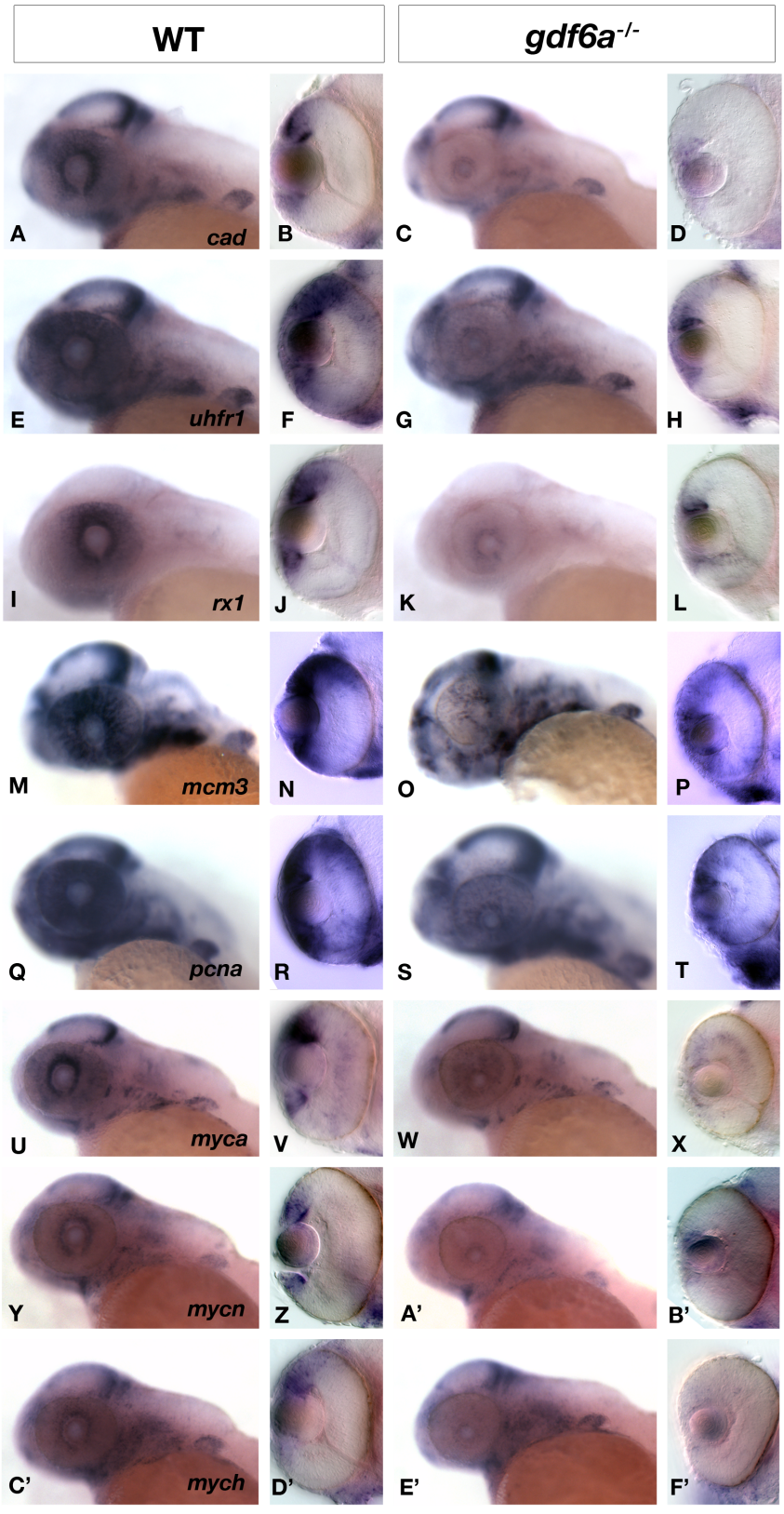
WT
gdf6a-/-
A
cad
B
C
D
E
uhfr1
F
G
H
I
rx1
J
K
L
M
mcm3
N
O
P
Q
pcna
R
S
T
U
myca
V
W
X
Y
mycn
Z
A'
B'
C'
mych
D'
E'
F'

Figure 3-5: In situ hybridization validation of Gdf6a responsive genes with known roles in cell cycle.

Gdf6a$^{-/-}$ embryos have ocular specific reduction in expression of genes with roles in the cell cycle. The expression of *cad* is almost completely lost in *gdf6a*$^{-/-}$ (A-D) while expression of *uhfr1* (E-H) and *rx1* (I-L) are down-regulated. The cell cycle regulators *mcm3* (M-P) and *pcna* (Q-T) are expressed at high levels throughout the eye including the CMZ at 2dpf, and are down-regulated in *gdf6a*$^{-/-}$ embryos. The expression of three zebrafish *C-Myc* paralogs is found in the CMZ at 2dpf, and is highly down-regulated (*myca*, U-X, *mycn* Y-B') or eliminated *(mych* C'-F') in *gdf6a*$^{-/-}$ eyes. Whole embryo pictures are taken at 90X, and cross section pictures are taken at 200X.

transcarbamylase, and *dihydroorotase* (*cad,* Figure 3-5 A-D)*, ubiquitin-like with PHD and ring finger domain containing 1* (*uhfr1* Figure 5E-H) and *retinal homeobox1* (*rx1,* Figure 3-5 I-L). Expression of *minichromosome maintenance complex component 3* (*mcm3,* Figure 3-5 M-P) and *proliferating cell nuclear antigen* (*pcna,* Figure 3-5 Q-T) are both highly down-regulated in the outer retina and CMZ in *gdf6a*$^{-/-}$ embryos but minimally changed elsewhere. Similar results are seen for three zebrafish paralogs of the cell cycle regulator, *C-Myc*. The expression of *myca,* found at high levels in CMZ, is strongly reduced in *gdf6a*$^{-/-}$ eyes (Figure 3-5 U-X). This is also the case for *mycn* (Figure 3-5 Y-B') and *mych* (Figure 3-5 C'-F'), which display strongly reduced expression in the CMZ of *gdf6a*$^{-/-}$ eyes, but are minimally affected in other areas of the embryo. Reduction in ocular expression of genes with roles in cell cycle progression suggests a role for *gdf6a* in cellular proliferation during eye development, and led to examination of possible anomalies in *gdf6a*$^{-/-}$ larvae.

Ocular proliferation during development is reduced in *gdf6a*$^{-/-}$ larvae

The decrease in ocular expression of multiple genes with roles in the cell cycle in *gdf6a*$^{-/-}$ implicates altered levels of cellular proliferation in the microphthalmia phenotype. Accordingly, the number of dividing cells was assayed using anti-phosphohistone H3 (PH3) antibodies at two time points: 2 dpf, when proliferation occurs primarily in the inner neural layer, and 4 dpf, when postmitotic retinal layers are present in *gdf6a* mutants and there is a greater contribution from the CMZ (FADOOL AND DOWLING 2008). To address potential confounding effects from reduced ocular size, the percentage of proliferating cells was quantified in addition to the total number of cells per section. While there is a difference in the number of proliferating cells per section at 2 dpf [*gdf6a*$^{-/-}$*:* number of cells (μ)=28, (n=7); WT: μ =47.5, n=6, p=0.0016, *t*-test], there is no significant difference in the proportion of PH3 positive cells per section [*gdf6a*$^{-/-}$: percent of cells (μ)=10.0% (n=7); WT: μ=11.7% (n=6); p=0.262, *t*-test] (Figure 3-6 A, B, E, F, I).

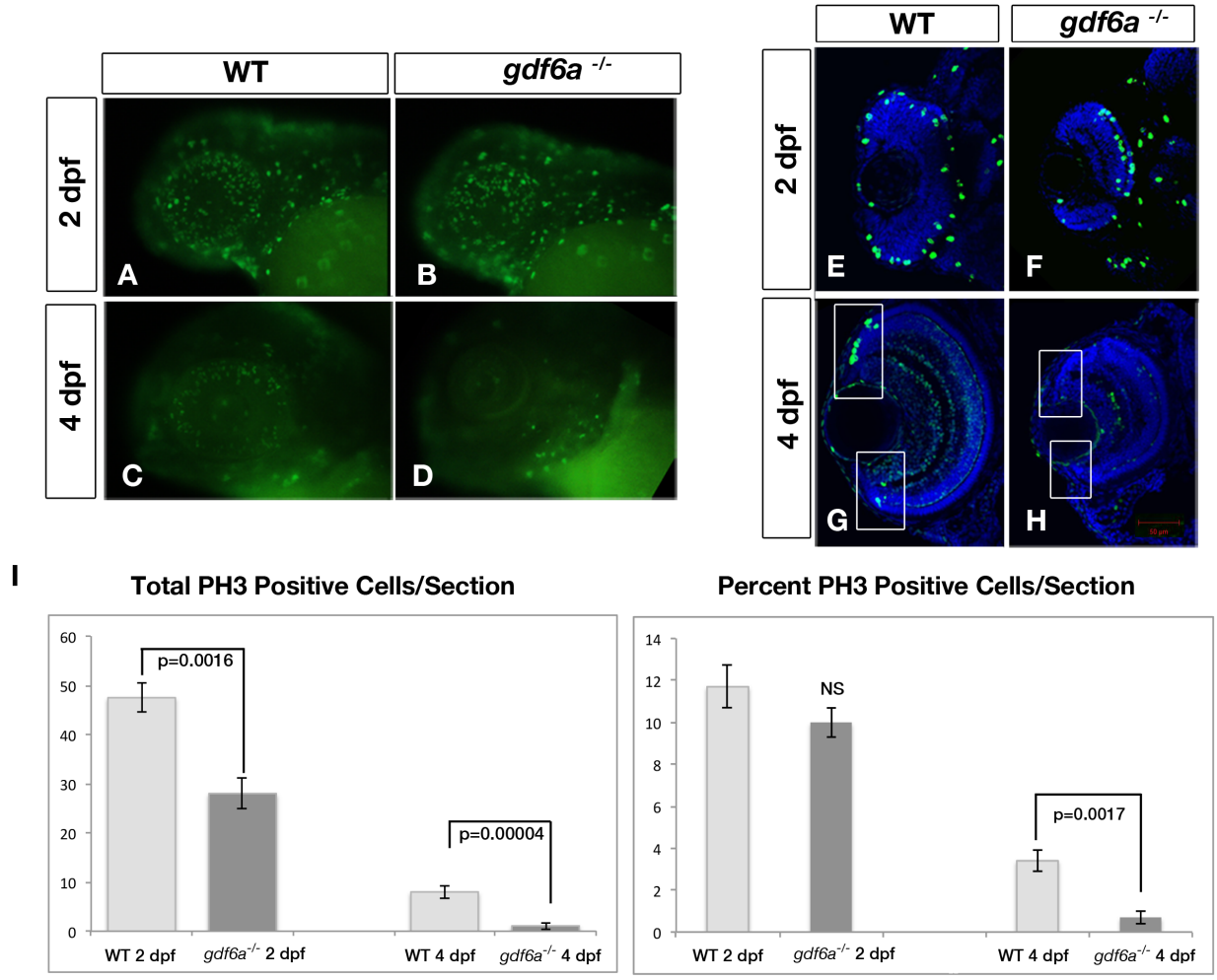

Figure 3-6: Gdf6a regulates cell proliferation in the developing eye.

The natural reduction in the level of proliferation between 2 and 4dpf in WT (A, C) is accelerated in *gdf6a*$^{-/-}$ embryos (B, D). Cross sections of WT embryos at 2 dpf show proliferating cells around the periphery of the eye (E), and confined to the CMZ at 4dpf (white boxes, G). There is a significant reduction of the number of proliferating cells at both 2 and 4dpf (F, H, I). To correct for the reduced number of cells in *gdf6a*$^{-/-}$ embryos, data were also quantified as the percentage of proliferating cells. Only at 4 dpf is the percentage of proliferating cells significantly different between WT and *gdf6a*$^{-/-}$ embryos (I). Total number of PH3 positive cells per section of ocular tissue shows a significant reduction at 2 dpf (*gdf6a*$^{-/-}$*:* μ=28, n=7; WT: μ =47.5, n=6, p=0.0016, *t*-test) (I) and 4dpf (*gdf6a*$^{-/-}$: μ=1.11, n=9; WT: μ=8, n=6, p=0.00004, *t*-test) (I). Quantification

of the percent of PH3 positive cells shows no significant difference at 2 dpf (*gdf6a*$^{-/-}$: μ=10.0%, n=7; WT: μ=11.7%, n=6, p=0.262, *t*-test), but a significant difference at 4 dpf between and WT (*gdf6a*$^{-/-}$: μ =0.68%, n=6; WT: μ=3.37%, n=6, p=0.0017, *t*-test). Graphical data are presented as mean ± standard error. Whole embryo pictures were taken at 90X.

By 4 dpf there is a statistically significant difference in the total number of PH3 positive cells in the CMZ [*gdf6a*$^{-/-}$: μ =1.1 (n=9); WT: μ =8 (n=6); p=0.00004, *t*-test]. These findings are validated by the proportion of positive cells [*gdf6a*$^{-/-}$: mean=0.7% (n=6); WT: mean=3.4% (n=6) p=0.0017, *t*-test] (Figure 3-6 C, D, G, H, I). The strongly reduced proportion of proliferating cells at 4 dpf suggest that loss of *gdf6a* during ocular development results in decreased proliferation in the CMZ, and, taken together with previous results, supports a role for *gdf6a* in regulation of both proliferation and apoptosis in the eye during development.

Expression of the forkhead box transcription factors *foxi1* and *foxi2* is altered in *gdf6a*$^{-/-}$ eyes

In addition to identifying altered expression of genes with roles in the cell cycle, microarray analysis also revealed genes with uncharacterized roles in ocular development and deregulated expression in *gdf6a*$^{-/-}$ embryos. The forkhead genes *foxi1* and *foxi2* show decreased (2.20 fold) and increased (1.97 fold) expression, respectively (Figure 3-4). Since these genes are members of the forkhead box family of transcription factors that have well documented roles in ocular development (XUAN *et al.* 1995; SEMINA *et al.* 2001; BERRY *et al.* 2006; SEO *et al.* 2012), we conducted additional studies to elucidate potential roles in determining ocular size. *In situ* analysis confirmed the microarray findings, and demonstrates that the two transcription factors are expressed in converse patterns in the dorsal (*foxi1*) and ventral (*foxi2*) CMZ (Figure 3-7 A, B, E, F). In WT embryos, *foxi1* is expressed in the dorsal retina in a similar pattern to *gdf6a* (Figure 3-1 E-F, Figure 3-7 A-B), with loss of *gdf6a* resulting in complete loss of *foxi1* expression in the dorsal CMZ (Fig. 3-7 C-D). The expression domain of *foxi2* is the mirror image of *foxi1* (Figure 3-7 E, F), and with loss of *gdf6a,* this ventral retinal expression of *foxi2* expands to encompass the dorsal CMZ where *foxi1* would normally reside (Figure 3-7 G, H). These findings indicate that *foxi1* and *foxi2* lie downstream of *gdf6a*. Their specific dorsal or ventral CMZ expression patterns are compatible with a role regulating proliferation in the CMZ, consistent with

previously characterized roles of *fox* transcription factors in regulation of the cell cycle(MYATT AND LAM 2007). Accordingly, we utilized gene specific morpholino injections to block *foxi2* function in *gdf6a*$^{-/-}$ embryos and non-mutant siblings and assessed consequent ocular size.

Injection of *foxi2* morpholino into *gdf6a* mutants further reduces eye size

Expression of *foxi* mRNAs delineates dorsal and ventral domains of the ciliary marginal zone. We assessed whether *foxi2* and *gdf6a* function in the same genetic pathway by morpholino inhibition of *foxi2* in both *gdf6a*$^{-/-}$ and *gdf6a*$^{+/-}$ embryos. Normally, the ocular size of *gdf6a*$^{+/-}$ embryos closely resembles that of *gdf6a*$^{+/+}$ (Figure 3-8 A & Figure 3-1 A, respectively) and genetic differences are only discernable upon genotyping. While injection of 4 ng of *foxi2* morpholino into WT embryos results in no discernable phenotype (data not shown), injection into *gdf6a*$^{+/-}$ embryos results in a small eye phenotype by 2 dpf [μ=76.6% of eye size, n=15, (p=0.004), *t*-test, (Figure 3-8 C and E)], similar to that of *gdf6a*$^{-/-}$ ocular size (Figure 3-8 B). Moreover, injection of *gdf6a*$^{-/-}$ embryos with *foxi2* morpholino results in a further reduction in eye size relative to uninjected *gdf6a*$^{-/-}$ embryos [Figure 3-8 D and E), μ= 77% of *gdf6a*$^{-/-}$ eye size, n=10 *gdf6a*$^{-/-}$; n=15 *gdf6a*$^{-/-}$ + Foxi2^{MO}, (p=0.00014), *t*-test]. On the basis of these findings, we observe a synergistic phenotype when we inject *foxi2* morpholino into *gdf6a*$^{+/-}$ embryos, consistent with these genes functioning on the same or converging genetic pathways.

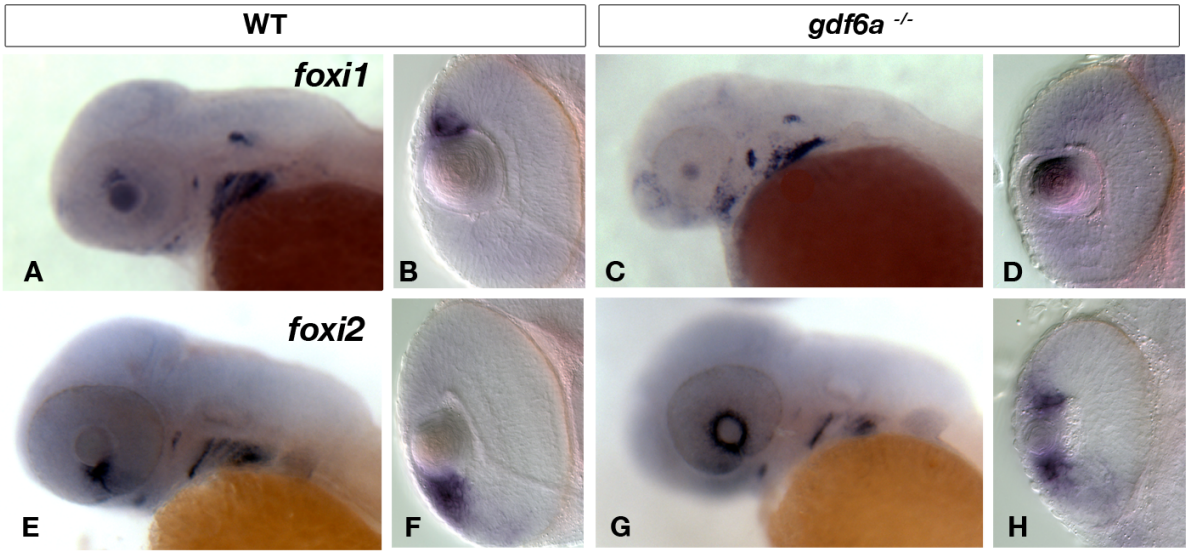

Figure 3-7: Altered *foxi* expression in the ciliary marginal zone of *gdf6a*$^{-/-}$ eyes.

At 48 hpf *foxi1* is expressed in the dorsal retina, CMZ, lens, otic vesicle and pharyngeal arches of WT fish (A, B), while in *gdf6a*$^{-/-}$ mutants *foxi1* expression is absent in the dorsal retina, reduced in the pharyngeal arches, and unchanged in the lens and otic vesicle (C, D). Expression of *foxi2* at 48hpf in WT embryos is in the ventral retinal and surrounding the choroid fissure (E, F), while in *gdf6a*$^{-/-}$ mutants it expands to the CMZ surrounding the lens with reduced expression also noted in the pharyngeal arches (G, H). *in situ* pictures were taken at 90X.

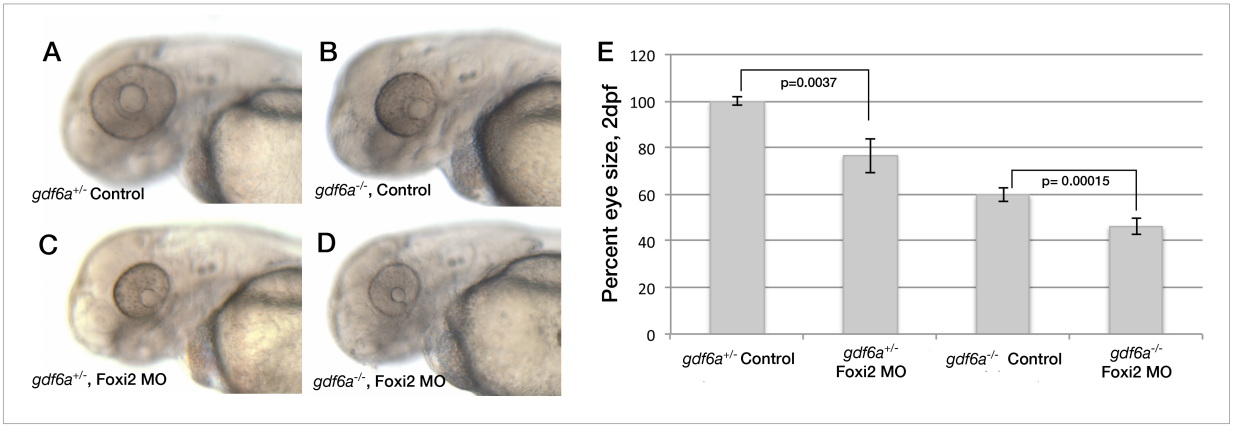

Figure 3-8: Loss of *foxi2* in *gdf6a*$^{+/-}$ fish results in microphthalmia.

Heterozygous (*gdf6a*$^{+/-}$) larvae have normal ocular size (A), in contrast to the microphthalmia evident in homozygous mutants (*gdf6a*$^{-/-}$) at 48hpf (B). Foxi2 morpholino injection into *gdf6a*$^{+/-}$ embryos results in *gdf6a*$^{+/-}$ larvae developing microphthalmic eyes [(C), n=15] almost indistinguishable from those of *gdf6a*$^{-/-}$ (B). Quantification of average eye size demonstrates that *gdf6a*$^{+/-}$ larvae injected with 4 ng of *foxi2*^{MO} have significantly smaller eyes than uninjected *gdf6a*$^{+/-}$ larvae [(E), μ=76.6% eye size, n=15, p=0.004, *t*-test]. Similarly, a reduction in the eye size of *gdf6a*$^{-/-}$ embryos is observed when compared to uninjected (D). Quantification of this change reveals significantly smaller eyes of *gdf6a*$^{-/-}$ larvae injected with *foxi2*^{MO} alone when compared with uninjected *gdf6a*$^{-/-}$ larvae [(E), μ= 77% of *gdf6a*$^{-/-}$ eye size, n=10 *gdf6a*$^{-/-}$; n=15 *gdf6a*$^{-/-}$ + Foxi2^{MO}, p=0.00014, *t*-test]. Graphical data are presented as mean ± standard error. Live pictures taken are at 90X.

3.3: Discussion

During zebrafish ocular development the neural retina is formed as progenitor cells exit the cell cycle and differentiate into populations of retinal neurons (CEPKO *et al.* 1996). Throughout the life of the fish, a population of self-renewing cells remains at the ciliary margin and adds new retinal neurons as the eye grows (WEHMAN *et al.* 2005; RAYMOND *et al.* 2006). We demonstrate that *gdf6a*, already known to initiate dorsal retina patterning and having a key role in lens development (FRENCH *et al.* 2009; GOSSE AND BAIER 2009), also regulates the cell cycle during retinal development. Parallels exist between the requirement of *gdf6a* for initiation of dorsal retina identity, and *gdf6a's* comparable role in specifying the dorsal identify of the CMZ. Notably, the CMZ has a polarized axis specified by *foxi1* and *foxi2*, with a requirement of *foxi2* in maintenance of ocular size in *gdf6a*$^{+/-}$ fish.

Mutations in *GDF6* result in microphthalmia, anophthalmia and coloboma, (ASAI-COAKWELL *et al.* 2007; ASAI-COAKWELL *et al.* 2009) phenotypes which are recapitulated in mouse, frog, and zebrafish model systems (HANEL AND HENSEY 2006; FRENCH *et al.* 2009; GOSSE AND BAIER 2009; DEN HOLLANDER *et al.* 2010). While the early role of *gdf6a* for dorsal retinal identity is well documented, few papers have addressed the mechanism underlying the small eye phenotype. Microphthalmia is observed as early as 24 hpf, and becomes more pronounced at later developmental stages. By 24 hpf, *gdf6a*$^{-/-}$ eyes contain less progenitor cells than their wild type or heterozygous counterparts, indicating a potential role for *gdf6a* in retinal precursor cell specification, or optic cup evagination as one facet of the microphthalmic phenotype. Consistent with this hypothesis, it has been shown that other Bmp ligands, such as Bmp2b, play a role in selecting the eye field from surrounding forebrain tissue (BIELEN AND HOUART 2012). Given *gdf6a's* expression adjacent to the early eye fields (FRENCH *et al.* 2009), it may also play a role in such processes.

The microphthalmia observed in *gdf6a* deficient zebrafish and *Xenopus* embryos has been attributed to increased levels of retinal apoptosis (HANEL AND HENSEY 2006; DEN HOLLANDER *et al.* 2010). Despite these reports, we found that inhibition of this apoptosis with P7C3, and anti-apoptotic compound thought to protect mitochondrial membrane integrity(PIEPER *et al.* 2010), does not rescue microphthalmia. Although incubation with this agent may have other effects on retinal cell development that were not tested, it is clearly able to inhibit retinal apoptosis with no associated increase in eye size. This lack of eye size rescue via incubation with P7C3 has also been observed up to 7 dpf (ASAI-COAKWELL *et al.* 2013). Although this result does not exclude an apoptotic contribution to the *gdf6a*$^{-/-}$ small eye phenotype, additional factors are clearly involved.

Increasing evidence supports a distinct role for *gdf6a* in regulating targets that control ocular proliferation during development. Indeed, there are significant alterations in the transcriptome after loss of *gdf6a* that are involved in cell cycle progression, such as *mcm3, pcna, myca, mycn* and *mych*. *MYC* genes have well documented roles in the regulation of proliferation in both normal and tumorigenic cells, and the *MYC* proto-oncogene is a known downstream target of the TGF-β signaling pathway (DANG 2012). *Myc* family members have previously implicated roles in ocular development, and are responsible for microphthalmic phenotypes seen in *meis1* mutant zebrafish, as *myca* expression is lost from the developing eye and co-injection of *c-myc* mRNA with *meis1* MO rescues cell cycle defects and eye size (BESSA *et al.* 2008). It has recently been demonstrated that knock-down of *hmx1* results in microphthalmia in part due to the failure of retinal progenitors to exit the cell cycle (BOISSET AND SCHORDERET 2012). Since *hmx1* is one of the most down-regulated genes on the microarray, it is likely that this may also contribute to *gdf6a*$^{-/-}$ induced microphthalmia. Similarly, *cad* expression is down regulated in *gdf6a* mutants, consistent with *cad* mutant phenotypes that involve small eyes and reduced retinal proliferation (WILLER *et al.* 2005). Taken together, our results indicate that Gdf6a regulates ocular

proliferation through multiple genetic pathways, similar to studies in mice where loss of Bmp receptors (*Bmpr1a* and *Bmpr1b*) affect eye size through multiple mechanisms(MURALI *et al.* 2005).

Although our data at 2 dpf accord with previous studies demonstrating no significant alteration in proliferation rates (DEN HOLLANDER *et al.* 2010), we observe a profound reduction in the number and proportion of proliferating cells at 4 dpf in the CMZ. From such findings, we conclude that the microphthalmia in *gdf6a*$^{-/-}$ larvae is due in part to significant decreased ocular proliferation. Although Gdf6a has been shown to regulate processes specifically in the dorsal retina (FRENCH *et al.* 2009; GOSSE AND BAIER 2009), the decrease in proliferation is uniform across the dorsal ventral axis. In addition, *gdf6a*$^{-/-}$ eyes are clearly smaller that their wild type siblings at earlier stages such as 24 hpf, and contain fewer progenitor cells, suggesting that specification of progenitors, or migration within the optic cup may influence early eye size in these animals. Apoptosis does not appear to have a major role in the induction of microphthalmia in *gdf6a* mutants as rescuing apoptosis does not significantly improve eye size; however, the possibility that cells that fail to progress through the cell cycle undergo apoptosis (at stages not tested), remains to be explored. We also cannot rule out other processes such as eye patterning and neural differentiation as contributing to *gdf6a*$^{-/-}$ induced microphthalmia, as Gdf6a is clearly involved in such processes.

The forkhead box transcription factors *foxi1* and *foxi2* are present at 28 hpf in WT embryos in multiple sites including the dorsal and ventral CMZ, respectively, otic vesicle and pharyngeal arches. Zebrafish *foxi1* has a key role in otic placode formation and jaw development through maintenance of survival of neural crest cell populations (HULANDER *et al.* 1998; NISSEN *et al.* 2003; SOLOMON *et al.* 2003a; OHYAMA AND GROVES 2004). Full elucidation of the developmental roles of *foxi2* has yet to occur; expression in the mouse neural retinal layer has been described,

and *Xenopus* Foxi2 was recently shown to be required for activation of Foxi1e, critical for subsequent ectodermal gene expression (WIJCHERS *et al.* 2005; CHA *et al.* 2012). *gdf6a*$^{-/-}$ embryos have significant alterations in ocular expression of *foxi1* and *foxi2*, as *foxi1* is lost from the dorsal CMZ and *foxi2* expands to encompass both the ventral and dorsal CMZ. The highly specific expression pattern of these transcription factors, coupled with loss of *foxi1* when dorsal retinal identity is not initiated, suggests that the CMZ has similar dorsal-ventral patterning to the retina. We are not aware of previous reports of CMZ patterning and cellular identity, which implies that stem cells in these areas may have differential proliferative or inductive potential. With *foxi1's* known role in maintenance of neural crest cell survival, and roles of other *fox's* in cell cycle control (OHYAMA AND GROVES 2004; TENG *et al.* 2008; KOO *et al.* 2012), we hypothesized that both *foxi1* and *foxi2* have a role in regulation of cell cycle progression in the CMZ and consequent ocular size. We examined possible anomalies in ocular proliferation and apoptosis in the previously described *foo* mutant (*foxi1*^{hi3747Tg}) (AMSTERDAM *et al.* 1999) that contains a retrovirus-induced mutation, and observed no changes in ocular size and proliferation (data not shown). It is possible that *foxi1* has redundant roles with *gdf6a* and other dorsal genes. Alternatively, expansion of *foxi2* expression may compensate for loss of *foxi1*. If the latter is correct, then loss of *foxi2* should increasingly result is reduced eye size in *gdf6a* mutants. This is indeed the case as transient knockdown of *foxi2* coupled with loss of one functional copy of *gdf6a* results in the occurrence of microphthalmia, revealing a novel requirement for this gene in controlling ocular size. The further reduction of eye size in *gdf6a* homozygous mutants injected with Foxi2 morpholino, compared to that of homozygous mutants alone, further supports our hypothesis of a compensatory role of *foxi2* in the determination of eye size in *gdf6a* mutants. Of great interest for the future is elucidation of developmental roles of *foxi2* and its transcriptional targets in the eye, as there is currently a lack in literature on this topic.

In summary, we have shown that central to microphthalmia in *gdf6a*$^{-/-}$ larvae is the reduction in ocular proliferation during development, due to significant changes in expression of genes responsible for cell cycle progression in the eye. Gdf6a induced ocular apoptosis does not appear to have a primary role in the determination of eye size, since inhibition does not rescue microphthalmia. Lastly, we have demonstrated that the CMZ has dorsal-ventral identity specified by *foxi1* and *foxi2*, with *foxi2* having a role in the control of ocular size.

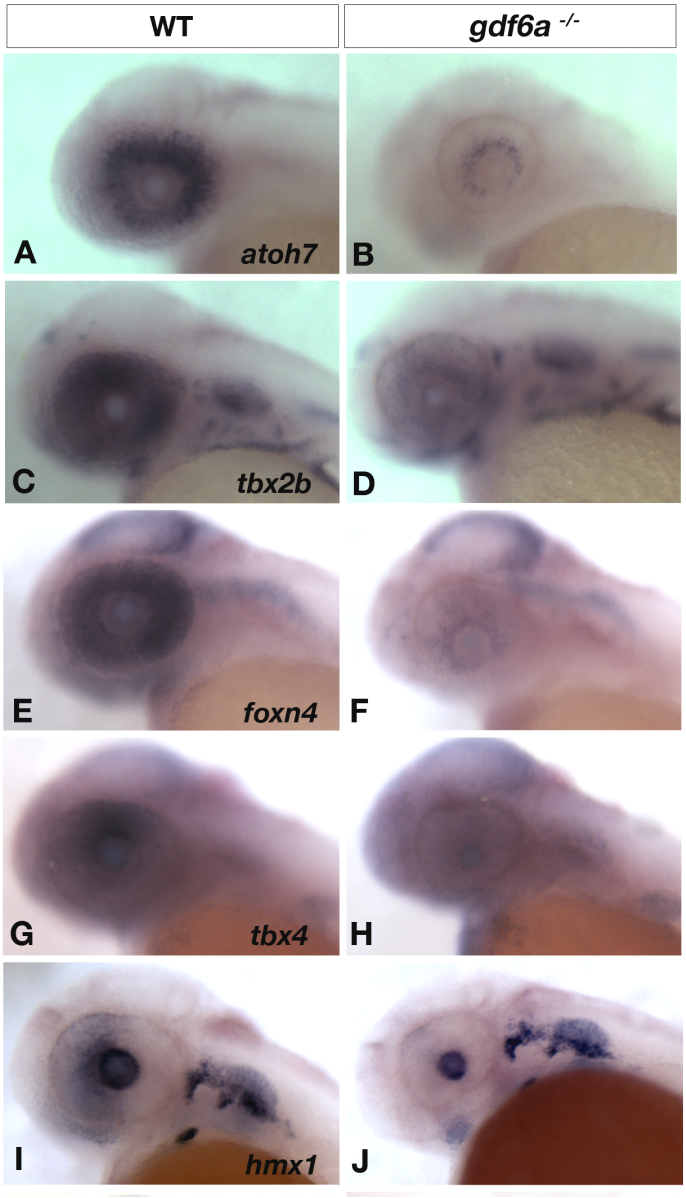

Figure 3-9. Microarray validation.

Atoh7, tbx2b and *foxn4* are expressed at high levels throughout the eye (A, C, E), but are highly down-regulated in *gdf6a*$^{-/-}$ eyes (B, D, F). *tbx4* expression is highest in the dorsal retina in WT (G) and lost in *gdf6a*$^{-/-}$ (H). *hmx1* is expressed in the nasal retina, lens and pharyngeal arches in WT (I), and expression is lost in *gdf6a*$^{-/-}$ mutant retina (J). All embryos are 2 dpf. *In situ* pictures are taken at 90X.

Chapter 4

Investigating the Roles of *foxi1* and *foxi2* in Ocular Patterning and Development

4.1: Introduction

Foxi1 and *foxi2* appear to be key players in ocular development based on their unique, polarized expression patterns of the CMZ in the dorsal and ventral retina, respectively, with this localization having implications in retinal patterning and control of ocular size. FOX transcription factors have a critical role in a number of ocular developmental processes, as illustrated by the range of ocular disease in patients with coding anomalies, chromosomal translocations and dosage alterations. For example, patients with duplication or deletion of the *FOXC1* locus have disorders of the anterior segment such as glaucoma, iris hypoplasia, and Axenfeld-Rieger syndrome (NISHIMURA *et al.* 1998; LEHMANN *et al.* 2000; MIRZAYANS *et al.* 2000), and anterior segment anomalies can also occur if *FOXC2, FOXL2* or *FOXE3* are affected. The importance of the FOX family is further emphasized through evolutionary conservation, with similar developmental roles and ocular phenotypes present in murine and zebrafish models (SMITH *et al.* 2000; LEHMANN *et al.* 2003; SKARIE AND LINK 2009; SEO *et al.* 2012), and a requirement of *FOX* genes for ocular patterning and establishment of the retinotectal map (YUASA *et al.* 1996; HERRERA *et al.* 2004; PRATT *et al.* 2004; TIAN *et al.* 2008; CARRERES *et al.* 2011).

However, descriptions of *foxi1* and *foxi2* in eye development remain minimal. In zebrafish and mouse, *foxi1* is required for the development of the jaw and otic placode by maintaining the survival of neural crest cells (NCCs) (HULANDER *et al.* 1998; NISSEN *et al.* 2003; SOLOMON *et al.* 2003a; OHYAMA AND GROVES 2004). In humans, *FOXI1* (*FKHL10)* has been found to be expressed in fetal and adult kidney (LARSSON *et al.* 1995) and has been implicated in Pendred Syndrome (HULANDER *et al.* 2003; YANG *et al.* 2007). Neural retina expression in mice has been described for *Foxi2 (WIJCHERS et al. 2005)*, along with expression in developing chick pharyngeal arches (KHATRI AND GROVES 2013), and altered methylation of *FOXI2* in cancer cell lines (MITCHELL *et al.* 2014). A number of these functions for *foxi1* and *foxi2* are in keeping with

the classification of some FOX transcription factors as tumor suppressors and oncogenes, with roles in cell cycle and cell fate (MYATT AND LAM 2007), suggesting that irregular tissue growth phenotypes, such as MAC in *gdf6a*$^{-/-}$ fish, could be due to aberrant expression of *foxi1* and *foxi2*.

Based on ocular expression patterns of *foxi1* and *foxi2*, the respective down- (2.20 fold) and up- (1.97 fold) regulation in *gdf6a* mutant eyes at 2 dpf determined by microarray analysis, similar spatial and temporal locations of *foxi1* and *gdf6a,* and the fact that *foxi2* and *gdf6a* lie on converging pathways for determining ocular size, we propose that these transcription factors are critical for ocular growth and patterning.

4.2: Results

foxi1 and *foxi2* are expressed in the dorsal and ventral retina, respectively, during development

To determine the ocular expression patterns of *foxi1* and *foxi2,* I performed ISH on WT embryos from the 13 somite stage (~16 hpf), before optic cup invagination and neural retina formation (SCHMITT AND DOWLING 1994), to 48 hpf, when the retina has undergone lamination (SCHMITT AND DOWLING 1999). At both 13 and 16 somites, *foxi1* is expressed in presumptive neural crest cells located in the area of the developing hindbrain (Figure 4-1 A, B, C, D). At 24 hpf, *foxi1* is expressed in both the dorsal retina and branchial arches (Figure 4-1 E), and at 48 hpf *foxi1* expands to the pharyngeal pouches and dorsal portion of the otic vesicle (destined to form the ear), while retinal expression has become confined to the dorsal CMZ (Figure 4-1 F). Contrary to *foxi1, foxi2* is expressed early in the developing eye at 13 and 16 somites in the presumptive ventral retina, which at this stage is the anterior portion of the eye during the course of ocular rotation (Figure 4-1 G, H). At 24 hpf *foxi2* transcripts are strongly localized to the ventral retina, with expression on opposing sides of the open choroidal fissure, and in the branchial arches (Figure 4-1 I). At 48 hpf, *foxi2* ocular expression becomes the mirror image to that of *foxi1* in the dorsal retina, with *foxi2* in the ventral CMZ, and branchial arch expression remaining (Figure 4-

1 J). The parallel expression patterns of *foxi1* and *foxi2* in the CMZ, coupled with the identical expression patterns of *foxi1* and *gdf6a* at 48 hpf, led us to suspect a role for these transcription factors in ocular cell cycle and patterning.

Morpholino inhibition of *foxi1* results in microphthalmia, coloboma, and an alteration in dorsal-ventral retinal patterning

We hypothesized that *foxi1* is downstream of *gdf6a* and would thus be required for ocular growth and patterning based on the CMZ expression pattern of *foxi1* at 48 hpf, and absence of expression in *gdf6a*$^{-/-}$ embryos (Figure 3-7) (FRENCH *et al.* 2013). To discern the role of *foxi1* in the eye, I injected 2 ng of *foxi1* with 1 ng of *p53* MO to offset any non-specific MO phenotypes (EISEN AND SMITH 2008), and assayed for changes in gene expression and eye morphology at 48 hpf. For dorsal ocular patterning, I analyzed expression of *gdf6a, tbx5*, *aldh1a2,* and for ventral patterning, *vax2, foxi2* and *ephb2*. For *gdf6a* expression, my purpose was to discern if there is feedback signaling in place, with an increase in *gdf6a* expression after the loss of *foxi1*, which could be a major downstream effector of *gdf6a*. Analysis of the major dorsal and ventral ocular patterning genes would support a role for *foxi1* in maintenance of dorsal eye patterning. Knockdown of *foxi1* in WT embryos resulted in increased expression of *gdf6a* and *tbx5* (Figure 4-2: A, B, C, D, E & F) and no obvious change in the expression of *aldh1a2* (Figure 4-2: G, H). An increase in expression of key dorsal patterning genes after knockdown of *foxi1* suggests that *foxi1* may also be an effector at the at the top of this pathway, and that there is a feedback loop in place for maintenance of the dorsal patterning domain. With regard to ventral genes, the loss of *foxi1* results in an increase in *vax2* and *foxi2* (Figure 4-3: A, B, C, D, E, F), and no change in *ephb2* expression at 48 hpf (Figure 4-3: G, H), indicating that loss of *foxi1* disrupts dorsal-ventral retinal patterning.

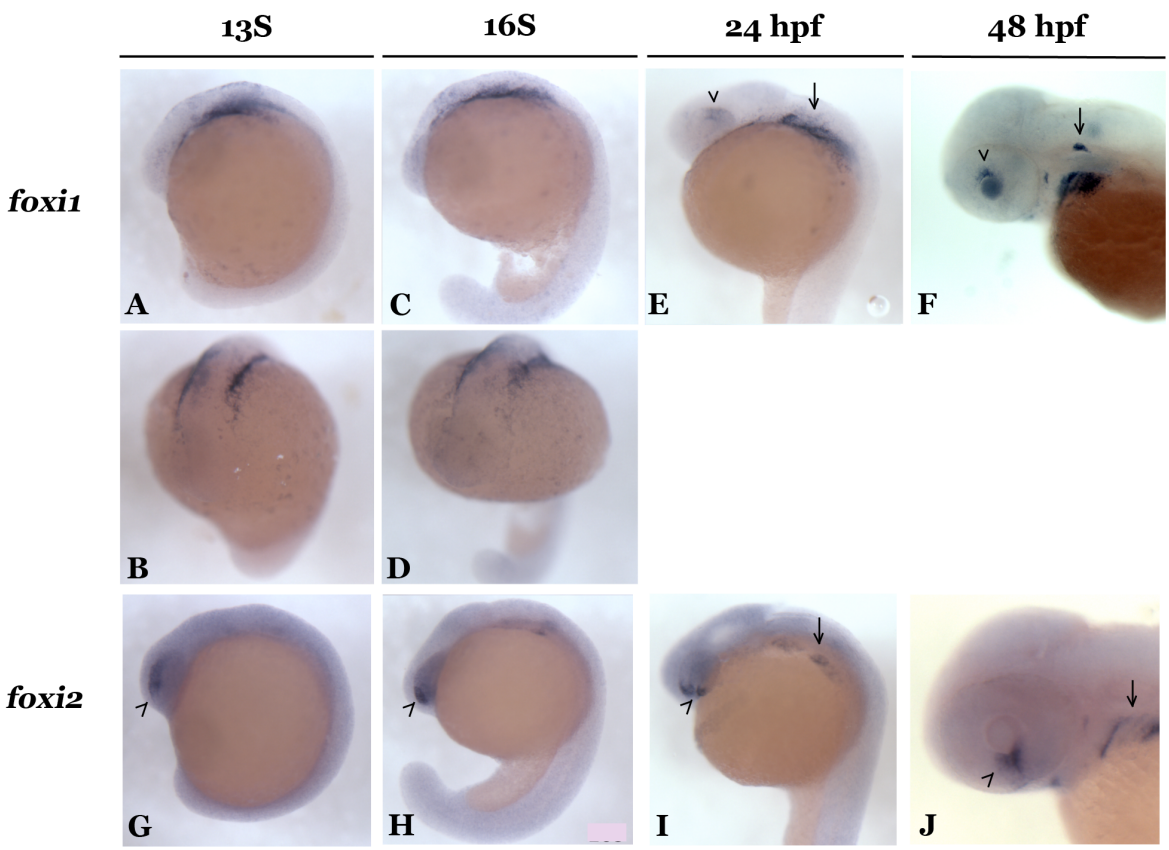

Figure 4-1: Time course expression of *foxi1* and *foxi2*.

foxi1 is expressed in presumptive neural crest cells in the hindbrain area at 13 somites [A (lateral view), B (frontal view)] and 16 somites [C (lateral view, D (frontal view)]. At 24 hpf, *foxi1* is present in the dorsal retina (arrowhead) and branchial arches (arrow) (E), and by 48 hpf, ocular *foxi1* expression has become restricted to the dorsal ciliary marginal zone (arrowhead), and remains in the branchial arches, pharyngeal pouches, and the dorsal part of the otic vesicle (arrow) (F). At 13 somites, *foxi2* is expressed anteriorly in the presumptive ventral retina (arrowhead) prior to the full rotation of the developing eye (G), with its ventral retinal localization (arrowhead) apparent by 16 somites (H). At 24 hpf, *foxi2* transcripts are on opposing sides of the closing choroid fissure (arrowhead) and in the branchial arches (arrow) (I), and at 48 hpf *foxi2* is expressed in the ventral ciliary marginal zone (arrowhead) and area of the closing choroid fissure, as well as in the pharyngeal pouches (arrow) (J).

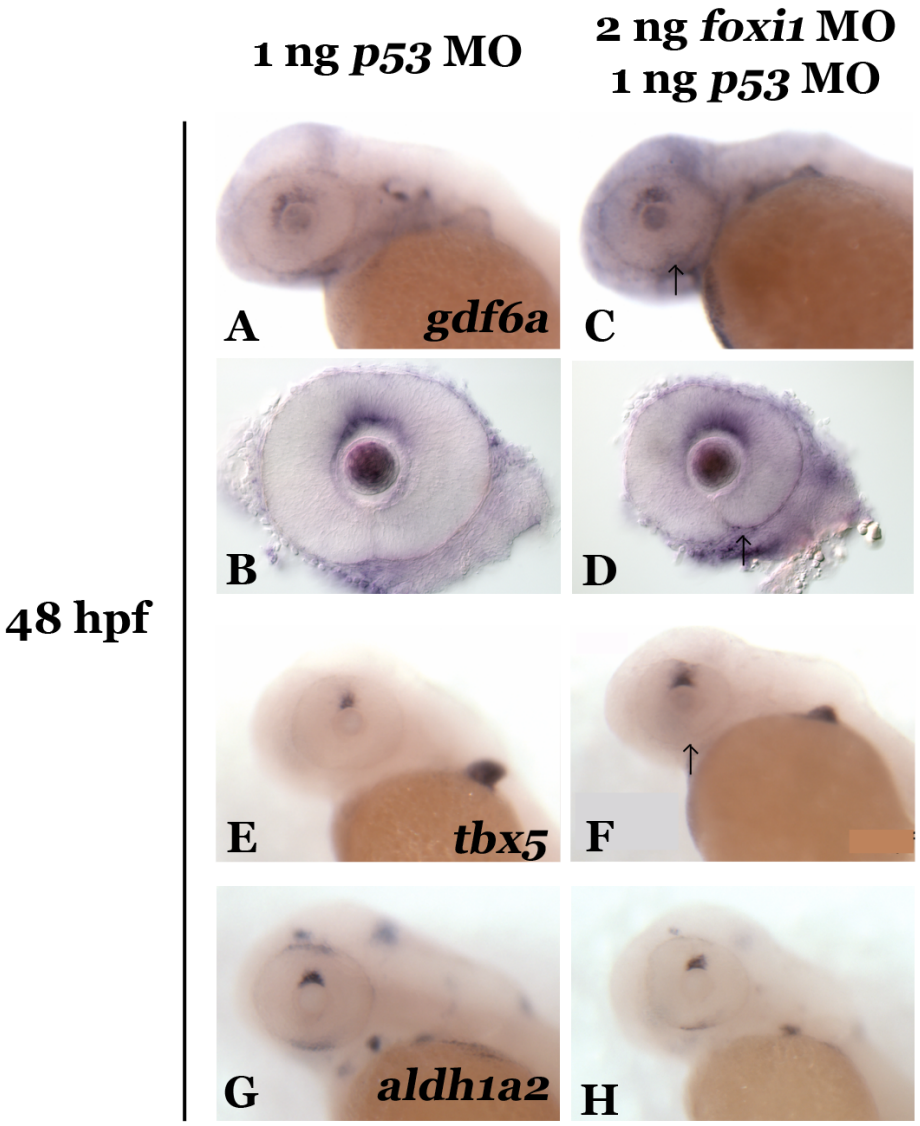

Figure 4-2: Knockdown of *foxi1* increases expression of select dorsal retinal markers and results in microphthalmia and coloboma.

Knockdown of *foxi1* results in an increase in dorsal retinal expression of *gdf6a* (A, B, C, D) and *tbx5* (E, F), and no obvious change in the expression of *aldh1a2* at 48 hpf (G, H), and causes microphthalmia and coloboma (D, F, H black arrows). All morphant embryos were staged to correct for delay in development.

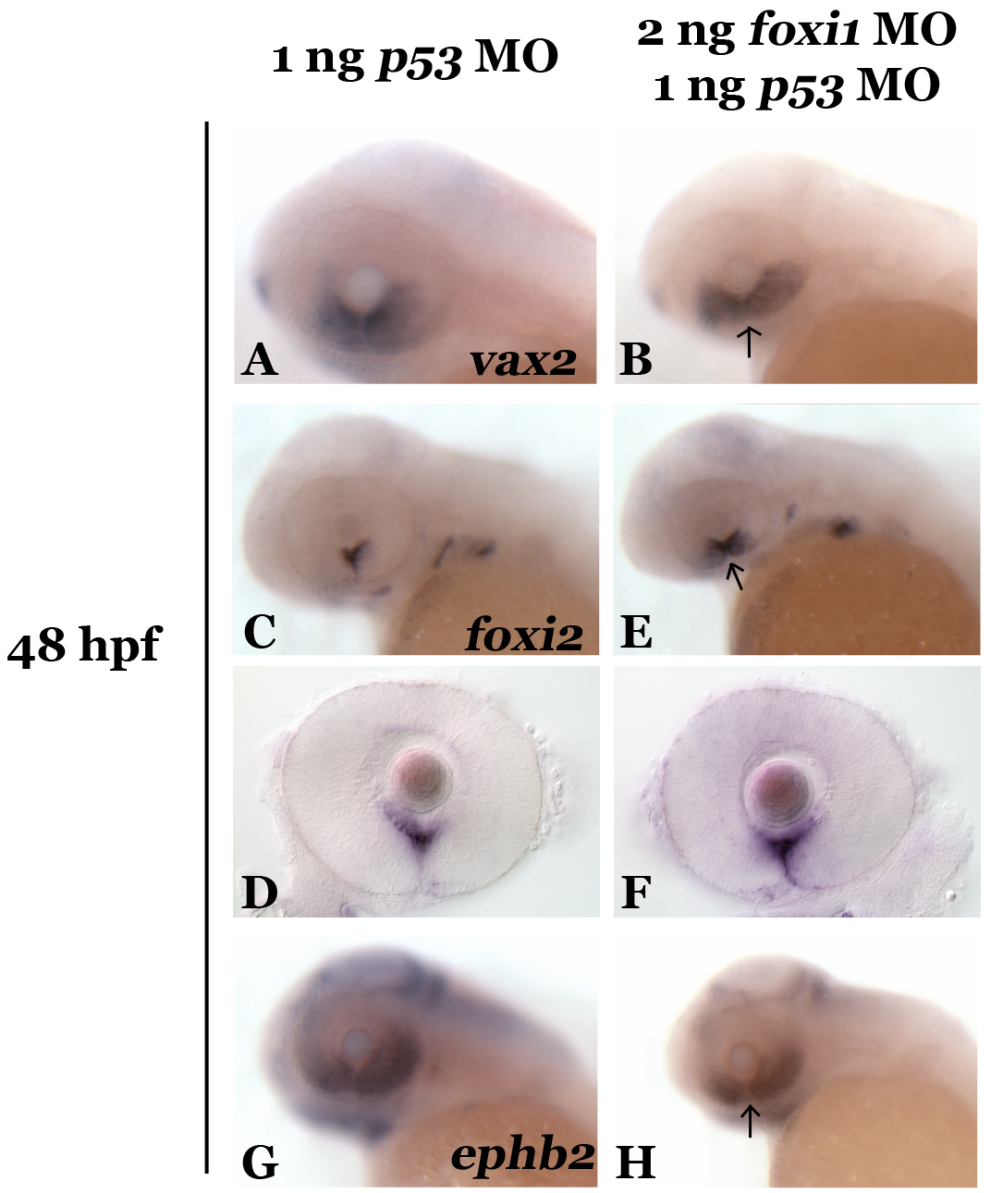

Figure 4-3: Knockdown of *foxi1* results in increased expression of select ventral retinal markers along with microphthalmia and coloboma.

Morpholino knockdown of *foxi1* results in increased ventral retinal expression of *vax2* (A, B) and *foxi2* (C, D, E, F), and no change in *ephb2* expression (G, H) at 48 hpf, and results in microphthalmia and coloboma. All morphant embryos were staged to correct for delay in development.

Additionally, knockdown of *foxi1* results in microphthalmia and coloboma at 48 hpf (Figure 4-2: C, D, F, H, Figure 4-3: B, E, F, H, black arrows), suggesting a role for *foxi1* in ocular cell cycle, and prompting our acquiring the *foo* line for analysis of changes in apoptosis and proliferation in *foxi1*$^{-/-}$ embryos and larvae, and to further discern the role of *foxi1* in retinal patterning.

foxi1$^{-/-}$ embryos and larvae lack apparent ocular phenotypes

To further elucidate the requirement for *foxi1* during ocular development, I used the previously described *foo* mutant (*foxi1*^{hi3747Tg} or *foxi1*$^{-/-}$) line (AMSTERDAM *et al.* 1999), which has a mutagenic proviral integration at the 5' end of the gene, which results in protein truncation before the forkhead box DNA binding domain (NISSEN *et al.* 2003). My goal was to further test and validate my previous findings of anomalies in retinal patterning, and to characterize any aberrations in ocular cell cycle resulting from the loss of *foxi1* that may be causing microphthalmia and coloboma. Many forkhead box transcription factors have roles in cell cycle regulation (LAM *et al.* 2013), and *foxi1* is thought to be required for proliferation and survival cues to NCCs (NISSEN *et al.* 2003). However, based on the preliminary findings outlined here, *foxi1*$^{-/-}$ embryos at 48 hpf and larvae at 72 hpf and 5 dpf appear to have no obvious gross eye morphological defects (Figure 4-4 A, B, C, D, E, F), no differences in ocular proliferation at 24 hpf (Figure 4-5 A, B), and no changes in ocular apoptosis at 72 hpf (Figure 4-5 C, D). Additionally, preliminary analysis of retinal gene expression in *foxi1*$^{-/-}$ embryos at 28 and 48 hpf showed no changes (data not shown), contrary to the aforementioned results obtained using *foxi1* MO. Lack of ocular phenotypes in *foxi1*$^{-/-}$ could be due to redundancy in function of *foxi1* with other ocular genes, such as *gdf6a,* or its ventral counterpart, *foxi2,* as there is an increase in *foxi2* expression in *foxi1* morphants (Figure 4-3 C, E). To determine if upregulation of *foxi2* is compensating for a loss of *foxi1*, I injected *foxi2* MO at 1, 2 and 4 ng into WT and *foxi1*$^{-/-}$ embryos, and found that loss of *foxi2* alone does not result in any gross morphological ocular

phenotypes (Figure 4-6 A, B, C, D), but in conjunction with the loss of *foxi1*, results in coloboma at 48 hpf (Figure 4-6 E, F, G, H). This suggests that lack of ocular phenotypes in *foxi1*$^{-/-}$ embryos and larvae may be, in part, attributable to compensation by other genes.

Morpholino knockdown of *foxi2* alters dorsal-ventral retinal gene expression and may result in microphthalmia

Based on the mirror CMZ expression patterns of *foxi1* and *foxi2* (Figure 3-7 A, B, E, F), the expansion of *foxi2* to the entire CMZ in *gdf6a*$^{-/-}$ embryos (Figure 3-7 E, F, G, H), and the requirement of *foxi2* in *gdf6a* heterozygous and mutant embryos for reduced ocular size (Figure 3-8), I investigated the role of *foxi2* in ocular development by MO knockdown. Similar to the analysis of gene expression after knockdown of *foxi1,* I analyzed expression of *gdf6a, tbx5, foxi1* and *aldh1a2* in the dorsal eye, and *vax2, aldh1a3* and *ephb2* in the ventral eye after knockdown of *foxi2*. Alteration in expression pattern of these genes would provide insights into the role of *foxi2* in initiation and maintenance of ocular patterning. Additionally, I performed analysis on the nasal retinal marker, *foxg1a*, to determine if *foxi2* has a role in pattering the nasal and temporal quadrants of the eye. In the dorsal eye, loss of *foxi2* has no effect on *gdf6a* expression at 48 hpf (Figure 4-7 A, B) or *tbx5* expression at 28 hpf (Figure 4-7 C, D). However, *tbx5* expression is affected at 48 hpf with significant expansion in the dorsal retina (Figure 4-7 E, F). Knockdown of *foxi2* also results in an increase in *foxi1* expression in the retina at 48 hpf (Figure 4-7 G, H), and there is an increase in ocular *aldh1a2* expression at 28 hpf (Figure 4-7 I, J, K, L). In the ventral eye, loss of *foxi2* results in an expansion of retinal *vax2* expression at 28 hpf (Figure 4-8 A, B) and 48 hpf, along with an increase in optic stalk and pineal gland expression at 48 hpf (Figure 4-8 C, D, E, F). Conversely, the loss of *foxi2* results in a decrease in *aldh1a3* ocular expression at 28 hpf (Figure 4-8 G, H, I, J), and has no effect on *ephb2* expression at 28 hpf (Figure 4-8 K, L), or on the nasal retinal marker, *foxg1a,* at 48 hpf (Figure 4-8 M, N). Based on aberrant retinal patterning that occurs after knockdown of *foxi2,* there may be a requirement for this transcription factor in the maintenance of the ventral retinal patterning domain.

Additionally, *foxi2* appears to have a role in ocular cell cycle during development, as *foxi2* morphants display microphthalmia with partial penetrance at 48 hpf (Figure 4-7 G, I & Figure 4-8 F, G), *foxi2* is expressed in the CMZ, and there is increasing severity of microphthalmia in *gdf6a* heterozygous and mutant embryos after loss of *foxi2*.

4.3: Discussion

In this chapter, I have conducted an analysis of the roles that *foxi1* and *foxi2* have in the determination of ocular size and patterning. Transient knockdown of *foxi1* using MO technology results in both morphogenic and patterning defects; however, recapitulation of these experiments using *foo*$^{-/-}$ embryos shows no ocular phenotypes. Non-specific MO phenotypes could be the cause of the previously observed phenotypes, or there could be compensation by the embryo for the loss of *foxi1* in *foo* mutants. Indeed, knockdown of *foxi2* in *foxi1*$^{-/-}$ embryos results in coloboma, suggesting redundancy in gene function. In addition for a requirement of *foxi2* for ocular growth, as knockdown of *foxi2* in WT fish results in partially penetrant microphthalmia, *foxi2* also appears to have a role in ocular patterning, with loss resulting in aberrant expression of dorsal and ventral markers.

The expression pattern of *foxi1* from 13 somites to 48 hpf is in agreement with previous studies in zebrafish (NISSEN *et al.* 2003; SOLOMON *et al.* 2003a; SPRAGUE *et al.* 2003; THISSE AND THISSE 2008). However, most of these studies pertain to *foxi1*'s early role in the formation of the otic vesicle, epibranchial placodes and jaw. With the exception of large-scale genomic screen data (SPRAGUE *et al.* 2003; THISSE AND THISSE 2008), this work is the first characterization of the later expression patterns of *foxi1* and its role during ocular development. Based on spatio-temporal retinal patterning and absence of ocular expression in *gdf6a*$^{-/-}$ embryos, it appeared that *foxi1* has a role downstream of *gdf6a* for maintenance of dorsal retinal identity

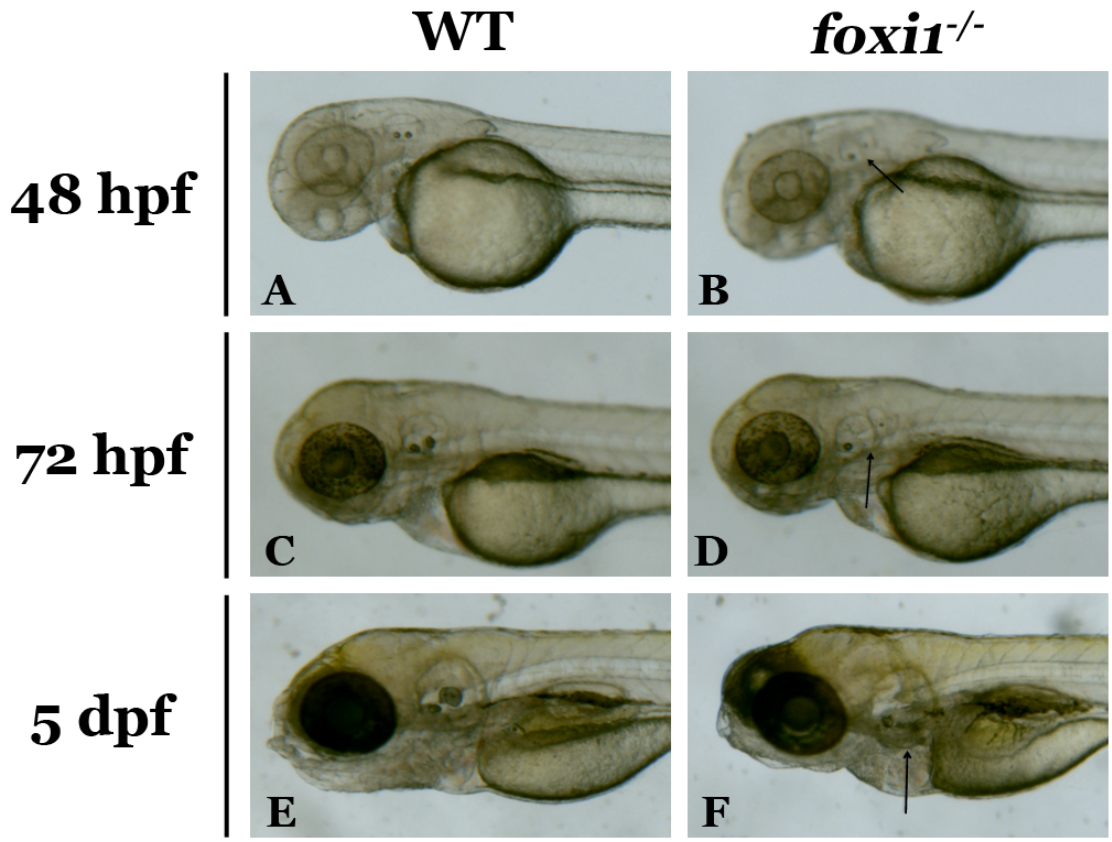

Figure 4-4: *foxi1*$^{-/-}$ *(foo)* mutant fish lack apparent ocular phenotypes.

As compared to WT fish at 48 hpf, 72 hpf and 5 dpf (A, C & E, respectively), *foxi1*^{hi3747Tg} larvae at 48 hpf, 72 hpf and 5 dpf have split and aberrantly developed otic vesicles (black arrows), but lack any obvious gross ocular phenotypes (B, D & F, respectively).

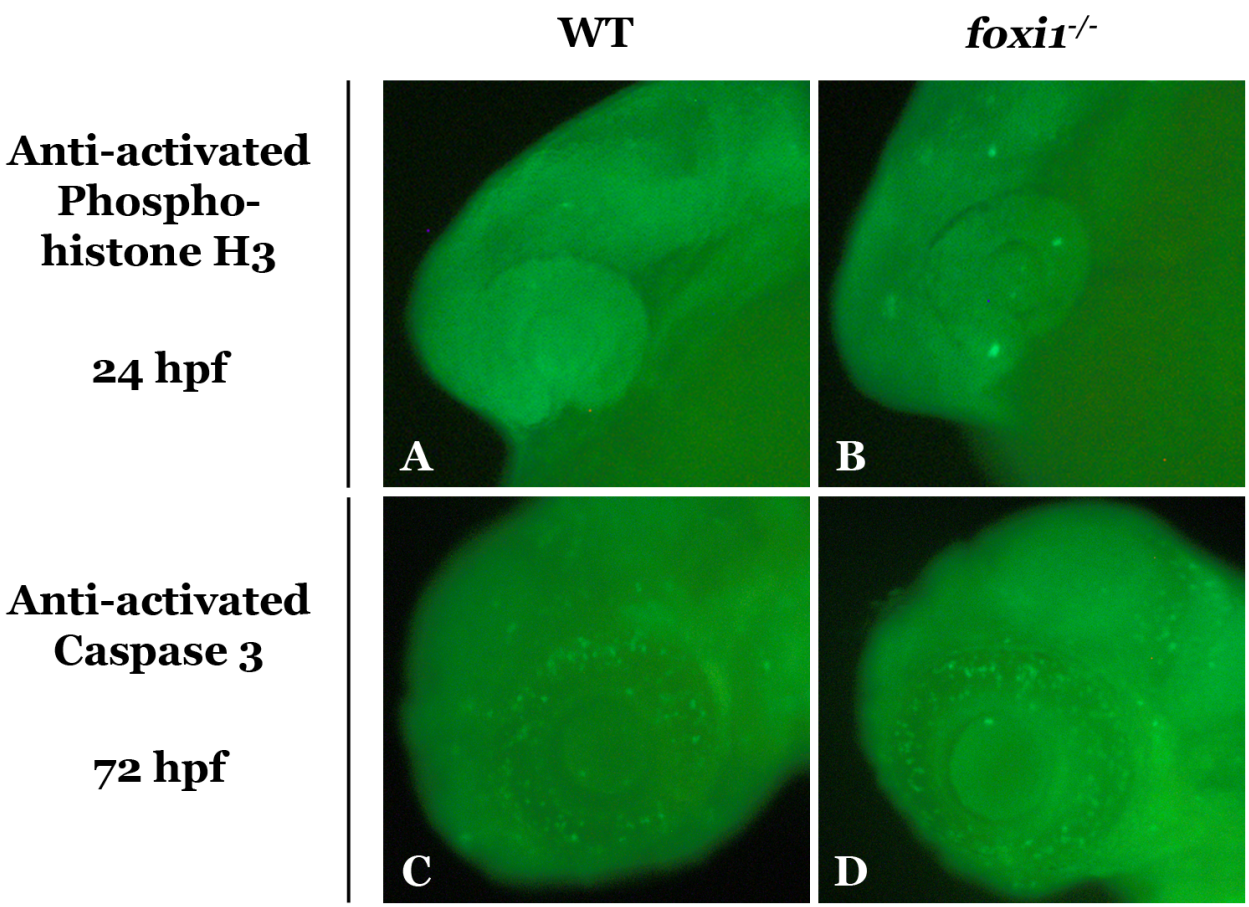

Figure 4-5: *foo* mutant fish do not have any obvious changes in ocular proliferation or apoptosis during development.

In this preliminary investigation, visualization of activated phosphohistone H3 at 24 hpf by immunohistochemistry shows no difference in ocular proliferation between WT and *foxi1*$^{-/-}$ embryos (A, B, n=1 biological replicates, n=4 technical replicates), while immunohistochemistry at 72 hpf for activated Caspase 3 shows no difference in ocular apoptosis (C, D, n=1 biological replicates, n=4 technical replicates).

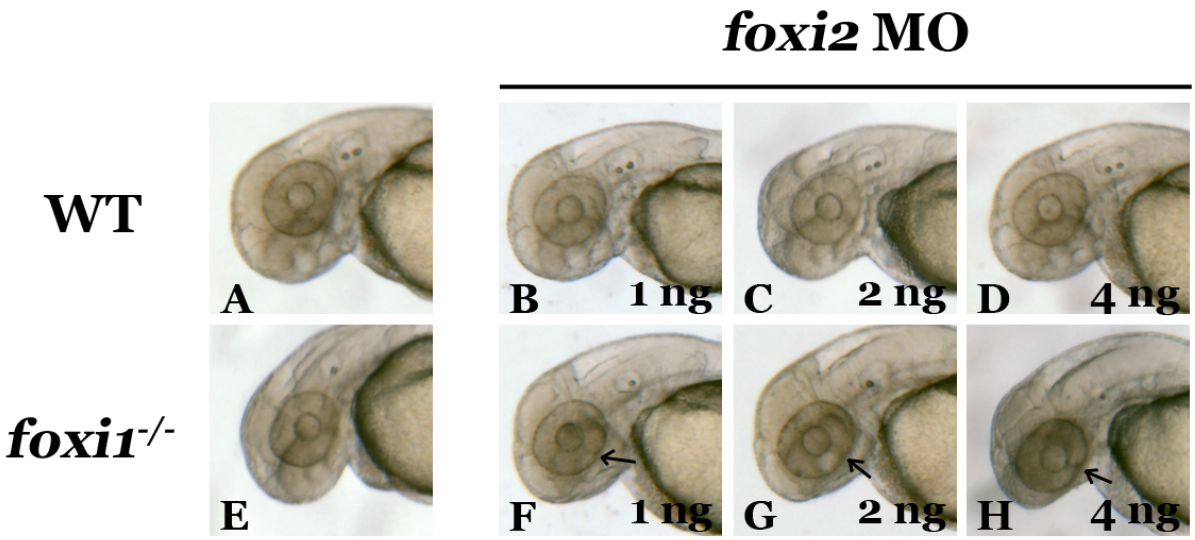

Figure 4-6: Knockdown of *foxi2* in *foo*$^{-/-}$ embryos results in coloboma.

Injection of *foxi2* MO into WT fish at 1, 2 and 4 ng does not result in any gross morphogenic ocular phenotypes at 48 hpf (A, B, C, D), while injection of 1, 2 and 4 ng of *foxi2* MO into *foxi1*$^{-/-}$ embryos results in coloboma (E, F, G, H, black arrows). n=1 biological replicates.

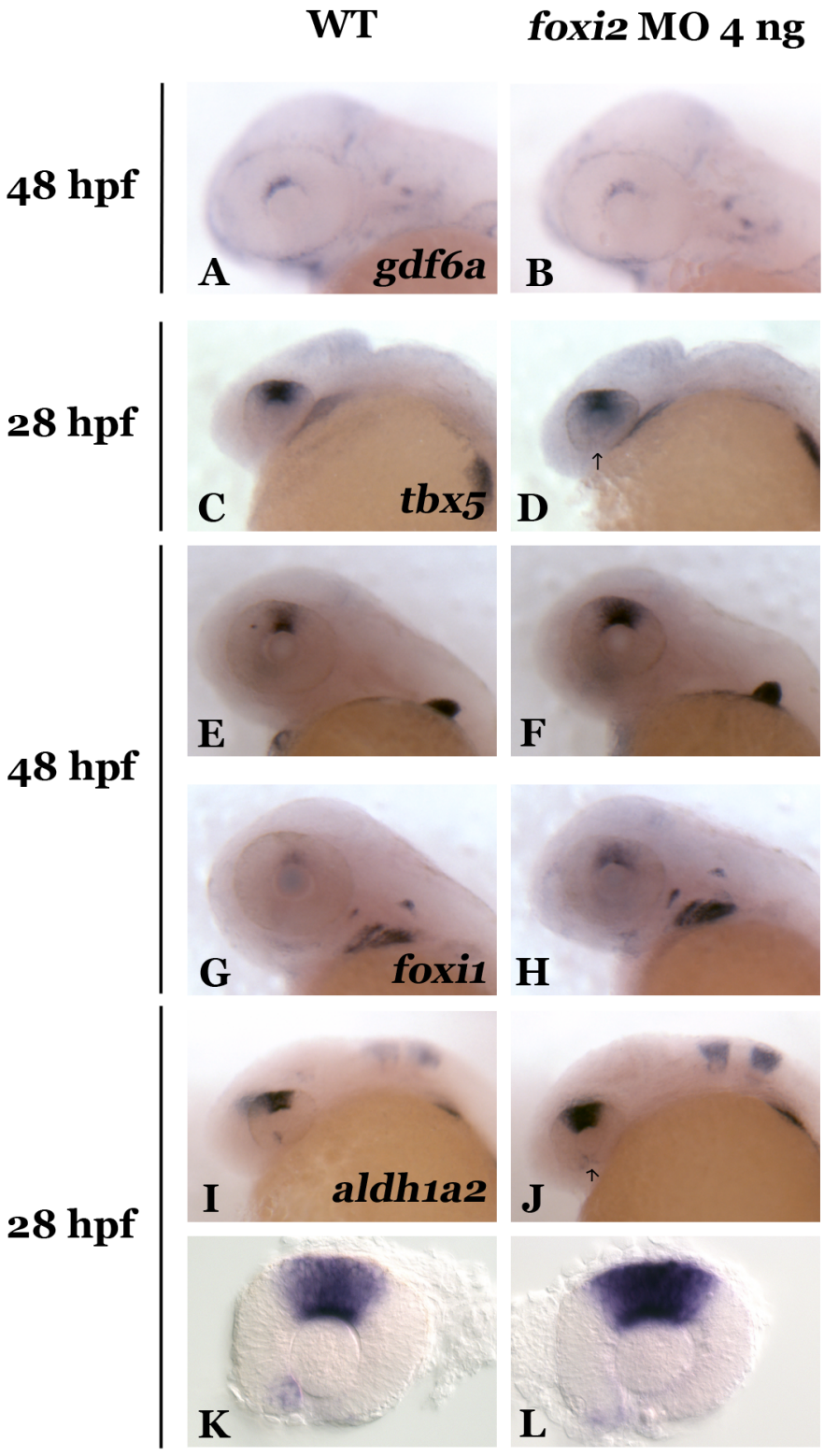
WT
foxi2 MO 4 ng
48 hpf
A
gdf6a
B
28 hpf
C
tbx5
D
48 hpf
E
F
G
foxi1
H
28 hpf
I
aldh1a2
J
K
L

Figure 4-7: Knockdown of *foxi2* affects dorsal retinal gene expression downstream of *gdf6a*.

In *foxi2* morphants at 48 hpf, *gdf6a* expression remains unchanged (A, B), as does *tbx5* at 28 hpf (C, D), while at 48 hpf, *tbx5* expression in the dorsal retina is expanded (E, F), along with *foxi1* expression (G, H), and morphants show a partially penetrant coloboma phenotype at 48 hpf (D, J, arrows). *aldh1a2* expression in the dorsal retina expansions after upon knockdown of *foxi2* at 28 hpf (I, J, K, L).

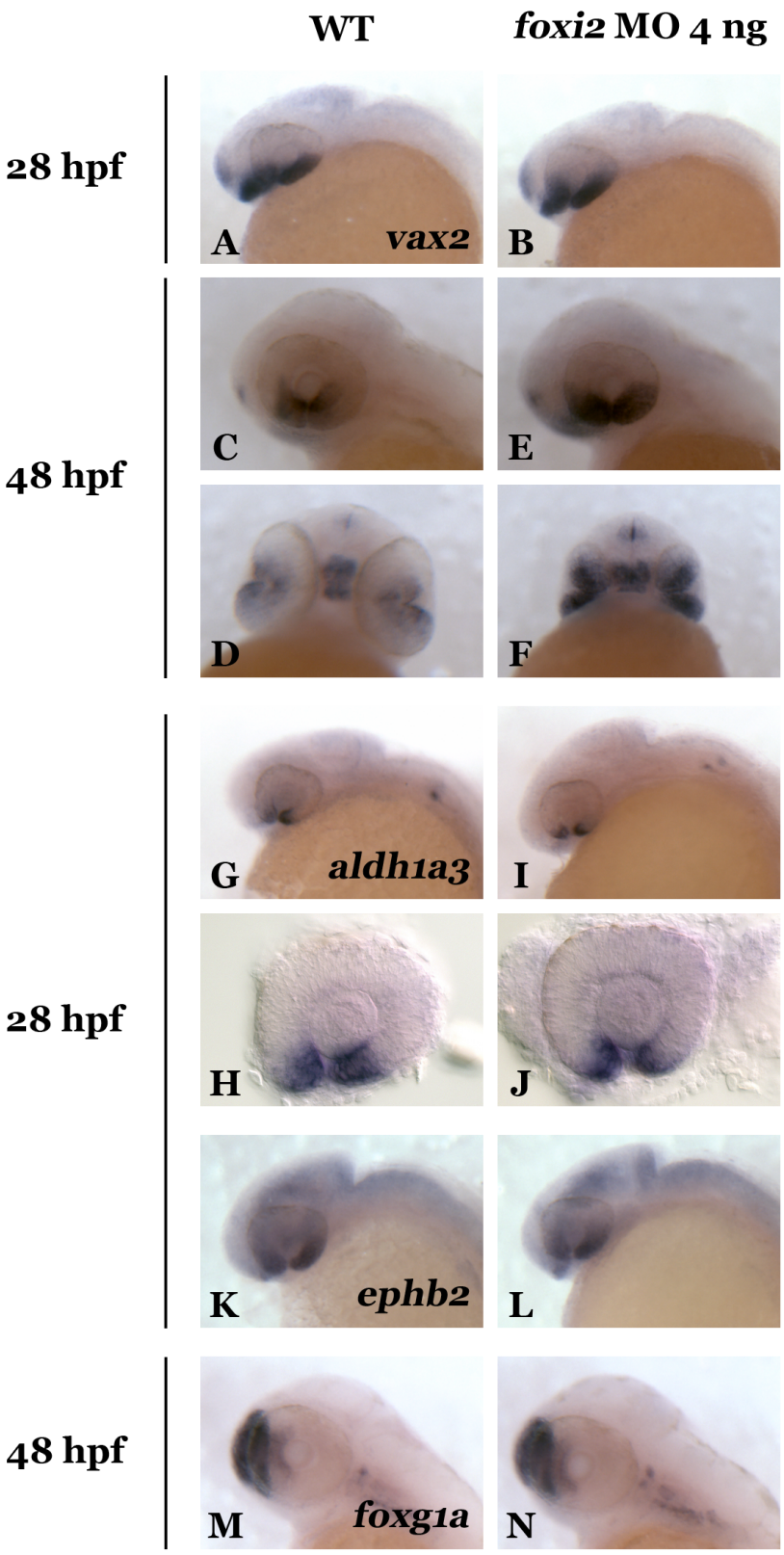
WT
foxi2 MO 4 ng
28 hpf
48 hpf
28 hpf
48 hpf
A
vax2
B
C
E
D
F
G
aldh1a3
I
H
J
K
ephb2
L
M
foxg1a
N

Figure 4-8: Knockdown of *foxi2* affects select ventral retinal genes, and does not affect expression of a nasal retinal marker.

Injection of 4 ng of *foxi2* MO results in increased retinal *vax2* expression at 28 hpf (A, B), and increased retinal, optic stalk and pineal gland expression at 48 hpf, and microphthalmia (C, D, E, F). Additionally, the loss of *foxi2* results in decreased *aldh1a3* retinal expression at 28 hpf (H, I, J, K), no change in *ephb2* expression at 28 hpf (L, M), and no change in *foxi2* expression at 48 hpf (N, O).

and ocular growth. However, only the decrease in *aldh1a2* expression is in agreement with previous studies documenting the change in dorsal retinal patterning after loss of *gdf6a* (FRENCH *et al.* 2009; GOSSE AND BAIER 2009), whereas *tbx5*, a major transcription factor in dorsal identity, and *gdf6a*, are increased in *foxi1* morphants. Possibly, *foxi1* is downstream of both *gdf6a* and *tbx5* and has a role in the maintenance of dorsal identity, and its loss results in an increase in upstream gene expression because of a feedback loop. It is also plausible that *foxi1* has a complex relationship with *aldh1a2,* and other genes that code for RA metabolic enzymes. Further investigation into this could show a requirement for *foxi1* in the migration of NCCs and POM to the eye, as *foxi1* has been previously shown to be required for the migration and survival of NCCs to the developing otic placode and jaw (HULANDER *et al.* 1998; NISSEN *et al.* 2003; SOLOMON *et al.* 2003a), and ocular RA attracts migrating NCCs (MATT *et al.* 2005; MATT *et al.* 2008; LUPO *et al.* 2011). To further discern this, *foxi1* transcriptional targets should be discerned with the use of RNA-sequencing.

After loss of *foxi1,* both *vax2* and *foxi2* expand dorsally, which is in agreement with previous findings showing the expansion of ventral markers after loss of *gdf6a,* as dorsal identity initiation and maintenance is lost (FRENCH *et al.* 2009; GOSSE AND BAIER 2009). This suggests that *foxi1* is required in some capacity for maintenance of dorsal identity in the eye. The expansion of *vax2* and *foxi2* could also be in response to expanded *tbx5* expression, as *tbx5* and *vax2* expression are antagonistic to maintain respective patterning domains (KOSHIBA-TAKEUCHI *et al.* 2000). Despite increased expression of *vax2* and *tbx5,* the patterning of *ephb2* remains unchanged in *foxi1* morphants. It is likely that this is due to a role for *foxi1* in the maintenance of retinal patterning and not for initiation, which has been shown to affect *eph* and *ephrin* expression (FRENCH *et al.* 2009).

Based on the microphthalmia and coloboma phenotype in *foxi1* morphants, I predicted that *foxi1* has a role in control of the ocular cell cycle. As MAC phenotypes are also observed in *gdf6a*$^{-/-}$ embryos, we hypothesized that the loss of *foxi1* would result in similar defects in proliferation and apoptosis. However, mutant *foo* fish (*foxi1*^{hi3747Tg}) have no gross morphogenic ocular defects up to 5 dpf, and preliminary analysis of proliferation and apoptosis shows no significant differences in mutant embryos. Additionally, *foo*$^{-/-}$ embryos have none of the aforementioned ocular patterning defects, suggesting that results obtained using *foxi1* MO could be due to non-specific morpholino effects. However, these findings are preliminary, and need to be repeated, expanded to include other time points, quantified, and other methods of assaying proliferation and apoptosis utilized. Working with MO technology can be highly advantageous due to ease of use, low cost, and short experimental time. However, there are a number of disadvantages. For example, it is difficult to determine how effective knockdown of a gene is without the appropriate antibody against the protein of interest, or if the MO is targeting another gene in addition to the gene it was designed against. Therefore, the off-target effects of *foxi1* MO could be due to the inhibition of both the gene of interest and others, resulting in the phenotype observed (EISEN AND SMITH 2008). Testing of the specificity of the *foxi1* and *foxi2* MO's could be done by co-injection with *foxi1* RNA not recognized by the MO, with the expectation that no phenotypes would result in this experiment. Additionally, many non-specific MO effects are due to increased apoptosis resulting from activation of p53 (EISEN AND SMITH 2008). To control for this, I co-injected with *p53* MO and did not perform analysis of cell cycle defects on morphants, instead using only mutants for this, anticipating that the microphthalmia and coloboma phenotypes were due to loss of *foxi1*. However, the *foxi1* mutants lacked all and any phenotypes present in the *foxi1* morphants. Again, this finding could be due to off-target MO effects, or to differences in compensation for the loss of *foxi1* by the embryo between MO technology and mutant lines. Authors of a recent large-scale mutagenesis screen note that there is often a lack of phenotypes present in lines with disruptive alleles, and that the location of a mutation in a gene is not always

a reliable predictor of mutation severity (KETTLEBOROUGH *et al.* 2013). Therefore, the *foxi1* ^{hi3747Tg} line may lack ocular defects, and initial investigators note that in the production of a number of disruptive *foxi1* alleles, severity of otic phenotypes differs (NISSEN *et al.* 2003). It is possible that use of another *foo* mutant line could yield similar ocular phenotypes as to those observed in the morphant. Alternatively, there may be compensation in *foo* mutant embryos through redundancy in the genome, or by upregulation of other genes, such as *foxi2,* as *foxi1*$^{-/-}$ embryos have coloboma after knockdown of *foxi2*. An expansion of *foxi2* expression, as seen in *foxi1* morphants, could be compensating for any ocular size defects, as it does in *gdf6a*$^{+/-}$ embryos. Additionally, previous studies have reported that FOX proteins are able to initiate cross talk between parallel signaling pathways in response to external environmental factors (BENAYOUN *et al.* 2011), which could be allowing for a rescue of any ocular phenotype in *foo*$^{-/-}$ embryos. However, the knockdown data of *foxi2* in *foo*$^{-/-}$ are preliminary, and further investigation into redundancy is required.

For the future, it would be of interest to discern where on the pathway of retinal patterning and cell cycle regulation *foxi1* lies, and the complexity of this pathway with regards to other members and feedback mechanisms in place. This would allow for determination of compensatory or redundant genes in place, and to perform knockdown of these genes to induce a similar phenotype, and to determine if the observed *foxi1* MO effects are off-target. It would also be worthwhile to investigate if *foxi1* has a role in NCC migration to the eye as it does elsewhere in the head. It is possible that patients with anterior segment defects have disruptions in *foxi1* regulated NCC migration, and a screening of these patients and the MAC panel could be undertaken.

With regards to *foxi2,* current knowledge regarding the function of this gene remains highly limited. Neural retina expression has been described during murine development (WIJCHERS *et*

al. 2005), as well as in zebrafish at 18 somites on opposing sides of the choroid fissure and at 48 hpf in the ventral CMZ (SOLOMON *et al.* 2003b). These patterns of expression are in agreement with my findings at 16 somites and 48 hpf, but I also found expression at the beginning of neural retina formation and ocular patterning, suggesting that *foxi2* may be required for initiation of ventral retinal patterning. Expression of *foxi2* on opposing sides of the open choroidal fissure also implies a role for *foxi2* in fissure closure, whether directly through cell cycle control or indirectly through downstream effectors. For instance, the knockdown of the major ventral patterning gene *vax2* results in coloboma in zebrafish (TAKE-UCHI *et al.* 2003), and there is upregulation of this gene in *foxi2* morphants. There is also a decrease in *aldh1a3* expression, and coloboma has been reported with aberrant levels of RA (WILSON *et al.* 1953; GREGORY-EVANS *et al.* 2004; LUPO *et al.* 2011; WILLIAMSON AND FITZPATRICK 2014). My hypothesis that *foxi2* is required for the initiation of ventral retinal identity appears to be incorrect, based on previous studies documenting the loss of Shh, which is required for the establishment of ventral retinal identity (EKKER *et al.* 1995). The ablation of cells that secrete Shh results in a reduction in the ventral patterning domain and decreased *vax* expression, and ectopic overexpression of Shh results in a decrease in genes required for dorsal retinal identity (ZHANG AND YANG 2001; SASAGAWA *et al.* 2002). However, it is thought that Shh and RA act independently of each other with regards to ventral eye development, with a requirement for RA for ventral ocular tissue formation, but for Shh in patterning (HYATT *et al.* 1996b; SASAGAWA *et al.* 2002). An increase in *vax2* after loss of *foxi2* suggests a role for maintenance of ventral retinal identity and a feedback loop, versus initiation where I would expect a decrease in *vax2* expression after loss of *foxi2*. In keeping with this, *foxi2* morphants do not have increased *gdf6a* expression, indicating that major genes that are required for initiation of dorsal identity are not affected. Rather, *tbx5* and *foxi1* expression are expanded at 48 hpf, which could have resulted due to a reduction in the maintenance of ventral identity, or an antagonistic expansion in response to an expansion in *vax2*. However, the expansion of *vax2* in other areas of the head after knockdown of *foxi2* also

indicates that this knockdown may not be specific to the eye, and further investigation into the role of *foxi2* into retinal patterning needs to be undertaken.

As opposed to initiation and maintenance of ventral patterning, a decrease in *aldh1a3* expression in *foxi2* morphants suggests that *aldh1a3* could be a direct target of *foxi2,* as *foxi1* could be to *aldh1a2*. *Foxi1* and *foxi2* may have a greater role in ventral eye morphogenesis than patterning, particularly with the coloboma seen after knockout in *foxi1*$^{-/-}$ embryos and its partial penetrance in *foxi2* morphants. Additionally, *aldh1a2* is expanded after loss of *foxi2,* which could be a compensatory response for the decrease in *aldh1a3*. Knockdown of *foxi2* has no effect on expression of the nasal marker, *foxg1a,* or the axon guidance gene *ephb2* at 28 hpf, which is surprising, based on previous studies showing that RA and Vax affect expression of guidance molecules (SEN *et al.* 2005). It is possible there is insufficient alteration in RA concentration and *vax2* expression in *foxi2* morphants. Additionally, changes in expression of other nasal and temporal markers after the knockdown of *foxi1* and *foxi2*, such as *foxg1b, efna5a, foxd1,* and *epha4b* should be addressed to further discern the roles of these *foxi* transcription factors in ocular patterning.

Much remains to be discerned with regards to the developmental roles of *foxi2*. It is likely that *foxi2* is required for migration of POM cells through the inferior fissure by control of *aldh1a3* expression and RA synthesis. Creation of a mutant *foxi2* line would allow for analysis of any changes in cell cycle, and this line could be outcrossed to others that have transgenically labeled NCC and POM cells. This would allow us to determine if the cause of coloboma and microphthalmia after *foxi2* knockdown is due to aberrant migration of these cells. It would also be of interest to determine if there is abnormal axonal pathfinding resulting from loss of either *foxi1* or *foxi2*, as this would be indicative of abnormal dorsal-ventral identity and confirm that the changes in retinal patterning seen have a significant impact on function. Or, conversely, this

would show no differences, and would indicate that *foxi1* and *foxi2* have roles in tissue morphogenesis instead of patterning. Discerning where *foxi2* lies in the ventral eye development pathway, i.e., with RA or Shh, would provide great insight into its role in eye development, and its expression should be examined in mutant zebrafish lines that affect both these genes. Based on the phenotypic differences between *foxi1* MO and *foo* embryos, the possibility that the phenotypes seen with *foxi2* MO are non-specific needs to be taken into consideration. Future experiments should address production and function of protein in morphant fish, and the creation and analysis of a *foxi2* mutant line. Additionally, further MO controls should be used, such as a 5 bp mismatch MO, a splice-blocking MO verified by RT-PCR in addition to the translation-blocking MOs used, and RNA rescue of the targeted gene.

The findings outlined here with regards to changes in gene expression after knockdown of *foxi1* and *foxi2* could be substantiated with the use of other quantification methods, and an increase in the number of biological replicates. For example, quantitative real-time PCR could be used to determine changes in gene expression, and western blot analysis to determine changes in protein production. Additionally, changes in ocular cell cycle in *foxi1* mutant embryos also needs to be supplemented with further studies to provide support to the data shown here.

In summary, I have shown that *foxi1* and *foxi2* are required during ocular development for dorsal-ventral retinal patterning and for morphogenesis, with knockdown resulting in irregular expression of patterning genes, along with microphthalmia and coloboma. Additionally, I have demonstrated differences in phenotypes that occur between MO technology and mutant lines. Both of these phenotypes merit further investigation, as does the role of *foxi1* and *foxi2* in ocular morphogenesis through potential regulation of RA and migration of NCCs to the eye.

Chapter 5

Identification of the Superior Ocular Fissure

5.1: Introduction

The formation of the inferior ocular fissure is a well-recognized developmental process, and is a result of morphogenic movement as the optic vesicle transitions from evagination to invagination, with failure of fissure closure resulting in inferior coloboma. However, 5 patients presenting with coloboma affecting structures of the superior eye is evidence for an additional, superior ocular fissure during development. To our knowledge, no previous reports of superior coloboma exist in the literature. The presence of this fissure in both zebrafish and humans indicates approximately 450 million years of evolutionary conservation and a central role for this structure during ocular development. If so, essential questions pertaining to the biology of the superior ocular fissure remain to be addressed. Namely, what is mediating the opening and closing of the fissure, what determines the location of where the fissure forms, and what is the purpose of this fissure?

In this chapter, I model the requirement for RA in superior and inferior ocular fissure closure, hypothesizing that mutations resulting in aberrant levels of this morphogen result in coloboma based on a proband with transheterozygous mutations in *CYP1B1*. Additionally, I address the roles of the FOX transcription factors *foxd1* and *foxg1* in determining the location of superior fissure formation, and a potential purpose of the fissure.

5.2: Results

The *CYP1B1* coding anomalies A287Pfsx6 and R368H may be pathogenic to superior coloboma and result in significantly reduced protein production and enzymatic activity

Discerned by Sanger sequencing, a superior coloboma proband (Figure 5-1 A)(Supplementary Table 5-1) is transheterozygous for the *CYP1B1* coding anomalies A287Pfsx6 (A287X) and R386H, and presents with unilateral superior coloboma and bilateral congenital glaucoma. In the province of Alberta, it is routine for patients with Primary Congenital Glaucoma to be screened for coding anomalies in *CYP1B1*. The R368H (c.1103G>A) and A287Pfsx6 (c.859delG)

CYP1B1 mutations in the proband were diagnosed and interpreted by the Molecular Diagnostic Laboratory in the Department of Medical Genetics at the University of Alberta, and confirmed by Erin Strachan of the Lehmann lab. *CYP1B1,* a 1632 bp gene, codes from the beginning of exon 2 to the end of exon 3 to produce a 543 amino acid protein, with exon 1 remaining untranslated (Figure 5-1 A, B). R368H (c.1103G>A) is a pathogenic allele that is causative of primary congenital glaucoma (REDDY *et al.* 2003; LI *et al.* 2011), and this missense mutation in exon 3 results in the production of a histidine instead of an arginine residue (Figure 5-1 A, B, C). A287Pfsx6 (c.859delG) is a frameshift mutation that results from a single nucleotide deletion in exon 2, resulting in a stop codon 18 nucleotides later (Figure 5-1 A, B, C). To discern the changes in biochemical function resulting from these variants, I first analyzed the amount of protein produced in transfected COS7 cells using α-tubulin as a control for cytosolic protein. As compared to the amount of WT CYP1B1 protein, the R368H variant results in production of approximately half the amount of 60 kDa protein (Figure 5-2 A). The A287X variant results in truncation of the open reading frame at 856 bp and is predicted to result in a ligand 32 kDa in size. The amount of the ligand made by COS7 cells is highly reduced, suggesting protein degradation (Figure 5-2 A). To determine if these variants result in altered protein function, I utilized a luminescent substrate assay that is a direct read out of CYP1B1 enzymatic activity. As compared to 100% WT CYP1B1 enzyme function, both R368H and A287X have only approximately 30% activity, with base-line activity of empty vector-transfected cells at 15% (Figure 5-2 B). These results strongly suggest that the coding anomalies R368H and A287X are pathogenic in the proband, resulting in reduced or absent protein levels and enzymatic activity.

Zebrafish have a superior ocular fissure present during development

Inferior coloboma results from the failure of the inferior fissure to close. Therefore, it is likely that superior coloboma results from the failure of a superior fissure to close. To determine if there is a superior ocular fissure during development, and if this structure is evolutionarily

conserved and present in zebrafish, I utilized anti-laminin immunofluorescence (IF) to visualize cell boundaries, which should be present between unfused ocular lobes. I found that at approximately 22 hpf, there is a highly transient superior ocular fissure present in zebrafish, visible using anti-laminin IF in *Tg*(*rx3*:*GFP)* and *gdf6a*$^{-/-}$ embryos (Figure 5-3 A, B, C). This structure is also visible on whole mount embryos viewed through a stereomicroscope (Figure 5-3 D). These findings confirm the existence of this previously undescribed developmental structure, and its presence in teleost fish indicates an evolutionary conserved function. Taken together with the apparently deleterious *CYP1B1* mutations in a proband, these findings indicate that an active metabolite produced by CYP1B1 is one factor required for fissure closure. We hypothesized that this metabolite is RA based on the recent characterization of a role for RA production by CYP1B1 (CHAMBERS *et al.* 2007), and previously described requirements for RA in inferior fissure closure.

Expression of the retinoic acid synthesis enzymes *aldh1a2, aldh1a3* and *cyp1b1* correspond with the locations of the superior and inferior ocular fissures

We hypothesized that the R368H and A287X alleles are pathogenic and cause superior coloboma in the proband due to reduced ocular RA. To test this, I first performed ISH to determine if there is corresponding spatio-temporal expression of *cyp1b1* and other RA synthesis enzymes in the developing eye. I found that at 28 hpf, *aldh1a2* is strongly expressed in the dorsal retina in the presumptive area of superior fissure formation, and transcripts are also present in the ventral retina at the inferior fissure (Figure 5-4 A, B). At 48 hpf this dorsal expression pattern remains, in addition to peripheral ocular expression (Figure 5-4 C). Conversely, in the ventral retina, *aldh1a3* is present at 28 and 48 hpf on opposing sides of the closing inferior fissure (Figure 5-4 D, E, F). Interestingly, *cyp1b1* is present in both the area of the superior and inferior fissure. At 28 hpf, transcripts are present in a vertical streak through and behind the eye from the area of the superior to inferior fissure, with strongest expression on the nasal portion of the eye, and at the anterior of the eye on the nasal half of the closing inferior fissure (Figure 5-4 G, H). At 48

hpf, the expression of *cyp1b1* is located at the 12 and 6 o'clock positions of the eye, corresponding to where the superior and inferior fissures had previously formed (Figure 5-4 I, J). The localization of transcripts of genes coding for RA synthesizing enzymes suggests that there is a required homeostatic concentration of this morphogen at both ocular fissures for closure during development. To show this, I next supplemented a coloboma model with Vitamin A during development.

Vitamin A supplementation can rescue inferior coloboma in *gdf6a*$^{-/-}$ larvae

Inferior ocular fissure closure is complete at approximately 36 hpf in zebrafish. At 48 hpf, control treated WT embryos have closed inferior ocular fissures, while *gdf6a*$^{-/-}$ larvae have inferior coloboma (Figure 5-5 A, B, C, D). Vitamin A (retinol) supplementation during development to WT embryos does not change inferior fissure closure at 48 hpf (Figure 5-5 E, F), where supplementation of *gdf6a*$^{-/-}$ embryos with Vitamin A rescues inferior fissure closure in 58% of mutant larvae (Figure 5-5 G, H, I). These findings strongly implicate a role for vitamin A, and its active derivative, RA, in ocular fissure closure.

A

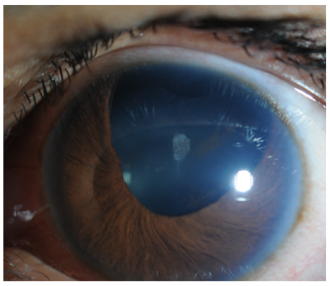

```
ATGGGCACCAGCCTCAGCCCGAACGACCCTTGGCCGCTAAACCCGCTGTCCATCCAGCAGACCACGCTCCT
GCTACTCCTGTCGGTGCTGGCCACTGTGCATGTGGGCCAGCGGCTGCTGAGGCAACGGAGGCGGCAGCTCC
GGTCCGCGCCCCCGGGCCCGTTTGCGTGGCCACTGATCGGAAACGCGGCGGCGGTGGGCCAGGCGGCTCAC
CTCTCGTTCGCTCGCCTGGCGCGGCGCTACGGCGACGTTTTCCAGATCCGCCTGGGCAGCTGCCCCATAGT
GGTGCTGAATGGCGAGCGCGCCATCCACCAGGCCCTGGTGCAGCAGGGCTCGGCCTTCGCCGACCGGCCGG
CCTTCGCCTCCTTCCGTGTGGTGTCCGGCGGCCGCAGCATGGCTTTCGGCCACTACTCGGAGCACTGGAAG
GTGCAGCGGCGCGCAGCCCACAGCATGATGCGCAACTTCTTCACGCGCCAGCCGCGCAGCCGCCAAGTCCT
CGAGGGCCACGTGCTGAGCGAGGCGCGCGAGCTGGTGGCGCTGCTGGTGCGCGGCAGCGCGGACGGCGCCT
TCCTCGACCCGAGGCCGCTGACCGTCGTGGCCGTGGCCAACGTCATGAGTGCCGTGTGTTTCGGCTGCCGC
TACAGCCACGACGACCCCGAGTTCCGTGAGCTGCTCAGCCACAACGAAGAGTTCGGGCGCACGGTGGGCGC
GGGCAGCCTGGTGGACGTGATGCCCTGGCTGCAGTACTTCCCCAACCCGGTGCGCACCGTTTTCCGCGAAT
TCGAGCAGCTCAACCGCAACTTCAGCAACTTCATCCTGGACAAGTTCTTGAGGCACTGCGAAAGCCTTCGG
CCCGGGGCCGCCCCCCGCGACATGATGGACGCCTTTATCCTCTCTGCGGAAAAGAAGGCGGCCGGGGACTC
GCACGGTGGTGGCGCGCGGCTGGATTTGGAGAACGTACCGGCCACTATCACTGACATCTTCGGCGCCAGCC
AGGACACCCTGTCCACCGCGCTGCAGTGGCTGCTCCTCCTCTTCACCAGGTATCCTGATGTGCAGACTCGA
GTGCAGGCAGAATTGGATCAGGTCGTGGGGAGGGACCTTCTGCCTTGTATGGGTGACCAGCCCAACCTGCC
CTATGTCCTGGCCTTCCTTTATGAAGCCATGCGCTTCTCCAGCTTTGTGCCTGTCACTATTCCTCATGCCA
CCACTGCCAACACCTCTGTCTTGGGCTACCACATTCCCAAGGACACTGTGGTTTTTGTCAACCAGTGGTCT
GTGAATCATGACCCAGTGAAGTGGCCTAACCCGGAGAACTTTGATCCAGCTCGATTCTTGGACAAGGATGG
CCTCATCAACAAGGACCTGACCAGCAGAGTGATGATTTTTTCAGTGGGCAAAAGGCGGTGCATTGGCGAAG
AACTTTCTAAGATGCAGCTTTTTCTCTTCATCTCCATCCTGGCTCACCAGTGCGATTTCAGGGCCAACCCA
AATGAGCCTGCGAAAATGAATTTCAGTTATGGTCTAACCATTAAACCCAAGTCATTTAAAGTCAATGTCAC
TCTCAGAGAGTCCATGGAGCTCCTTGATAGTGCTGTCCAAAATTTACAAGCCAAGGAAACTTGCCAATAA
```

B

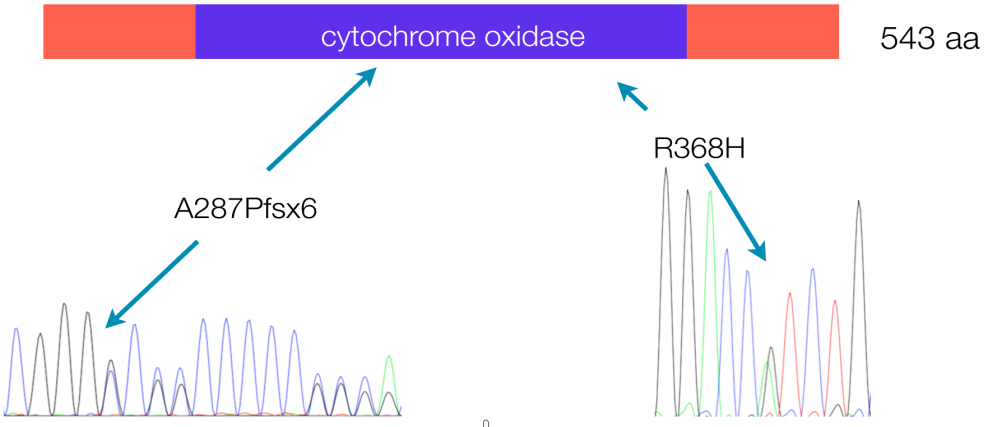

C

```
0
WT…MGTSLSPNDPWPLNPLSIQQTTLLLLLSVLATVHVGQRLLRQRRRQLRSAPPGPFAWPLI
HA…MGTSLSPNDPWPLNPLSIQQTTLLLLLSVLATVHVGQRLLRQRRRQLRSAPPGPFAWPLI

61
WT…GNAAAVGQAAHLSFARLARRYGDVFQIRLGSCPIVVLNGERAIHQALVQQGSAFADRPAFA
HA…GNAAAVGQAAHLSFARLARRYGDVFQIRLGSCPIVVLNGERAIHQALVQQGSAFADRPAFA

122
WT…SFRVVSGGRSMAFGHYSEHWKVQRRAAHSMMRNFFTRQPRSRQVLEGHVLSEARELVAL
HA…SFRVVSGGRSMAFGHYSEHWKVQRRAAHSMMRNFFTRQPRSRQVLEGHVLSEARELVAL

181
WT…LVRGSADGAFLDPRPLTVVAVANVMSAVCFGCRYSHDDPEFRELLSHNEEFGRTVGAGSL
HA…LVRGSADGAFLDPRPLTVVAVANVMSAVCFGCRYSHDDPEFRELLSHNEEFGRTVGAGSL

241                                                    A287P
WT…VDVMPWLQYFPNPVRTVFREFEQLNRNFSNFILDKFLRHCESLRPGAAPRDMMDAFILSA
HA…VDVMPWLQYFPNPVRTVFREFEQLNRNFSNFILDKFLRHCESLRPGPPPAT.--------

301
WT…EKKAAGDSHGGGARLDLENVPATITDIFGASQDTLSTALQWLLLLFTRYPDVQTRVQAEL
HA…------------------------------------------------------------

361
WT…DQVVGRDRLPCMGDQPNLPYVLAFLYEAMRFSSFVPVTIPHATTANTSVLGYHIPKDTVV
HA…------------------------------------------------------------

421
WT…FVNQWSVNHDPVKWPNPENFDPARFLDKDGLINKDLTSRVMIFSVGKRRCIGEELSKMQL
HA…------------------------------------------------------------

481
WT…FLFISILAHQCDFRANPNEPAKMNFSYGLTIKPKSFKVNVTLRESMELLDSAVQNLQAKE
HA…------------------------------------------------------------

      543
WT…TCQ.
HA…---
```

```
0                                                              60
WT…MGTSLSPNDPWPLNPLSIQQTTLLLLLSVLATVHVGQRLLRQRRRQLRSAPPGPFAWPLI
HA…MGTSLSPNDPWPLNPLSIQQTTLLLLLSVLATVHVGQRLLRQRRRQLRSAPPGPFAWPLI

61                                                             121
WT…GNAAAVGQAAHLSFARLARRYGDVFQIRLGSCPIVVLNGERAIHQALVQQGSAFADRPAFA
HA…GNAAAVGQAAHLSFARLARRYGDVFQIRLGSCPIVVLNGERAIHQALVQQGSAFADRPAFA

122                                                            180
WT…SFRVVSGGRSMAFGHYSEHWKVQRRAAHSMMRNFFTRQPRSRQVLEGHVLSEARELVAL
HA…SFRVVSGGRSMAFGHYSEHWKVQRRAAHSMMRNFFTRQPRSRQVLEGHVLSEARELVAL

181                                                            240
WT…LVRGSADGAFLDPRPLTVVAVANVMSAVCFGCRYSHDDPEFRELLSHNEEFGRTVGAGSL
HA…LVRGSADGAFLDPRPLTVVAVANVMSAVCFGCRYSHDDPEFRELLSHNEEFGRTVGAGSL

241                                                            300
WT…VDVMPWLQYFPNPVRTVFREFEQLNRNFSNFILDKFLRHCESLRPGAAPRDMMDAFILSA
HA…VDVMPWLQYFPNPVRTVFREFEQLNRNFSNFILDKFLRHCESLRPGAAPRDMMDAFILSA

301                                                            360
WT…EKKAAGDSHGGGARLDLENVPATITDIFGASQDTLSTALQWLLLLFTRYPDVQTRVQAEL
HA…EKKAAGDSHGGGARLDLENVPATITDIFGASQDTLSTALQWLLLLFTRYPDVQTRVQAEL

361      R368H                                                 420
WT…DQVVGRDRLPCMGDQPNLPYVLAFLYEAMRFSSFVPVTIPHATTANTSVLGYHIPKDTVV
HA…DQVVGRDRLPCMGDQPNLPYVLAFLYEAMRFSSFVPVTIPHATTANTSVLGYHIPKDTVV

421                                                            480
WT…FVNQWSVNHDPVKWPNPENFDPARFLDKDGLINKDLTSRVMIFSVGKRRCIGEELSKMQL
HA…FVNQWSVNHDPVKWPNPENFDPARFLDKDGLINKDLTSRVMIFSVGKRRCIGEELSKMQL

481                                                            540
WT…FLFISILAHQCDFRANPNEPAKMNFSYGLTIKPKSFKVNVTLRESMELLDSAVQNLQAKE
HA…FLFISILAHQCDFRANPNEPAKMNFSYGLTIKPKSFKVNVTLRESMELLDSAVQNLQAKE

      543
WT…TCQ.
HA…TCQ.
```

Figure 5-1: The *CYP1B1* coding anomalies A287Pfsx6 and R368H in proband HA with unilateral superior coloboma and bilateral congenital glaucoma.

The superior coloboma proband has a large superior iris coloboma (OS) (A). The human *CYP1B1* transcript is composed of three exons, an untranslated exon 1 (401 bp, not shown), and translated exon 2 and exon 3 (1632 bp) (A), which code for a 543 amino acid protein (B). The proband HA is heterozygous for the coding anomaly A287Pfsx6, which is a 1 nucleotide deletion in exon 2 (A - red G) that results in the formation of a stop codon 18 nucleotides, or 5 amino acids, downstream (B, C). Proband HA is also heterozygous for R368H [A - blue G, (7940G>A) B], resulting in the production of a histidine instead of an arginine at residue 368 (B, C).

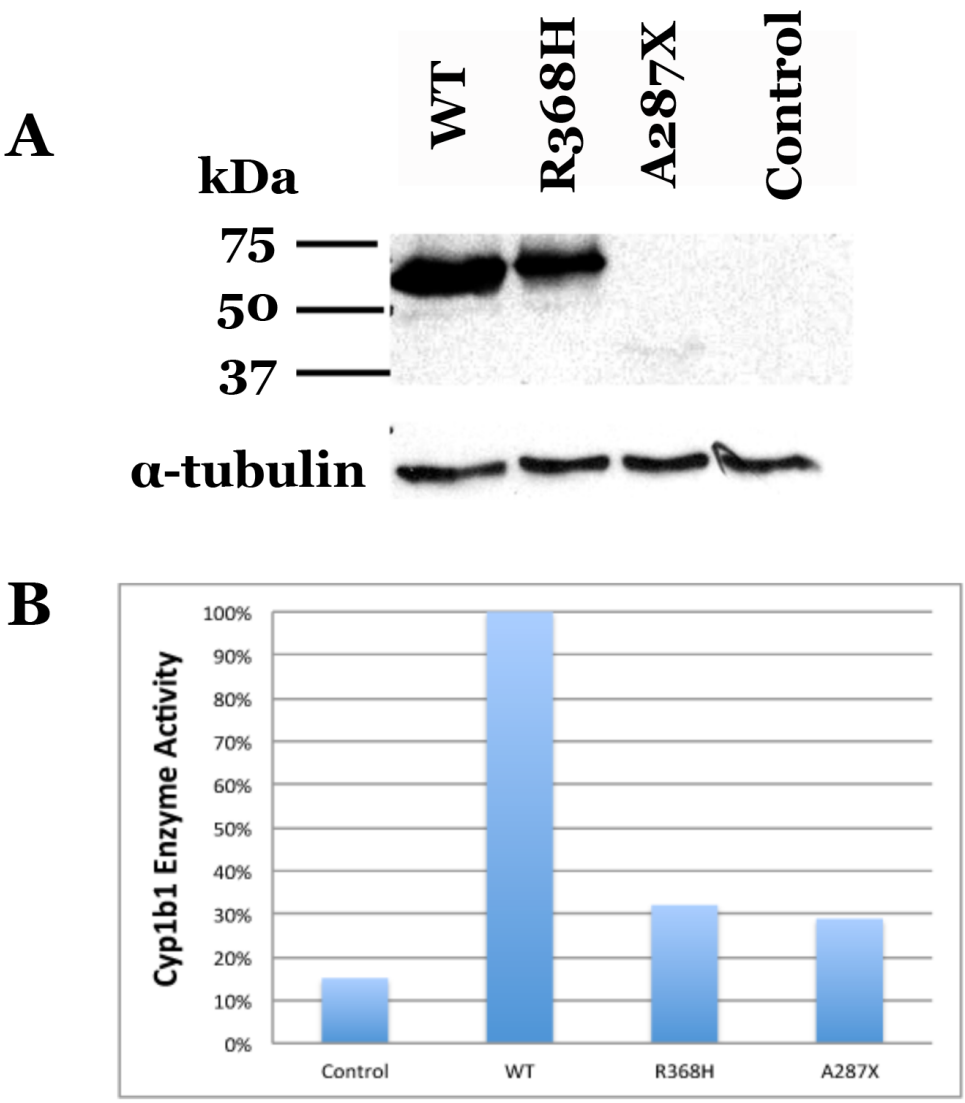

Figure 5-2: Evidence of altered biochemical function in proband HA with the heterozygous *CYP1B1* variants A287X and R368H.

Western blot analysis demonstrates a reduced amount of 60 kDa R368H ligand, and a near absence of 32 kDa A287X ligand, compared with 60 kDa WT ligand in the cell-lysate (A), with an untransfected plate of Cos-7 cells as a control. Biological replicates n=2. CYP1B1 luciferase reporter analysis shows a decrease in R368H (32% activity) and A287X (28.8% activity) CYP1B1 enzymatic activity as compared to wild type (100% activity)(B). Alpha-tubulin was utilized as a cytosolic control, and empty pCS2+ vector as the control for base CYP1B1 activity in Cos-7 cells (15% activity). Biological replicates n=1, with 6 technical replicates.

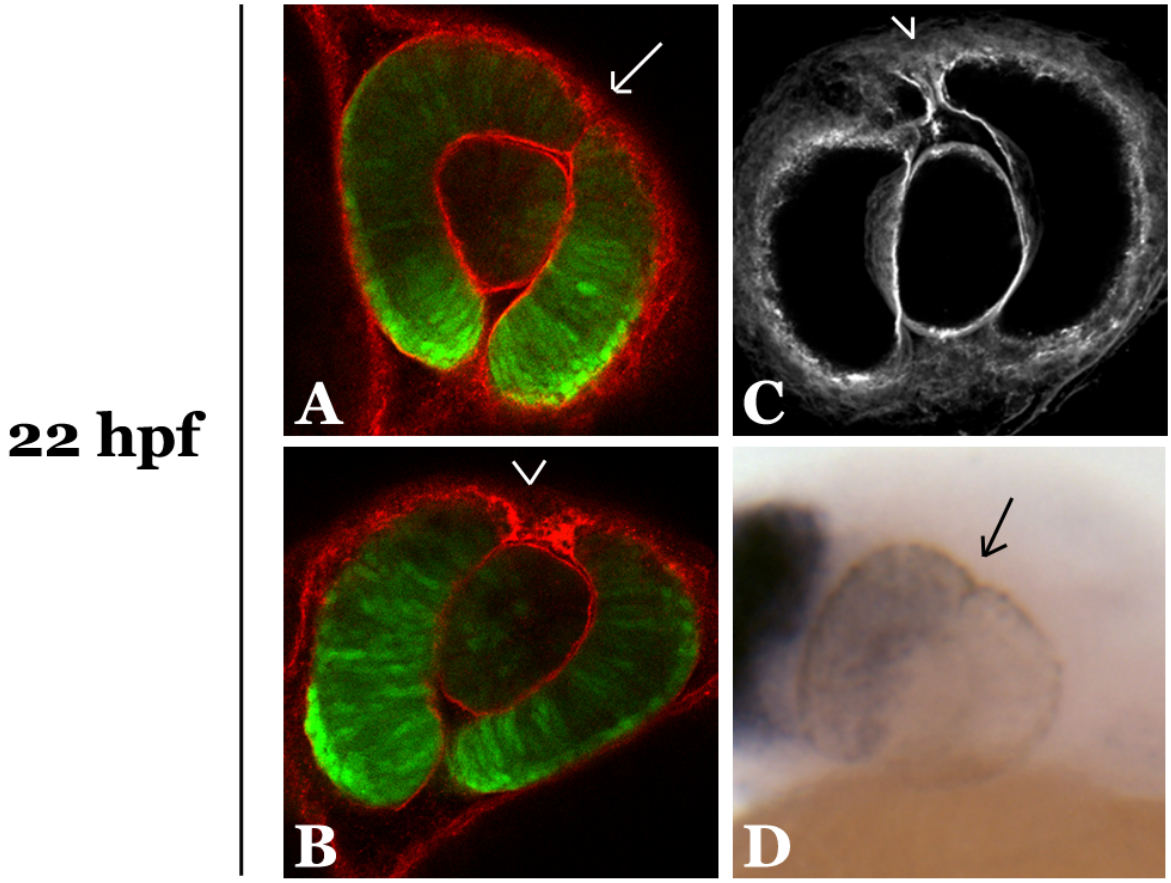

Figure 5-3: Evidence for existence of a superior fissure in zebrafish.

At approximately 22 hpf the superior ocular fissure can be visualized using anti-laminin immunofluorescence in *Tg*(*rx3*:*GFP)* embryos (A, B, white arrow & arrowhead), in *gdf6a*$^{-/-}$ embryos (C, white arrowhead), and in WT whole images of embryos on the yolk viewed through a stereoscope (D, black arrow).

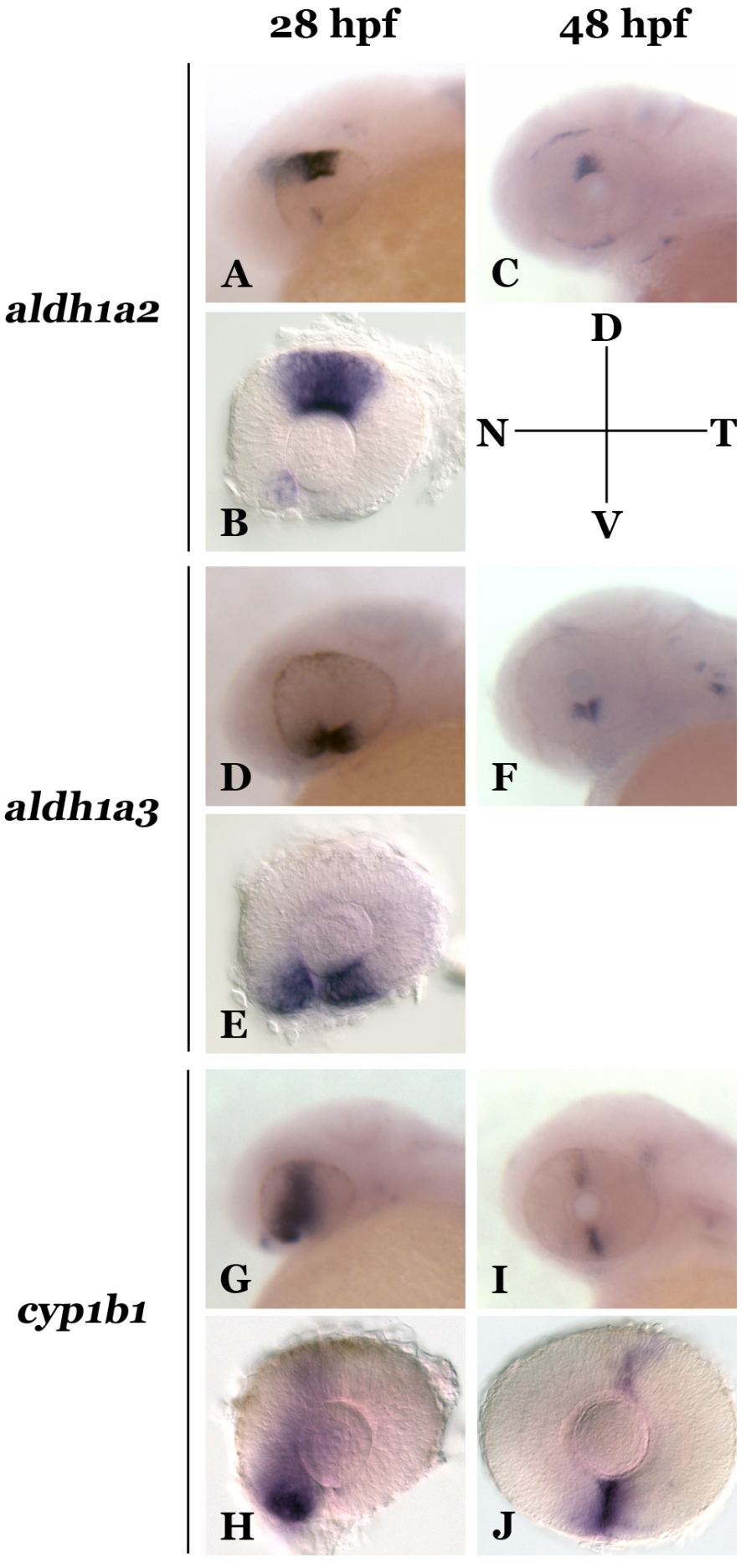
28 hpf
48 hpf
aldh1a2
A
C
B
D
N
T
V
aldh1a3
D
F
E
cyp1b1
G
I
H
J

Figure 5-4: The ocular localization of the retinoic acid synthesis genes *aldh1a2, aldh1a3* and *cyp1b1* corresponds to the locations of the superior and inferior fissures.

At 28 hpf, *aldh1a2* is strongly expressed in the dorsal retina and faintly in the ventral retina, localized to the area of the inferior fissure (A, B). This dorsal expression pattern remains at 48 hpf, with some peripheral localization of transcripts (C). In the ventral retina, *aldh1a3* is strongly expressed on opposing sides of the closing choroidal fissure at both 28 and 48 hpf. *cyp1b1* has a highly dynamic ocular expression pattern; at 28 hpf, transcripts are present in a vertical stripe in and behind the eye, extending from the location of the superior to inferior fissure, with strongest expression inferiorly (G, H). At 48 hpf, *cyp1b1* ocular expression is shown in two linear domains, broken by the lens, which correspond exactly with the locations of the now closed superior and inferior ocular fissures (I, J).

The ocular expression patterns of *foxd1* and *foxg1a* demarcate the temporal and nasal eye and correspond with the locations of the superior and inferior fissures

While the formation of the inferior ocular fissure is concurrent with a morphogenic event, the mechanism underlying the formation of the superior fissure is unknown. We hypothesized that the FOX proteins foxd1, foxg1a and foxg1b, may be determining the location of fissure formation, based on their ocular expression patterns and boundaries. At 28 and 48 hpf, *foxd1* transcripts are localized to the temporal portion of the retina, with expression becoming more tightly localized around the lens at 48 hpf (Figure 5-6 A, B, C, D). Expression of *foxg1a* in the nasal retina mirrors the expression of *foxd1* in the temporal retina at 28 and 48 hpf (Figure 5-6 E, F, G, H). The expression of these transcription factors is separated at the 12 and 6 o'clock boundaries created by the respective superior and inferior ocular fissures, with a late closing superior fissure occasionally visible at 28 hpf (Figure 5-6 E). While the localization of *foxd1* and *foxg1a* ocular transcripts is tightly demarked by the fissures, the expression pattern of a paralog of *foxg1a, foxg1b*, encompasses nearly the entirety of the eye, with exception for a small portion of the nasal and temporal portion of the ventral retina at 28 hpf, and a portion of the ventral temporal retina at 48 hpf (Figure 5-6 I, J, K, L). The expression of a third *foxg1a* paralog, *foxg1c*, is very faint and expressed in the area of the midbrain and hindbrain at 28 and 48 hpf (Figure 5-6 M, N). From the localization of *foxd1* and *foxg1a* transcripts, it appears that these FOX genes are responsible for controlling the location of the superior fissure. However, the expression of *foxg1b* throughout the retina implies that a complex interaction between these transcription factors may mediate superior fissure location and formation. To discern the distinct roles of *foxg1a, foxg1b* and *foxd1* in superior fissure formation, I knocked down their expression and examined any changes in transcript localization of RA synthesis genes, which would provide insights into a change in fissure location and closure.

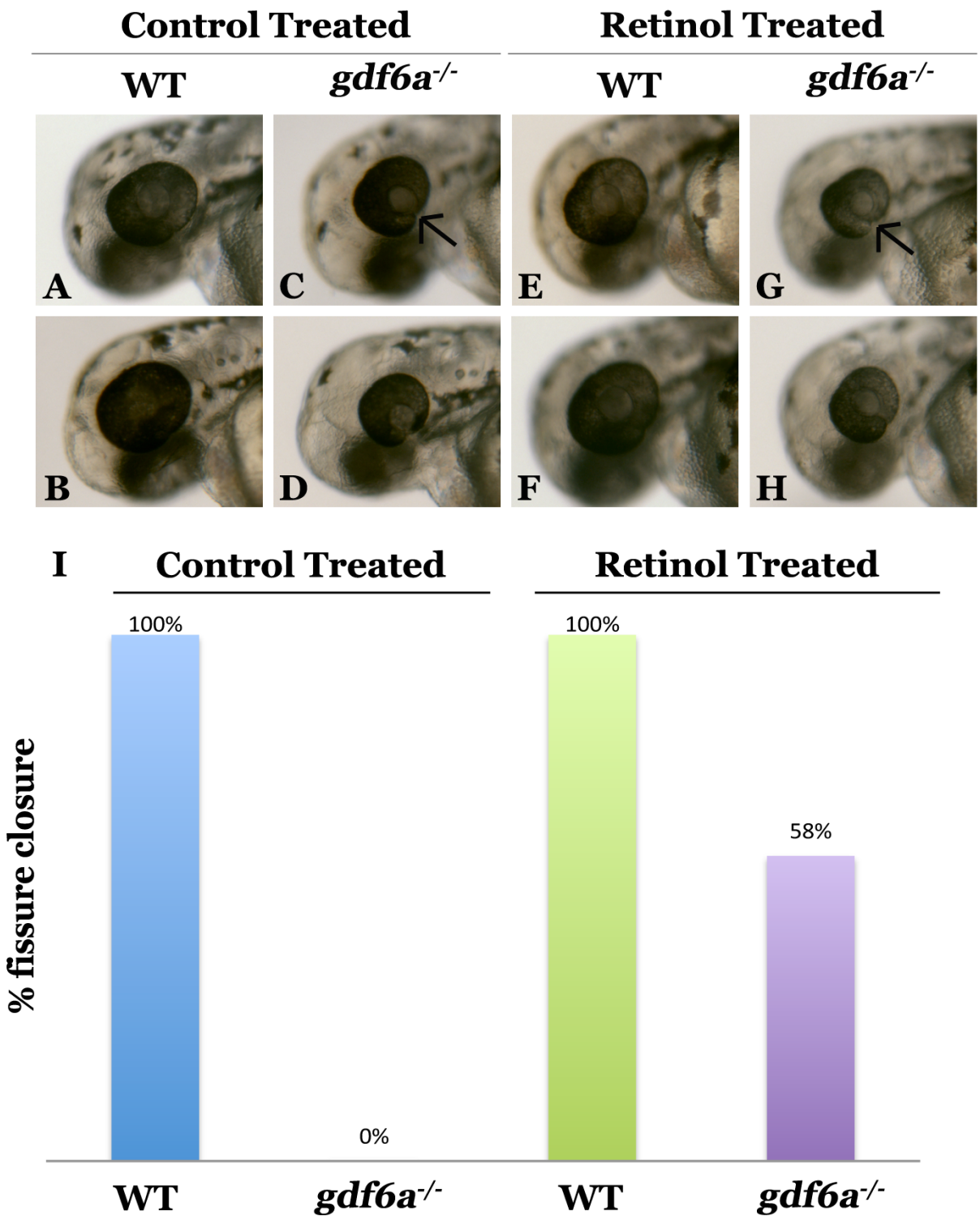
Control Treated
Retinol Treated
WT
gdf6a-/-
WT
gdf6a-/-
A
C
E
G
B
D
F
H
I
Control Treated
Retinol Treated
% fissure closure
100%
0%
100%
58%
WT
gdf6a-/-
WT
gdf6a-/-

Figure 5-5: Inferior coloboma in *gdf6a*$^{-/-}$ larvae can be rescued with retinol supplementation during development.

Control treated 48 hpf WT larvae have fully closed inferior ocular fissures (A, B), while *gdf6a*$^{-/-}$ larvae have inferior coloboma (C, D). Treatment with 0.6 μM all trans retinol at ~%75 epiboly results in no difference in inferior fissure closure in WT larvae (E, F, n=66), but results in a 58% increase in inferior fissure closure in *gdf6a*$^{-/-}$ larvae (G, H, I, n=7/12). Biological replicates n=2, 5 technical replicates per experiment.

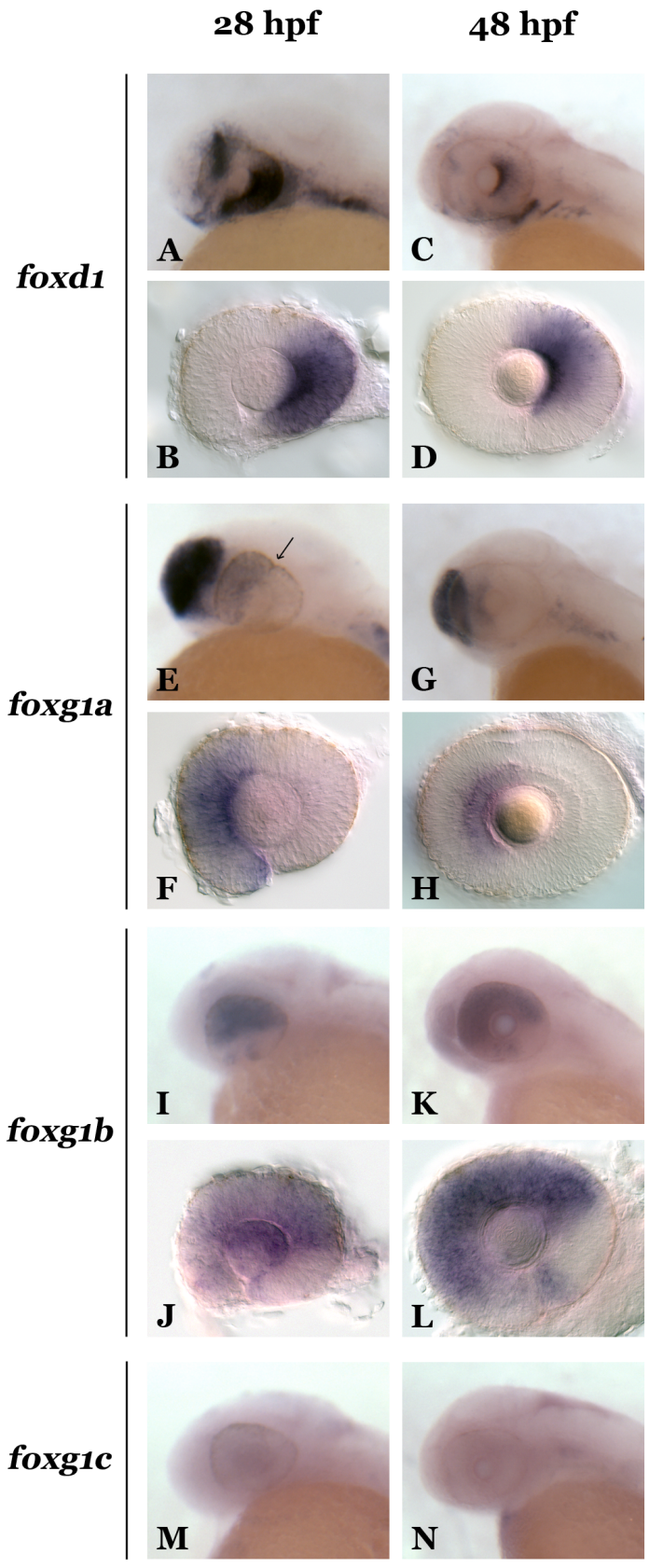
28 hpf
48 hpf
foxd1
foxg1a
foxg1b
foxg1c
A
B
C
D
E
F
G
H
I
J
K
L
M
N

Figure 5-6: Ocular expression patterns of the forkhead box transcription factors *foxd1, foxg1a, foxg1b* and *foxg1c* at 28 and 48 hpf.

foxd1 and *foxg1a* transcripts are localized to opposite halves of the retina, with *foxd1* expressed temporally and *foxg1a* nasally at both 28 and 48 hpf, with a clear boundary between expression at 12 and 6 o'clock, or the presumptive locations of the superior and inferior fissure, respectively (A, B, C, D, E – arrow to superior fissure, F, G, H). The *foxg1a* paralog *foxg1b* is expressed throughout the eye at both 28 and 48 hpf, with the exception of a small portion of the ventral portions of the nasal and temporal retina at 28 hpf, and a small part of the ventral temporal retina at 48 hpf (I, J, K, L). The *foxg1a* paralog *foxg1c* is expressed only faintly at the mid-hindbrain boundary at 28 and 48 hpf (M, N).

Knockdown of *foxd1* and *foxg1* results in differential ocular expression of *aldh1a2, aldh1a3* and *cyp1b1*

Knockdown of the temporally expressed *foxd1* results in a decrease in dorsal retinal expression of *aldh1a2* (Figure 5-7 A, B), and a concomitant decrease in ventral retinal expression of *aldh1a3*, along with partially penetrant coloboma at 28 hpf (Figure 5-7 C, D, E, F). Ocular expression of *cyp1b1* at both 28 and 48 hpf remains unchanged in *foxd1* morphants (Figure 5-7 G, H, I, J). Knockdown of the nasal genes *foxg1a* and *foxg1b*, utilizing lower and higher doses of the MO, also results in altered expression of RA synthesizing genes in the retina at 48 hpf. At both MO doses, *aldh1a2* expression in the dorsal retina is decreased (Figure 5-8 A, B, C), while *aldh1a3* expression remains unchanged at the lower dose (Figure 5-8 D, E). *Cyp1b1* expression at 48 hpf is typically demonstrated by two vertical stripes at the 12 and 6'oclock positions (Figure 5-6 F, G), and knockdown of *foxg1a* and *foxg1b* at a lower dose results in a slight shift of the dorsal, 12 o'clock stripe, to the nasal portion of the retina, and an expansion and shift of the ventral, 6 o'clock stripe to the nasal portion of the retina (Figure 5-8 H, I). At the higher MO dose, the loss of *foxg1a* and *foxg1b* results in partially penetrant coloboma, and a profound alteration in *cyp1b1* expression. In the dorsal retina there is a shift of the *cyp1b1* expression domain nasally, and an expanded patch of expression and numerous stripes, many that are only present in the top half of the retina (Figure 5-8 J). In the ventral retina, *cyp1b1* expression expands to opposing sides of the ventral fissure, and just as described in the dorsal retina, there is a shift to the nasal portion where there are many vertical stripes of expression, some of which are present in the bottom half of the ventral retina (Figure 5-8 J, K). The change in ocular expression of RA synthesis genes after knockdown of *foxd1, foxg1a,* and *foxg1b* prompted my subsequent analysis of the location of superior fissure formation after knockdown of these transcription factors.

The knockdown of *foxd1* and *foxg1* results in aberrant superior fissure formation

To discern whether *foxg1a*, *foxg1b* and *foxd1* control the location of superior fissure formation, I utilized anti-laminin IF after MO knockdown. The superior fissure is a highly transient structure

in zebrafish, and is present at approximately 22 hpf directly opposite the ventral fissure, at a 12 o'clock position in WT embryos (Figure 5-9 A, B). Knockdown of *foxd1* results in the formation of more than one superior fissure, with one fissure forming in the nasal portion of the dorsal eye, and another forming in the temporal portion of the dorsal eye (p=0.03, Figure 5-9 C, D, E). Using *Tg*(*rx3*:*GFP)* embryos, the superior fissure is also visible at 22 hpf (Figure 5-10 A, B), and knockdown of both *foxg1a* and *foxg1b* (knockdown of *foxg1a* alone does not cause a superior fissure phenotype) results in a shift of the fissure into the nasal region (p=0.09, Figure 5-10 C, D, E). These findings support the hypothesis that the transcription factors *foxg1a, foxg1b* and *foxd1* have a role in determining the location of superior fissure formation.

foxg1b$^{-/-}$ larvae do not have irregular ocular vasculature at 48 hpf

We hypothesized that a purpose of the superior fissure is to allow for the passage of ocular vasculature, and that a shift in the location of the superior fissure would result in a corresponding shift in vasculature. To test this hypothesis, I outcrossed *foxg1b*$^{+/-}$ and *Tg*(*flk1:EGFP*) fish and analyzed vascular phenotypes. 48 hpf *foxg1b*$^{+/+}$ larvae have a ventral radial vessel, a nasal radial vessel, and either one or two dorsal radial vessels (Figure 5-11 A, B). This phenotype is also present in *foxg1b*$^{+/-}$ and *foxg1b*$^{-/-}$ larvae (Figure 5-11 C, D, E, F), suggesting that there are no vasculature phenotypes present at this stage, there is redundancy in function with *foxg1a,* or that the superior fissure serves a different developmental purpose.

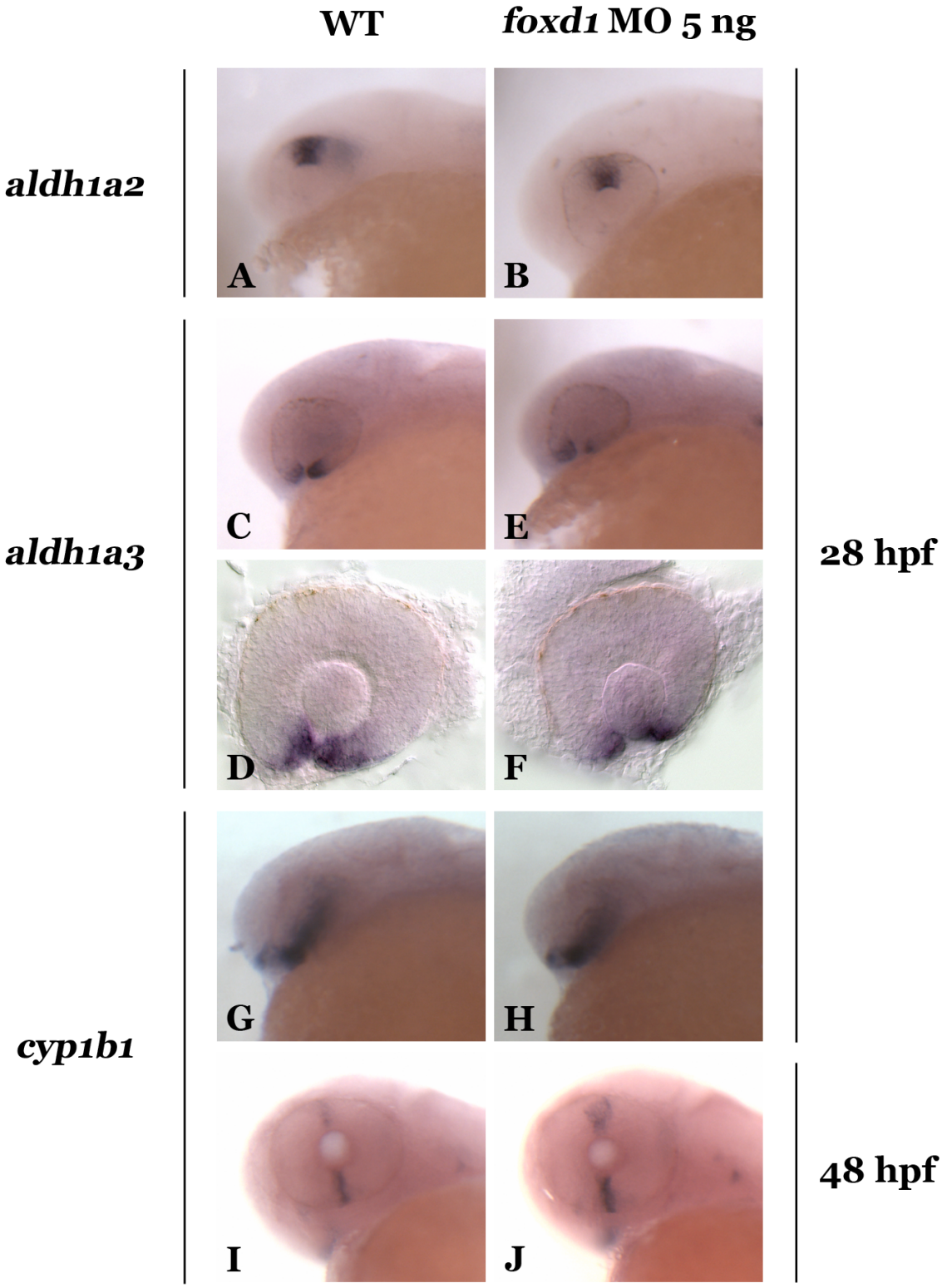
WT
foxd1 MO 5 ng
aldh1a2
aldh1a3
cyp1b1
A
B
C
E
D
F
G
H
I
J
28 hpf
48 hpf

Figure 5-7: The ocular expression of *aldh1a2* and *aldh1a3* is decreased after knockdown of *foxd1*, whereas *cyp1b1* expression is unaffected.

Knockdown of *foxd1* via injection of 5 ng of MO results in a moderate decrease in expression of *aldh1a2* in the dorsal retina (A, B), and a decrease in expression of *aldh1a3* in the ventral retina (C, D, E, F), both at 28 hpf. Knockdown of *foxd1* expression has no effect on ocular *cyp1b1* expression at 28 or 48 hpf (G, I, H, J).

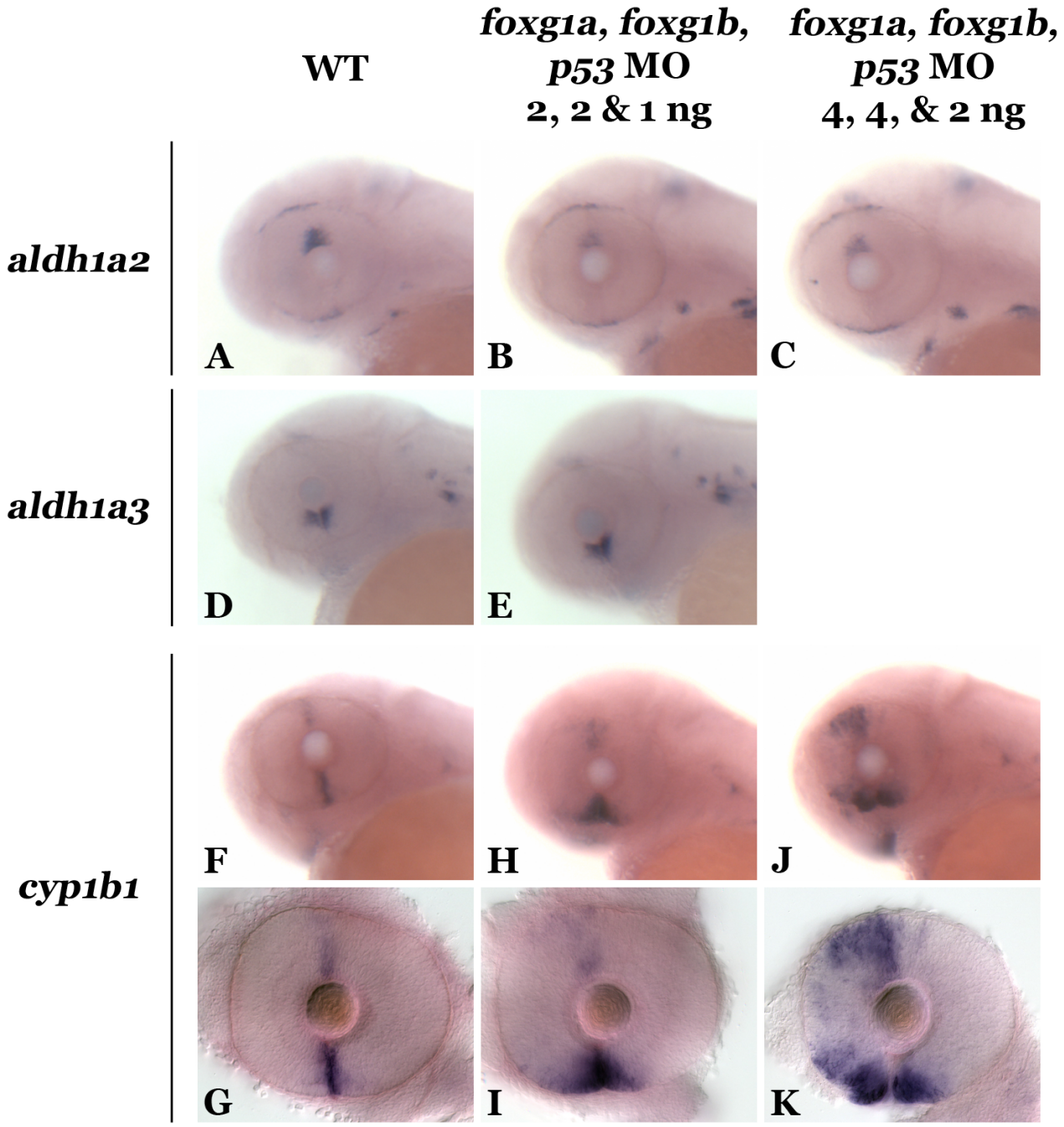

Figure 5-8: Knockdown of both *foxg1a* and *foxg1b* results in decreased *aldh1a2* expression, no change in *aldh1a3* expression and aberrant expansion and shift in *cyp1b1* retinal expression.

Knockdown of *foxg1a, foxg1b* and *p53* by injection of either 2, 2 and 1 ng, or 4, 4 and 2 ng, respectively, results in a decrease in dorsal retinal *aldh1a2* expression (A, B, C), and no change in

ventral retinal *aldh1a3* expression (D, E) at 48 hpf. At the 2 ng dose, *cyp1b1* expression becomes expanded in the ventral retina at the location of the inferior fissure and into the nasal retina, and there is a slight shift in dorsal retina expression from its WT 12 o'clock expression into the nasal retina at 48 hpf (F, G, H, I). At the 4 ng dose, *cyp1b1* expression is greatly expanded in the ventral and dorsal retina, with aberrant expression into the nasal retina from both locations, and a shift in the dorsal 12 o'clock strip into the nasal retina (J, K).

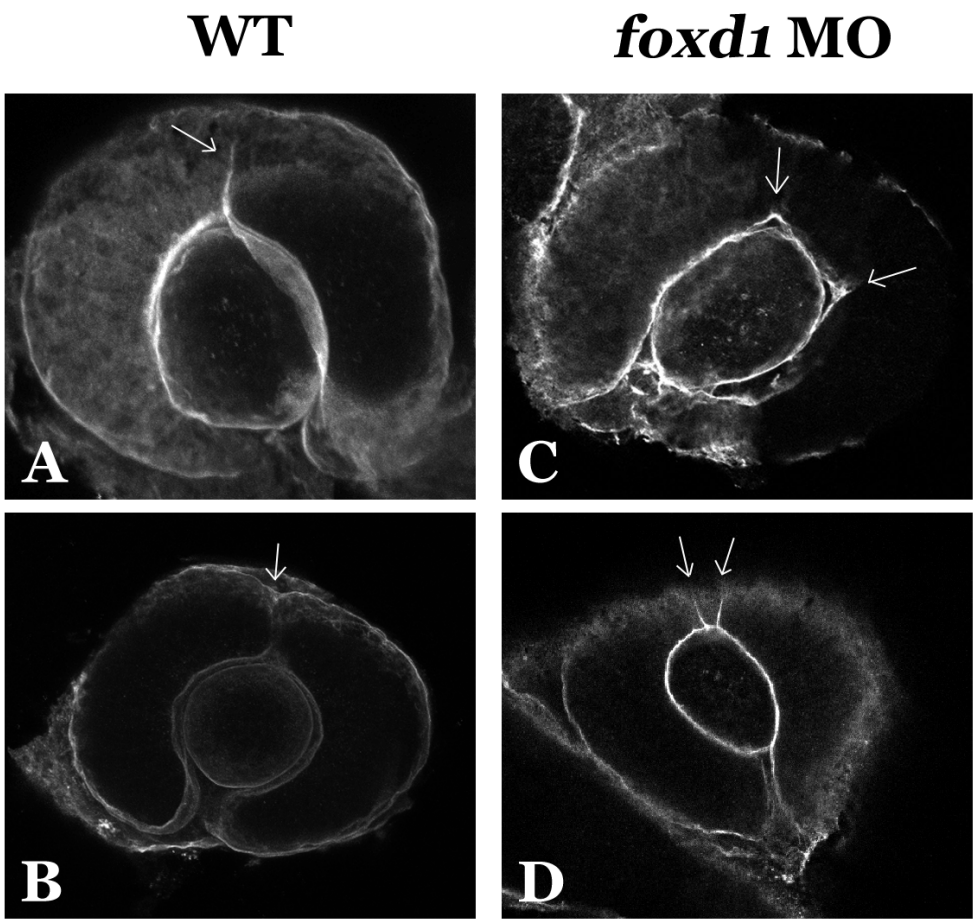
WT
foxd1 MO
A
B
C
D

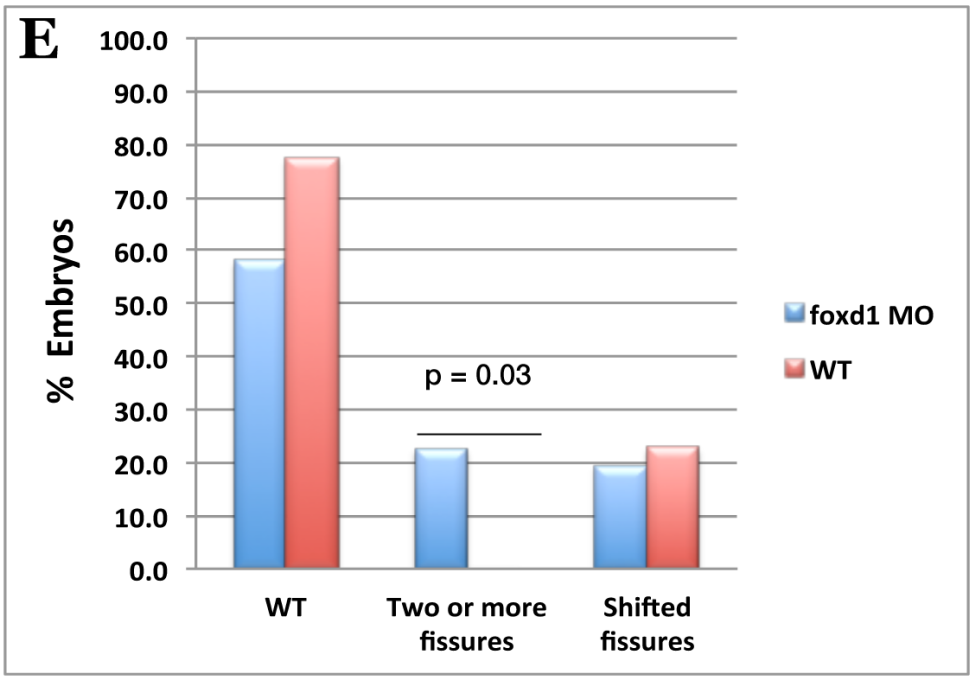
E
100.0
90.0
80.0
70.0
60.0
50.0
40.0
30.0
20.0
10.0
0.0
% Embryos
p = 0.03
WT
Two or more fissures
Shifted fissures
foxd1 MO
WT

Figure 5-9: Knockdown of *foxd1* results in aberrant superior fissure formation.

At approximately 22 hpf, the superior ocular fissure is open in the dorsal retina directly opposite to the inferior ocular fissure at 12 o'clock (A, B, white arrows). Injection of 5 ng of *foxd1* into AB embryos results in the formation of more than one superior fissure offset from 12 o'clock, with one fissure in the nasal region and another in the temporal region (C, D, white arrows). Quantification of fissure formation shows that 58% (n=18/31) of *foxd1* morphants and 77% (n=17/22) uninjected embryos have the WT fissure phenotype, 22% (n=7/31) of morphants and 0% (n=0/22) of uninjected embryos have two or more superior fissures (p=0.03), and 20% (n=6/31) of morphants and 23% (n=5/22) of uninjected embryos have shifted ocular fissures, as determined by a blind scoring assessment and Fisher's exact test (E). Biological replicates n=2, 6 technical replicates per experiment.

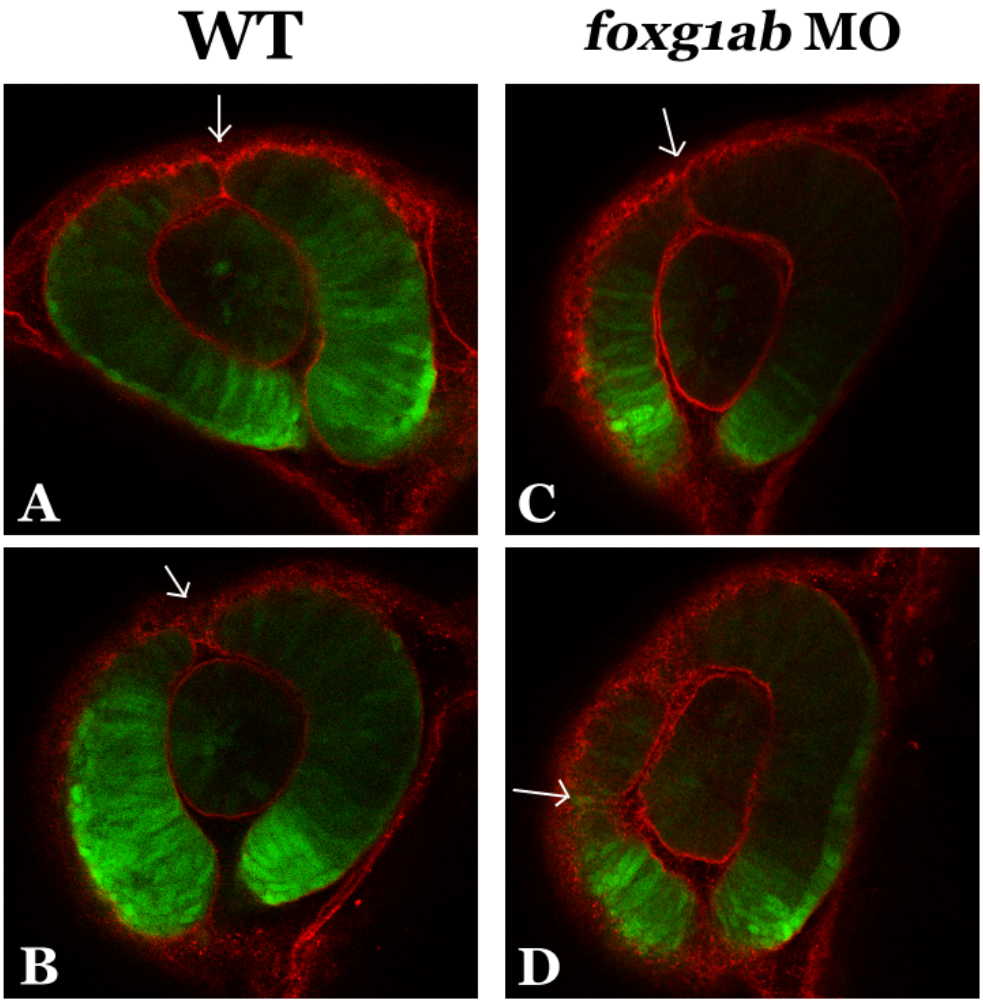
WT
foxg1ab MO
A
C
B
D

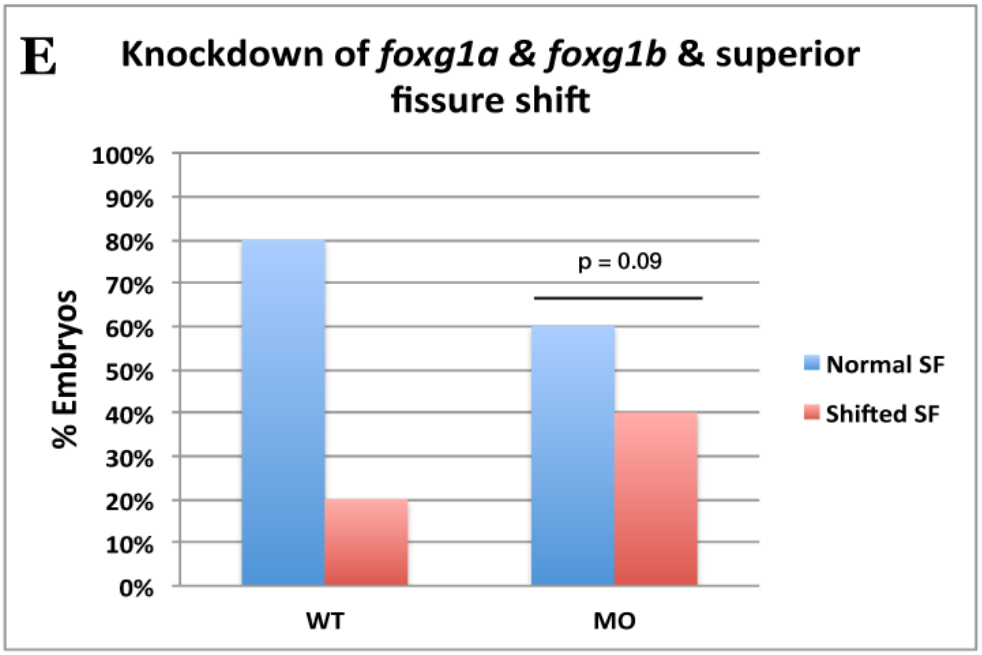
E
Knockdown of foxg1a & foxg1b & superior fissure shift
% Embryos
100%
90%
80%
70%
60%
50%
40%
30%
20%
10%
0%
p = 0.09
WT
MO
Normal SF
Shifted SF

Figure 5-10: Knockdown of *foxg1a* and *foxg1b* results in superior fissure shift.

At approximately 22 hpf, the superior ocular fissure is open in the dorsal retina directly opposite to the inferior ocular fissure at 12 o'clock (A, B, white arrows). Injection of 4 ng of *foxg1a,* 4 ng of *foxg1b* and 2 ng of *p53* MO into *Tg*(*rx3*:*GFP)* embryos results in the shift of the superior fissure from the 12 o'clock position into the nasal portion of the eye (C, D, white arrows). Quantification of fissure formation shows that 80% (n=28/35) of uninjected WT embryos had a normal superior fissure position and 20% (n=7/35) had a shifted superior fissure, while 60% (n=27/45) of morphant embryos had a normal superior fissure position and 36% (n=18/45) had a shifted superior fissure (p=0.09), as determined by a blind scoring assessment and Fisher's Exact Test (E). Visualization of epithelial boundaries was performed by anti-laminin immunofluorescence. Biological replicates n=1, 6 technical replicates.

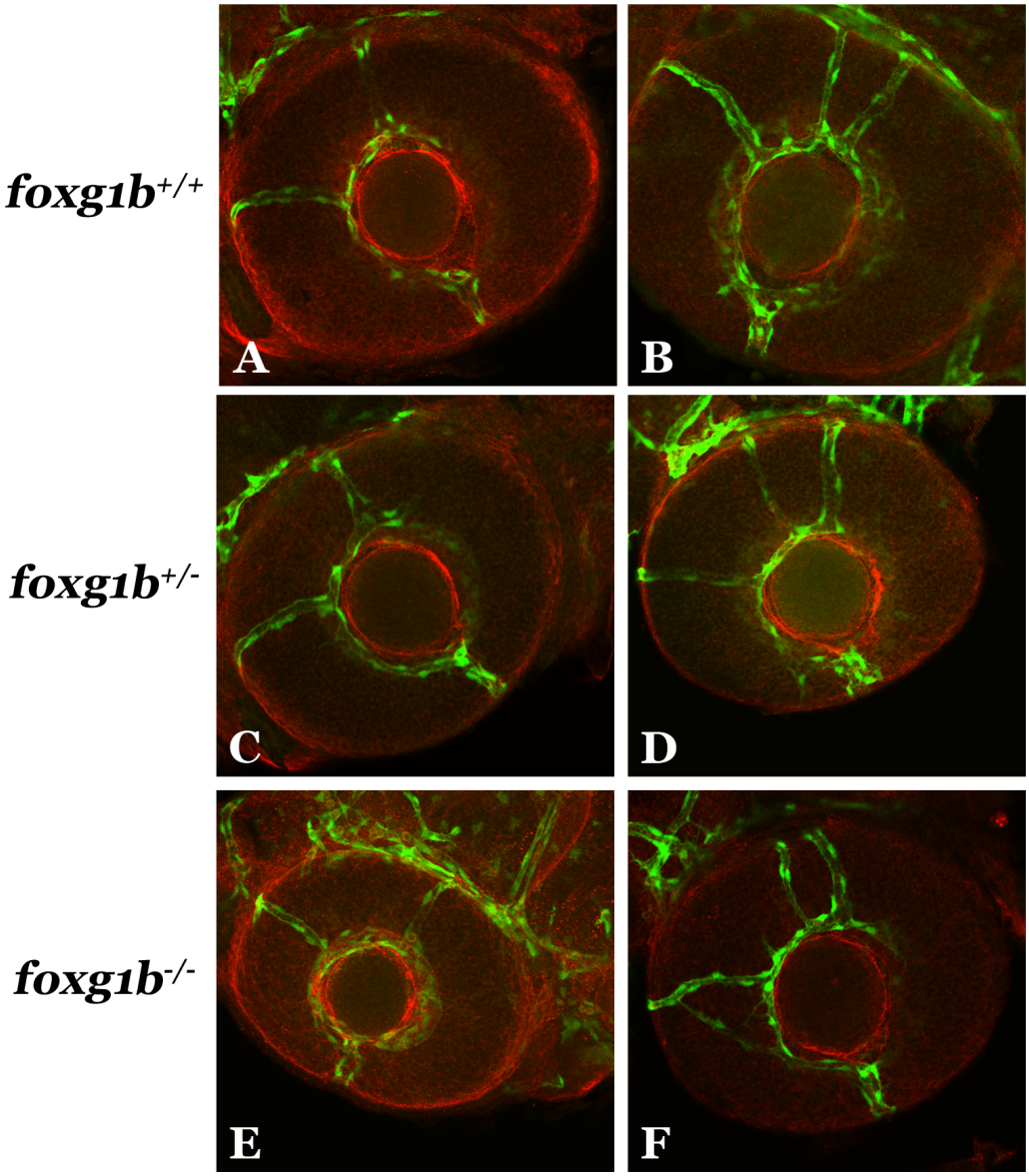

Figure 5-11: *foxg1b*$^{-/-}$ larvae do not have irregular ocular vasculature at 48 hpf.

At 48 hpf, *foxg1b*$^{+/+}$;*Tg*(*flk1:EGFP*) larvae have a ventral radial vessel, a nasal radial vessel, and either one (n=2/6) or two dorsal radial vessels (n=4/6) (A, B). *foxg1b*$^{+/-}$;*Tg*(*flk1:EGFP*) (n=8/11 and n=3/11 with singular or duplicated dorsal radial vessels, respectively) and *foxg1b*$^{-/-}$;*Tg*(*flk1:EGFP*) larvae have highly similar vasculature phenotypes, with no visible abnormalities (n=5/7 and n=2/7 with singular or duplicated dorsal radial vessels, respectively) (C, D, E, F). Biological replicates n=1.

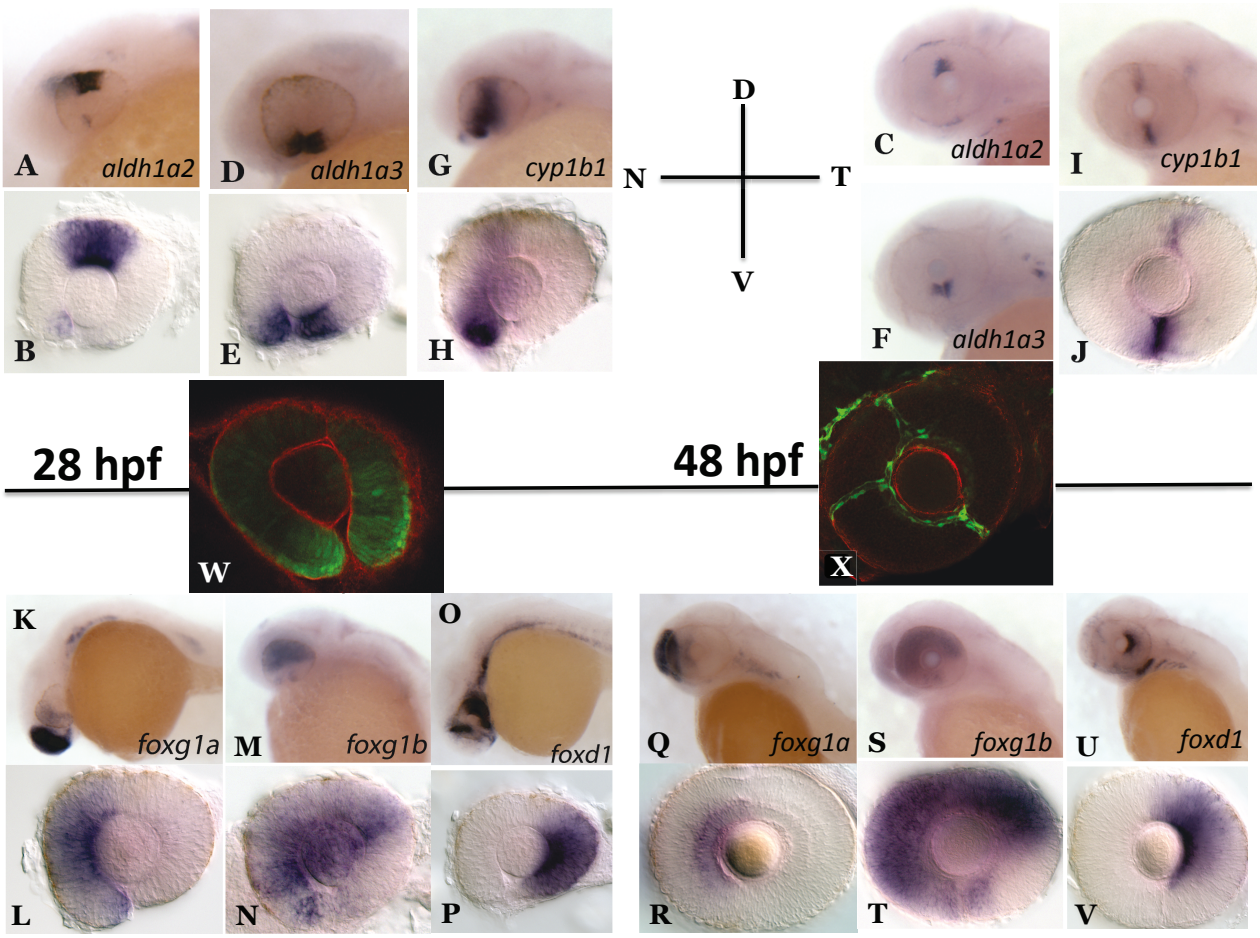

Figure 5-12: Timeline of expression of genes hypothesized to have a role in superior ocular fissure biology.

Expression of genes that code for enzymes that metabolize Vitamin A to its active derivative, retinoic acid, are expressed in the dorsal and ventral retina at the areas of the superior and inferior fissure, respectively, at both 28 and 48 hpf. *aldh1a2* is expressed in the dorsal retina and partially in the ventral retina (A, B, C), *aldh1a3* is expressed in the ventral retina (D, E, F), and *cyp1b1* in both the dorsal and ventral retina (G, H, I, J). The expression of the FOX transcription factors *foxg1a, foxg1b* and *foxd1* correspond with the location of superior fissure formation, with *foxg1a* and *foxg1b* in the nasal retina at 28 and 28 hpf (K, L, M, N, Q, R, S, T), and *foxd1* in the temporal retina at 28 and 48 hpf (O, P, U, V). From approximately 22 – 28 hpf the superior fissure can be visualized using anti-laminin immunofluorescence in *Tg*(*rx3*:*GFP)* embryos (W),

and at 48 hpf the location of the dorsal and ventral radial vessel corresponds with that of the superior and inferior ocular fissures, respectively, visualized in *foxg1b*$^{+/-}$;*Tg*(*flk1:EGFP*) larvae (X).

Supplementary Table 5-1: Clinical features of patients diagnosed with superior coloboma

Patient	Age in 2014	Ocular Phenotypes	Systemic Disease & Other Findings	Genotype
1	30	Unilateral iris coloboma (OS) & anomalous retinal vasculature inferiorly	Tuberous Sclerosis	Unknown
2	25	Large superior iris coloboma (OS), small lenticular coloboma (OS), and small gap in lens zonule (12 o'clock OS), two small superior iris lesions (OD)	Bilateral Congenital Glaucoma Iraqi ancestry	*CYP1B1* – R368H & A287X
3	8	Unilateral lenticular coloboma (OS) at 10 – 11 o'clock	None	Unknown
4	4	Unilateral superior scleral defect (OD), associated superior retinal colobomatous changes, situs inversus (displaced vessels)	None	Unknown
5		Unilateral superior retinal and optic nerve coloboma (OS)	Dandy-Walker Syndrome	Unknown

OD = right eye, OS = left eye

Gene & Patient	NGS Results	Sanger Sequencing Results
BMP2 – Bone Morphogenetic Protein 2		
Patient 1	Heterozygous non-synonymous coding change resulting in E675G (gAa/gGa at position 79808400)	No coding anomalies detected
Patient 2	No coding anomalies detected	No coding anomalies detected
Patient 3	No coding anomalies detected	No coding anomalies detected
Patient 4	Heterozygous intron coding change (position 79754726)	No coding anomalies detected
Patient 5	Data unavailable	No coding anomalies detected
CYP1A1 – Cytochrome P450 1A1		
Patient 1	No coding anomalies detected	Data unavailable
Patient 2	Heterozygous for the non-synonymous coding change P238S (Cct/Tct at position 75014727) & for the non-synonymous coding change I286T (aTt/aCt at position 75014027)	No coding anomalies detected
Patient 3	No coding anomalies detected	Data unavailable
Patient 4	No coding anomalies detected	Data unavailable
Patient 5	Data unavailable	Data unavailable
DACH2 – Dachshund Homolog 2		
Patient 1	N/A	No coding anomalies detected
Patient 2	Heterozygous insertion/deletion at the splice	No coding anomalies

	site acceptor (position 86071034)	detected
Patient 3	Heterozygous non-synonymous coding change resulting in V141G (gTa/gGa at position 85404046)	Negative for V141G
Patient 4	Heterozygous insertion/deletion resulting in a frame shift (position 86071038)	No coding anomalies detected
Patient 5	Data unavailable	No coding anomalies detected
DIXDC1 – DIX domain containing 1		
Patient 1	Homozygous for an insertion/deletion resulting in a frame shift (position 111853106)	No coding anomalies detected
Patient 2	Homozygous for an insertion/deletion resulting in a frame shift (position 111853106)	No coding anomalies detected
Patient 3	Homozygous for an insertion/deletion resulting in a frame shift (position 111853106)	No coding anomalies detected
Patient 4	Heterozygous for a synonymous coding change (ctG/ccT at position 111853110)	No coding anomalies detected
Patient 5	Data unavailable	No coding anomalies detected
FZD4 – Frizzled Family Receptor 4		
Patient 1	Heterozygous non-synonymous coding change resulting in M159I (atG/atA at position 86663321)	Negative for M159I
Patient 2	No coding anomalies detected	No coding anomalies detected
Patient 3	No coding anomalies detected	No coding anomalies detected
Patient 4	Heterozygous synonymous coding change at V101 (gtT/gtA at position 86663495)	Negative for V101
Patient 5	No coding anomalies detected	No coding anomalies

		detected

5.3: Discussion

In this chapter I have described a novel developmental structure, the superior ocular fissure, and basic components of its biology. Five patients presenting with superior ocular coloboma prompted our initial investigation of this structure, and biochemical characterization of a proband's transheterozygous *CYP1B1* mutations began elucidation of the pathogenicity of this disease. The presence of a developmental structure causing superior coloboma, the superior ocular fissure, was confirmed in zebrafish. The biology of this transient structure appears to be highly similar to that of the inferior ocular fissure, with a requirement of RA for closure. However, the superior fissure differs in that the FOX transcription factors *foxd1* and *foxg1* appear to control the location of fissure formation, with knockdown resulting in a duplication or shift, respectively.

While the description in this thesis appears to be the first account of superior coloboma and the superior fissure, examination of early zebrafish literature provides description of a similar developmental structure. Using scanning electron microscopy (SEM), Ellen Schmitt and John Dowling described in 1994 a "posterior groove" in zebrafish that forms at 14 somites, is directly opposite to the choroid fissure at 24 hpf, and assumes a dorsal location at 36 hpf (SCHMITT AND DOWLING 1994). This description of the posterior groove appears to be the actual first account of what we refer to as the superior fissure, although there are a number of discrepancies between their report and ours. Specifically, the authors state that this fissure is present for up to 12 hours, contrary to our findings that it is only present for approximately 2-4 hours. Differences in viewing power between SEM and a stereomicroscope could easily account for this disagreement. Another early paper from the same research group also describes the formation of an ectopic fissure in the dorsal eye, resulting from the implantation of a RA soaked bead (HYATT *et al.* 1996b). The authors state that this fissure appears to be an ectopic choroidal fissure, and that

implantation of the bead was able to induce fissure formation in any quadrant of the eye (HYATT *et al.* 1996b). A repeat of this experiment and examination of patterning changes could reveal whether a second inferior fissure was forming, or if this was an exacerbation of the superior fissure phenotype due to high RA levels. In support of this, mammalian eyes typically have higher RA levels in the ventral eye than in the dorsal eye (MCCAFFERY *et al.* 1992), which can explain the morphological differences in fissure size and duration between the dorsal and ventral retina in teleosts, or represent an unknown mechanism by which differences in RA levels specify dorsal-ventral ocular polarity. Despite these reports of the superior fissure there are no reported cases to date of superior coloboma, which appears to be highly rare as compared to inferior coloboma, ~11% of blind European children are afflicted with inferior coloboma (CHANG *et al.* 2006). The rarity of superior coloboma suggests a highly complex disease etiology and numerous redundancies in place to ensure its correct development, and a likely combination of genomic and environmental factors. Indeed, my preliminary biochemical characterization of the proband's two non-functional *CYP1B1* alleles has indicated that both mutations result in reduced protein production and almost complete loss of enzymatic function. Although we suspect these alleles to be pathogenic with regards to superior coloboma, and the R368H allele has been previously described as pathogenic in glaucoma (REDDY *et al.* 2003), it is highly likely that there are additional contributing factors in this proband. In support of this theory, none of the other superior coloboma probands have *CYP1B1* mutations, and RA deficiency during gestation cannot be ruled out, thereby implicating other causative alleles. However, the rarity and complexity of superior coloboma may account for the lack of prior investigations concerning the biology of its structure, the superior fissure, despite previous reports of this developmental structure by another name.

Based on the proband's *CYP1B1* mutations, I addressed the apparent requirement for an active metabolite of Cyp1b1, RA, in ocular fissure closure. A role for RA in ocular development has been

extensively documented in human, rodent and zebrafish, with ocular defects and coloboma resulting from a deficiency or excess of RA during development (Chapter 1 – Retinoic Acid). The localization of *cyp1b1, aldh1a2* and *aldh1a3* transcripts correlates with that of the superior and inferior fissures, although my description of the expression pattern of *cyp1b1* in zebrafish is relatively novel, with limited reports of its expression during development (YIN *et al.* 2008), and none with regards to its role in ocular development. *gdf6a*$^{-/-}$ embryos have severe inferior coloboma and aberrant expression of RA metabolic genes, with a loss of *aldh1a2* and expansion of *aldh1a3* expression (FRENCH *et al.* 2009), and we have initial reports of the loss of dorsal *cyp1b1* expression. The aberrant expression of these genes may account for why the loss of an initiator for dorsal retinal identity results in coloboma of the inferior eye. In support of this theory, supplementation of *gdf6a*$^{-/-}$ embryos with retinol rescues coloboma in approximately 60% of mutants. However, explaining how this supplementation leads to rescue is difficult to discern. It is possible that the upregulation in *aldh1a3,* a highly efficient metabolizer of retinol, has used up all of the maternal supplies early in ocular development, and supplementation provides another source. It is also likely that expression of *cyp26a1* and *cyp26b1* in *gdf6a*$^{-/-}$ embryos is aberrant, and these enzymes could be breaking down RA at an increased rate. Additionally, it is still unknown how RA mediates ocular fissure closure. While is it probable that fissure closure is occurring by attraction of migrating POM cells, and integration of these cells into the eye and formation of derivatives, such as tissues of the anterior segment (HOLT 1980; MATT *et al.* 2005; LUPO *et al.* 2011; BOHNSACK AND KAHANA 2013), exact mechanisms remain to be described. In the murine system, RA is required for cell death at the inferior fissure (MATT *et al.* 2005; MATT *et al.* 2008), while in zebrafish RA stimulates proliferation for fissure closure (HYATT *et al.* 1996b; BOHNSACK AND KAHANA 2013). Reports also indicate that RA is not the only mediator of ocular fissure closure through regulation of NCCs, with the thyroid hormone receptor heterodimerizing with RAR for transcriptional regulation of NCC migration (BOHNSACK AND KAHANA 2013). In this respect, future work with regards to the thyroid hormone metabolic

pathway in patients and zebrafish could provide further insight into ocular fissure biology. It is also likely that there are other metabolites of Cyp1b1 in the eye with a role in ocular development.

As the *CYP1B1* proband is afflicted with bilateral glaucoma, a disease of the anterior segment, it is possible that superior coloboma is also a result of anterior segment malformation, which is often due to improper migration and cell cycle regulation of neural crest and POM cells. *PITX2* coding anomalies result in Axenfeld-Rieger syndrome (TUMER AND BACH-HOLM 2009), and *pitx2* has been shown to be a downstream transcriptional target of RA for regulation of NCCs (BOHNSACK *et al.* 2012). Further support for this theory is provided by our observations that the superior fissure may be more akin to a dorsal groove than a fully penetrant fissure. This groove could act as a channel for the migration of POM cells into the superior and anterior portions of the eye, and for guidance of vasculature growth. This could explain why the superior fissure is highly transient and difficult to visualize as compared to the fully penetrant inferior fissure. Investigation of patients and animal models with anterior segment anomalies could yield insight into disease etiology.

While the zebrafish model system is a powerful tool, the presence of a superior fissure in other model organisms, such as chick and mouse should be investigated. In zebrafish, the time course of superior fissure opening and closure using SEM technology should be documented, and cellular movements closely examined, as this could provide insights as to why the SF opens. Namely, is the superior fissure required for the same purpose as the inferior, i.e. for entry of migrating POM cells and blood vessels, and if so, why is there a significant difference in morphologies of the fissures. To discern this, one could use transgenic zebrafish lines that have fluorescently labeled NCCs and POM cells, and visualize their respective migration during development. Using lineage-tracing experiments of these labeled NCC and POM cells, it would

be possible to determine which derivatives are forming from the cells that enter through the superior fissure, and how aberrant migration or differentiation contributes to coloboma.

Future experiments should address the biological concentration of RA required for optimal ocular development, along with differences in RA concentration between the superior and inferior eye that may result in differential ocular morphogenesis. To determine ocular RA concentrations, one could use high-performance liquid chromatography (HPLC) on eyes extracted during embryonic development (MCCAFFRERY *et al.* 1993), along with a novel technology that uses fluorescence resonance energy transfer (FRET) to visualize free RA in zebrafish (SHIMOZONO *et al.* 2013). Downstream targets of RA transcriptional control should be discerned by performing RNA sequencing on WT, RA supplemented or RA depleted zebrafish eyes at different developmental stages. Lastly, the creation of a *cyp1b1* mutant fish and examination of predicted superior fissure phenotypes would be of great value to model the ocular disease present in the patient. Anticipating a sustained superior fissure opening, a rescue of the phenotype with *cyp1b1* and *CYP1B1* RNA would confirm the requirement of this enzyme for fissure closure, without rescue provided by R368H and A287X RNA.

The antagonistic interaction between *foxd1, foxg1a* and *foxg1b* appears to control the site of superior fissure formation. Previously known as Brain Factor-1 (BF-1, *foxg1*) and Brain Factor-2 (BF-2, *foxd1),* both transcription factors have extensive roles in brain, eye and ear development in human, mouse, chick and zebrafish (HATINI *et al.* 1994; XUAN *et al.* 1995; HANASHIMA *et al.* 2004; PRATT *et al.* 2004). In mammalian brain development, *Foxg1* controls cellular proliferation and differentiation (XUAN *et al.* 1995; HANASHIMA *et al.* 2004) and coding anomalies in *FOXG1* result in Rett syndrome (JACOB *et al.* 2009). With regards to ocular development, both *foxd1* and *foxg1* pattern the optic chiasm, temporal and nasal retina, and control the downstream effectors eph and ephrin that are critical for topographic mapping,

axonal projection and pathfinding (YUASA *et al.* 1996; HERRERA *et al.* 2004; PRATT *et al.* 2004; TIAN *et al.* 2008; CARRERES *et al.* 2011). Given these extensive roles in brain development and retinal patterning, the definition of another ocular boundary and control of a neural developmental structure is in keeping with previously defined function. However, how *foxg1* and *foxd1* mediate superior fissure location remains unknown. Although there is clear definition at 12 and 6 o'clock by *foxg1a* and *foxd1,* transcript localization of *foxg1b* is confounding, but clearly necessary for fissure formation, since knockdown of only *foxg1a* does not result in any phenotypes. I hypothesize that the antagonism of these factors provides permissive cues for superior fissure formation, as knockdown of transcripts results in weakened antagonism and ectopic fissure formation. Determining the efficacy of knockdown using these MOs and protein production could provide insights, as would the knockdown of all three transcription factors, with the expectation that many superior fissures would form. Perhaps, as found with implantation of a RA soaked bead, the entire eye is permissive to fissure formation, with *foxd1* and *foxg1* mediating inhibition, with the exception of a boundary of low transcript expression at 12 o'clock. This area could also be permissive for the expression of *cyp1b1,* whose expression pattern is highly ectopic and expanded in *foxg1* morphants. In keeping with this, *foxd1* and *foxg1* appear to partially mediate the expression of *cyp1b1, aldh1a2* and *aldh1a3,* but it is unclear whether the location of RA synthesis determines the location of fissure formation, or if the formation of the fissure promotes expression of the RA genes. To discern whether *foxg1* and *foxd1* are responsible for expression of these genes, and to identify others that may be responsible for fissure formation, RNA sequencing analysis could be performed on WT and morphant eyes and their transcriptomes compared.

A potential developmental role of the superior fissure, consistent with the synthesis of RA at this location, is to allow for passage of migrating POM cells and ocular blood vessels, similar to the inferior fissure. However, preliminary examination of *foxg1b*$^{-/-}$ larvae with fluorescently labeled

blood vessels does not demonstrate any anomalies in the positioning of the dorsal or nasal radial vessels, and the occasional formation of two dorsal radial vessels is typical, since blood vessel development is stochastic. Further examination of blood vessel phenotypes should be carried out with the addition of *foxg1a* MO, by the creation of double *foxg1a* and *foxg1b* mutant embryos, with *foxd1* MO and *foxd1* mutants, and at various time points of superior fissure formation. Additionally, analysis of the requirement for the fissure for entry of migrating cells could be done by outcrossing *foxg1* and *foxd1* mutant lines to reporter lines that label NCCs and POM cells. The confirmation of a superior fissure and the role that *foxd1* and *foxg1* play in its biology should be further examined in zebrafish and in other model organisms.

Chapter 6

General Discussion and Conclusions

In my thesis research, I have characterized the apoptotic and proliferative defects underlying the microphthalmia in *gdf6a*$^{-/-}$ embryos, and for the first time I have shown the polarization of the ciliary marginal zone by the transcription factors *foxi1* and *foxi2*. I have described two different *foxi1* phenotypes resulting from different knockdown technologies, and have demonstrated that *foxi2* has a role in ocular growth and retinal patterning. Finally, I have reported the existence of a novel developmental structure, the superior ocular fissure, whose failed closure appears to result from insufficient retinoic acid, and the control of superior ocular fissure location by *foxd1* and *foxg1*.

Gdf6a regulates the cell cycle during retinal development

Gdf6a is essential for ocular development, and is required for dorsal retinal patterning and lens formation, with loss of this gene resulting in microphthalmia, anophthalmia and coloboma, demonstrated both in zebrafish and in patients with *GDF6* coding anomalies (ASAI-COAKWELL *et al.* 2007; ASAI-COAKWELL *et al.* 2009; FRENCH *et al.* 2009; GOSSE AND BAIER 2009; DEN HOLLANDER *et al.* 2010). However, the mechanisms underlying how reduced transcript levels of *gdf6a* result in a small eye phenotype remains to be defined. We have shown, contrary to previous reports (HANEL AND HENSEY 2006; DEN HOLLANDER *et al.* 2010), that apoptotic defects are not the sole contributing factor. A reduced number of progenitor cells, a significant decrease in the expression of cell cycle regulators, and decreased proliferation during ocular development all contribute to microphthalmia. However, it is likely that there are additional, undefined mechanisms by which Gdf6a is controlling ocular size and development, as microphthalmia is present at 24 hpf in *gdf6a* mutants, and the cell cycle defects described here are from 28 hpf – 4 dpf. Gdf6a could have roles in specification of ocular progenitors that contribute to formation of the retinal anlage, or in the differentiation of these progenitors, with failure of either of these resulting in microphthalmia. Further roles of Gdf6a in regulation of ocular development still remain to be discerned. Intriguingly, these results also indicate that genes with roles in ocular

patterning are also required for control of the cell cycle, with the mechanisms remaining to be defined. Microarray analysis to determine potential downstream effectors of *gdf6a* and their subsequent validation by ISH revealed significant ocular changes in the transcription factors *foxi1* and *foxi2,* whose expression polarizes the ciliary marginal zone, an area of retinal progenitor cells, into dorsal and ventral domains. This is the first report characterizing the CMZ as an area with spatial identity, and has implications for therapies pertaining to ocular growth and repair. Finally, the ventral CMZ patterning gene, *foxi2,* appears to lie on a converging pathway with *gdf6a* in the determination of ocular size, and provides compensation for ocular size in both *gdf6a*$^{+/-}$ and *gdf6a*$^{-/-}$ embryos during development. These findings are highly significant with regards to defining a mechanism behind ocular disease and the developmental of preventative therapeutics.

Foxi1 and foxi2 have roles in retinal patterning and ocular growth

The discovery that *foxi1* and *foxi2* polarize the ciliary marginal zone prompted my investigation into their role in ocular development. Use of antisense MO technology implicated *foxi1* in the maintenance of retinal patterning and ocular growth, much like its upstream effector, *gdf6a*. However, preliminary analysis of the *foo* mutant, previously characterized for otic vesicle defects and created in a retro-viral insertion screen, indicated that the loss of *foxi1* has no consequences on ocular development. The difference in phenotypes between these technologies highlights a challenge the zebrafish research community faces as the generation of mutant lines becomes easier. In particular, a large-scale mutant screen and analysis of phenotypes showed that only 6% of disruptive alleles resulted in obvious phenotypes (KETTLEBOROUGH *et al.* 2013), which is in sharp contrast to previously reported phenotypes obtained using morpholinos. These findings have been attributed to toxicity and non-specificity associated with the random knockdown of other genes in addition to the target gene. However, an alternative theory postulates that zebrafish have remarkable plasticity in fitting with their regenerative capabilities (GEMBERLING

et al. 2013), and while unable to cope in the short-term with the knockdown of a gene, can compensate from the onset of development for a constitutional mutation by upregulation of other genes that perform redundant functions. In particular, duplication of the teleost genome supports this explanation, and although only approximately 25% of duplicated genes were retained with neo and sub functionalization, there appears to be a high degree of redundancy, particularly for critical developmental pathways. The roles of *foxi1* and *foxi2* merit further investigation based on intriguing changes in the expression of RA synthesizing enzymes, in addition to previous reports of a role for *foxi1* in NCC migration and survival. It is possible that *foxi1* and foxi2 perform similar roles in migration of NCCs to the eye by regulation of RA signaling. Additionally, examination of human orthologues and investigation of disease resulting from coding anomalies in *foxi1* and *foxi2* would provide insight into the roles of these genes in mammalian ocular development.

The superior ocular fissure as a novel developmental structure

The superior ocular fissure is a novel developmental structure whose biology remains to be fully elucidated. Although our characterization appears to be one of discovery, early zebrafish literature indicates that this may not be the first description of this fissure despite its presence remaining unreported for approximately 20 years following initial reports. A possible explanation for this is the prevailing opinion of the zebrafish community regarding the presence of only one ocular fissure, with previous reports being rejected or rationalized as a ventralization of the dorsal eye and the formation of a second choroidal fissure. The biology of the structure presents several challenges to its future study, as it is highly transient, does not appear to fully penetrate ocular tissue, has a complex and robust etiology and to date, there are only 5 documented cases of failed fissure closure worldwide. In comparison, the inferior fissure is highly apparent during development and there are thousands of inferior coloboma cases reported to date in both patients and model organisms. What appears to be central to closure of

both ocular fissures is an unknown, homeostatic concentration of retinoic acid. Unfortunately, it is very difficult to discern the required concentration of RA in the eye during development, and excess RA is just as damaging as a deficiency. Future research should target this deficiency in our knowledge for a progression to preventative therapeutics that supplement a molecule with a very narrow therapeutic index. When compared to the inferior fissure, the superior fissure has a different set of mechanisms in place to control the location of its formation. Namely, how antagonism between two transcription factors, *foxd1* and *foxg1,* provides a permissive cue that allows for fissure formation is unknown. However, the identification of these cues, whether they mediate expression of *cyp1b1,* and what downstream effectors facilitate the separation of ocular tissue, remains to be determined. With regards to developmental disorders, elucidation of the biology of the superior fissure will provide insights about other diseases of failed fissure closure, such as spina bifida and cleft palate, and has the potential for the generation of numerous treatments and preventative therapeutics.

In conclusion, I have characterized the apoptotic and proliferative defects present in a microphthalmic BMP model. For the first time, I have shown the polarization of the ciliary marginal zone by *foxi1* and *foxi2,* and demonstrated a role for these transcription factors in ocular patterning and development. Finally, I have reported the existence of a novel developmental structure, the superior ocular fissure, described a requirement for retinoic acid in the closure of the ocular fissures, and implicated *foxg1* and *foxd1* in localizing the formation of the superior fissure.

Bibliography

Abouzeid, H., T. Favez, A. Schmid, C. Agosti, M. Youssef *et al.*, 2014 Mutations in ALDH1A3 Represent a Frequent Cause of Microphthalmia/Anophthalmia in Consanguineous Families. Hum Mutat 35**:** 949-953.

Amsterdam, A., S. Burgess, G. Golling, W. Chen, Z. Sun *et al.*, 1999 A large-scale insertional mutagenesis screen in zebrafish. Genes Dev 13**:** 2713-2724.

Amsterdam, A., R. M. Nissen, Z. Sun, E. C. Swindell, S. Farrington *et al.*, 2004 Identification of 315 genes essential for early zebrafish development. Proc Natl Acad Sci U S A 101**:** 12792-12797.

Asai-Coakwell, M., C. R. French, K. M. Berry, M. Ye, R. Koss *et al.*, 2007 GDF6, a novel locus for a spectrum of ocular developmental anomalies. Am J Hum Genet 80**:** 306-315.

Asai-Coakwell, M., C. R. French, M. Ye, K. Garcha, K. Bigot *et al.*, 2009 Incomplete penetrance and phenotypic variability characterize Gdf6-attributable oculo-skeletal phenotypes. Hum Mol Genet 18**:** 1110-1121.

Asai-Coakwell, M., L. March, X. H. Dai, M. Duval, I. Lopez *et al.*, 2013 Contribution of growth differentiation factor 6-dependent cell survival to early-onset retinal dystrophies. Hum Mol Genet 22**:** 1432-1442.

Bagiyeva, S., G. Marfany, O. Gonzalez-Angulo and R. Gonzalez-Duarte, 2007 Mutational screening of CYP1B1 in Turkish PCG families and functional analyses of newly detected mutations. Mol Vis 13**:** 1458-1468.

Bakrania, P., M. Efthymiou, J. C. Klein, A. Salt, D. J. Bunyan *et al.*, 2008 Mutations in BMP4 cause eye, brain, and digit developmental anomalies: overlap between the BMP4 and hedgehog signaling pathways. Am J Hum Genet 82**:** 304-319.

Bardakjian, T. M., and A. Schneider, 2011 The genetics of anophthalmia and microphthalmia. Curr Opin Ophthalmol 22**:** 309-313.

Behesti, H., J. K. Holt and J. C. Sowden, 2006 The level of BMP4 signaling is critical for the regulation of distinct T-box gene expression domains and growth along the dorso-ventral axis of the optic cup. BMC Dev Biol 6**:** 62.

Benayoun, B. A., S. Caburet and R. A. Veitia, 2011 Forkhead transcription factors: key players in health and disease. Trends Genet 27**:** 224-232.

Berry, F. B., M. A. Lines, J. M. Oas, T. Footz, D. A. Underhill *et al.*, 2006 Functional interactions between FOXC1 and PITX2 underlie the sensitivity to FOXC1 gene dose in Axenfeld-Rieger syndrome and anterior segment dysgenesis. Hum Mol Genet 15**:** 905-919.

Bessa, J., M. J. Tavares, J. Santos, H. Kikuta, M. Laplante *et al.*, 2008 meis1 regulates cyclin D1 and c-myc expression, and controls the proliferation of the multipotent cells in the early developing zebrafish eye. Development 135**:** 799-803.

Bielen, H., and C. Houart, 2012 BMP signaling protects telencephalic fate by repressing eye identity and its Cxcr4-dependent morphogenesis. Dev Cell 23**:** 812-822.

Bohnsack, B. L., and A. Kahana, 2013 Thyroid hormone and retinoic acid interact to regulate zebrafish craniofacial neural crest development. Dev Biol 373**:** 300-309.

Bohnsack, B. L., D. S. Kasprick, P. E. Kish, D. Goldman and A. Kahana, 2012 A zebrafish model of axenfeld-rieger syndrome reveals that pitx2 regulation by retinoic acid is essential for ocular and craniofacial development. Invest Ophthalmol Vis Sci 53**:** 7-22.

Boisset, G., and D. F. Schorderet, 2012 Zebrafish hmx1 promotes retinogenesis. Exp Eye Res 105**:** 34-42.
Bower, M., R. Salomon, J. Allanson, C. Antignac, F. Benedicenti *et al.*, 2012 Update of PAX2 mutations in renal coloboma syndrome and establishment of a locus-specific database. Hum Mutat 33**:** 457-466.
Bronner, M. E., and N. M. LeDouarin, 2012 Development and evolution of the neural crest: an overview. Dev Biol 366**:** 2-9.
Brownell, I., M. Dirksen and M. Jamrich, 2000 Forkhead Foxe3 maps to the dysgenetic lens locus and is critical in lens development and differentiation. Genesis 27**:** 81-93.
Carlsson, P., and M. Mahlapuu, 2002 Forkhead transcription factors: key players in development and metabolism. Dev Biol 250**:** 1-23.
Carreres, M. I., A. Escalante, B. Murillo, G. Chauvin, P. Gaspar *et al.*, 2011 Transcription factor Foxd1 is required for the specification of the temporal retina in mammals. J Neurosci 31**:** 5673-5681.
Casey, J., R. Kawaguchi, M. Morrissey, H. Sun, P. McGettigan *et al.*, 2011 First implication of STRA6 mutations in isolated anophthalmia, microphthalmia, and coloboma: a new dimension to the STRA6 phenotype. Hum Mutat 32**:** 1417-1426.
Cepko, C. L., C. P. Austin, X. Yang, M. Alexiades and D. Ezzeddine, 1996 Cell fate determination in the vertebrate retina. Proc Natl Acad Sci U S A 93**:** 589-595.
Cermak, T., E. L. Doyle, M. Christian, L. Wang, Y. Zhang *et al.*, 2011 Efficient design and assembly of custom TALEN and other TAL effector-based constructs for DNA targeting. Nucleic Acids Res 39**:** e82.
Cha, S. W., M. McAdams, J. Kormish, C. Wylie and M. Kofron, 2012 Foxi2 is an animally localized maternal mRNA in Xenopus, and an activator of the zygotic ectoderm activator Foxi1e. PLoS One 7**:** e41782.
Chambers, D., L. Wilson, M. Maden and A. Lumsden, 2007 RALDH-independent generation of retinoic acid during vertebrate embryogenesis by CYP1B1. Development 134**:** 1369-1383.
Chang, L., D. Blain, S. Bertuzzi and B. P. Brooks, 2006 Uveal coloboma: clinical and basic science update. Curr Opin Ophthalmol 17**:** 447-470.
Chassaing, N., N. Ragge, A. Kariminejad, A. Buffet, S. Ghaderi-Sohi *et al.*, 2013 Mutation analysis of the STRA6 gene in isolated and non-isolated anophthalmia/microphthalmia. Clin Genet 83**:** 244-250.
Chuang, J. C., and P. A. Raymond, 2001 Zebrafish genes rx1 and rx2 help define the region of forebrain that gives rise to retina. Dev Biol 231**:** 13-30.
Cirillo, L. A., and K. S. Zaret, 2007 Specific interactions of the wing domains of FOXA1 transcription factor with DNA. J Mol Biol 366**:** 720-724.
Clark, K. L., E. D. Halay, E. Lai and S. K. Burley, 1993 Co-crystal structure of the HNF-3/fork head DNA-recognition motif resembles histone H5. Nature 364**:** 412-420.
Crisponi, L., M. Deiana, A. Loi, F. Chiappe, M. Uda *et al.*, 2001 The putative forkhead transcription factor FOXL2 is mutated in blepharophimosis/ptosis/epicanthus inversus syndrome. Nat Genet 27**:** 159-166.
Dahm, R., H. B. Schonthaler, A. S. Soehn, J. van Marle and G. F. Vrensen, 2007 Development and adult morphology of the eye lens in the zebrafish. Exp Eye Res 85**:** 74-89.
Dang, C. V., 2012 MYC on the path to cancer. Cell 149**:** 22-35.

Davoody, A., I. P. Chen, R. Nanda, F. Uribe and E. J. Reichenberger, 2012 Oculofaciocardiodental syndrome: a rare case and review of the literature. Cleft Palate Craniofac J 49**:** e55-60.
den Hollander, A. I., J. Biyanwila, P. Kovach, T. Bardakjian, E. I. Traboulsi *et al.*, 2010 Genetic defects of GDF6 in the zebrafish out of sight mutant and in human eye developmental anomalies. BMC Genet 11**:** 102.
Dhomen, N. S., K. S. Balaggan, R. A. Pearson, J. W. Bainbridge, E. M. Levine *et al.*, 2006 Absence of chx10 causes neural progenitors to persist in the adult retina. Invest Ophthalmol Vis Sci 47**:** 386-396.
Dowling, J. E., and G. Wald, 1960 The Biological Function of Vitamin a Acid. Proc Natl Acad Sci U S A 46**:** 587-608.
Duester, G., 2008 Retinoic acid synthesis and signaling during early organogenesis. Cell 134**:** 921-931.
Duggan, C. D., S. DeMaria, A. Baudhuin, D. Stafford and J. Ngai, 2008 Foxg1 is required for development of the vertebrate olfactory system. J Neurosci 28**:** 5229-5239.
Eisen, J. S., and J. C. Smith, 2008 Controlling morpholino experiments: don't stop making antisense. Development 135**:** 1735-1743.
Ekker, S. C., A. R. Ungar, P. Greenstein, D. P. von Kessler, J. A. Porter *et al.*, 1995 Patterning activities of vertebrate hedgehog proteins in the developing eye and brain. Curr Biol 5**:** 944-955.
Fadool, J. M., and J. E. Dowling, 2008 Zebrafish: a model system for the study of eye genetics. Prog Retin Eye Res 27**:** 89-110.
Fang, J., S. L. Dagenais, R. P. Erickson, M. F. Arlt, M. W. Glynn *et al.*, 2000 Mutations in FOXC2 (MFH-1), a forkhead family transcription factor, are responsible for the hereditary lymphedema-distichiasis syndrome. Am J Hum Genet 67**:** 1382-1388.
Fares-Taie, L., S. Gerber, N. Chassaing, J. Clayton-Smith, S. Hanein *et al.*, 2013 ALDH1A3 mutations cause recessive anophthalmia and microphthalmia. Am J Hum Genet 92**:** 265-270.
French, C. R., T. Erickson, D. V. French, D. B. Pilgrim and A. J. Waskiewicz, 2009 Gdf6a is required for the initiation of dorsal-ventral retinal patterning and lens development. Dev Biol 333**:** 37-47.
French, C. R., T. R. Stach, L. D. March, O. J. Lehmann and A. J. Waskiewicz, 2013 Apoptotic and proliferative defects characterize ocular development in a microphthalmic BMP model. Invest Ophthalmol Vis Sci 54**:** 4636-4647.
Fuhrmann, S., 2010 Eye morphogenesis and patterning of the optic vesicle. Curr Top Dev Biol 93**:** 61-84.
Gammill, L. S., and M. Bronner-Fraser, 2003 Neural crest specification: migrating into genomics. Nat Rev Neurosci 4**:** 795-805.
Gemberling, M., T. J. Bailey, D. R. Hyde and K. D. Poss, 2013 The zebrafish as a model for complex tissue regeneration. Trends Genet 29**:** 611-620.
Gerth-Kahlert, C., K. Williamson, M. Ansari, J. K. Rainger, V. Hingst *et al.*, 2013 Clinical and mutation analysis of 51 probands with anophthalmia and/or severe microphthalmia from a single center. Mol Genet Genomic Med 1**:** 15-31.
Golling, G., A. Amsterdam, Z. Sun, M. Antonelli, E. Maldonado *et al.*, 2002 Insertional mutagenesis in zebrafish rapidly identifies genes essential for early vertebrate development. Nat Genet 31**:** 135-140.

Gongal, P. A., and A. J. Waskiewicz, 2008 Zebrafish model of holoprosencephaly demonstrates a key role for TGIF in regulating retinoic acid metabolism. Hum Mol Genet 17**:** 525-538.
Gonzalez-Rodriguez, J., E. L. Pelcastre, J. L. Tovilla-Canales, J. E. Garcia-Ortiz, M. Amato-Almanza *et al.*, 2010 Mutational screening of CHX10, GDF6, OTX2, RAX and SOX2 genes in 50 unrelated microphthalmia-anophthalmia-coloboma (MAC) spectrum cases. Br J Ophthalmol 94**:** 1100-1104.
Gosse, N. J., and H. Baier, 2009 An essential role for Radar (Gdf6a) in inducing dorsal fate in the zebrafish retina. Proc Natl Acad Sci U S A 106**:** 2236-2241.
Gregory-Evans, C. Y., M. J. Williams, S. Halford and K. Gregory-Evans, 2004 Ocular coloboma: a reassessment in the age of molecular neuroscience. J Med Genet 41**:** 881-891.
Grocott, T., S. Johnson, A. P. Bailey and A. Streit, 2011 Neural crest cells organize the eye via TGF-beta and canonical Wnt signalling. Nat Commun 2**:** 265.
Hanashima, C., S. C. Li, L. Shen, E. Lai and G. Fishell, 2004 Foxg1 suppresses early cortical cell fate. Science 303**:** 56-59.
Hanel, M. L., and C. Hensey, 2006 Eye and neural defects associated with loss of GDF6. BMC Dev Biol 6**:** 43.
Hannenhalli, S., and K. H. Kaestner, 2009 The evolution of Fox genes and their role in development and disease. Nat Rev Genet 10**:** 233-240.
Hata, A., G. Lagna, J. Massague and A. Hemmati-Brivanlou, 1998 Smad6 inhibits BMP/Smad1 signaling by specifically competing with the Smad4 tumor suppressor. Genes Dev 12**:** 186-197.
Hatini, V., W. Tao and E. Lai, 1994 Expression of winged helix genes, BF-1 and BF-2, define adjacent domains within the developing forebrain and retina. J Neurobiol 25**:** 1293-1309.
Herrera, E., R. Marcus, S. Li, S. E. Williams, L. Erskine *et al.*, 2004 Foxd1 is required for proper formation of the optic chiasm. Development 131**:** 5727-5739.
Hill, R. E., J. Favor, B. L. Hogan, C. C. Ton, G. F. Saunders *et al.*, 1992 Mouse Small eye results from mutations in a paired-like homeobox-containing gene. Nature 355**:** 750.
Hogan, B. L., 1996 Bone morphogenetic proteins: multifunctional regulators of vertebrate development. Genes Dev 10**:** 1580-1594.
Holly, V. L., S. A. Widen, J. K. Famulski and A. J. Waskiewicz, 2014 Sfrp1a and Sfrp5 function as positive regulators of Wnt and BMP signaling during early retinal development. Dev Biol 388**:** 192-204.
Holt, C., 1980 Cell movements in Xenopus eye development. Nature 287**:** 850-852.
Hornby, S. J., C. E. Gilbert, J. K. Rahi, A. K. Sil, Y. Xiao *et al.*, 2000 Regional variation in blindness in children due to microphthalmos, anophthalmos and coloboma. Ophthalmic Epidemiol 7**:** 127-138.
Howe, K., M. D. Clark, C. F. Torroja, J. Torrance, C. Berthelot *et al.*, 2013 The zebrafish reference genome sequence and its relationship to the human genome. Nature 496**:** 498-503.
Hu, M., and S. S. Easter, 1999 Retinal neurogenesis: the formation of the initial central patch of postmitotic cells. Dev Biol 207**:** 309-321.
Huillard, E., D. Laugier and M. Marx, 2005 Defects in chicken neuroretina misexpressing the BMP antagonist Drm/Gremlin. Dev Biol 283**:** 335-344.

Hulander, M., A. E. Kiernan, S. R. Blomqvist, P. Carlsson, E. J. Samuelsson *et al.*, 2003 Lack of pendrin expression leads to deafness and expansion of the endolymphatic compartment in inner ears of Foxi1 null mutant mice. Development 130**:** 2013-2025.
Hulander, M., W. Wurst, P. Carlsson and S. Enerback, 1998 The winged helix transcription factor Fkh10 is required for normal development of the inner ear. Nat Genet 20**:** 374-376.
Hyatt, G. A., E. A. Schmitt, J. M. Fadool and J. E. Dowling, 1996a Retinoic acid alters photoreceptor development in vivo. Proc Natl Acad Sci U S A 93**:** 13298-13303.
Hyatt, G. A., E. A. Schmitt, N. Marsh-Armstrong, P. McCaffery, U. C. Drager *et al.*, 1996b Retinoic acid establishes ventral retinal characteristics. Development 122**:** 195-204.
Hyatt, G. A., E. A. Schmitt, N. R. Marsh-Armstrong and J. E. Dowling, 1992 Retinoic acid-induced duplication of the zebrafish retina. Proc Natl Acad Sci U S A 89**:** 8293-8297.
Isken, A., M. Golczak, V. Oberhauser, S. Hunzelmann, W. Driever *et al.*, 2008 RBP4 disrupts vitamin A uptake homeostasis in a STRA6-deficient animal model for Matthew-Wood syndrome. Cell Metab 7**:** 258-268.
Jacob, F. D., V. Ramaswamy, J. Andersen and F. V. Bolduc, 2009 Atypical Rett syndrome with selective FOXG1 deletion detected by comparative genomic hybridization: case report and review of literature. Eur J Hum Genet 17**:** 1577-1581.
Janssen, N., J. E. Bergman, M. A. Swertz, L. Tranebjaerg, M. Lodahl *et al.*, 2012 Mutation update on the CHD7 gene involved in CHARGE syndrome. Hum Mutat 33**:** 1149-1160.
Jin, S. W., D. Beis, T. Mitchell, J. N. Chen and D. Y. Stainier, 2005 Cellular and molecular analyses of vascular tube and lumen formation in zebrafish. Development 132**:** 5199-5209.
Kallen, B., E. Robert and J. Harris, 1996 The descriptive epidemiology of anophthalmia and microphthalmia. Int J Epidemiol 25**:** 1009-1016.
Kari, G., U. Rodeck and A. P. Dicker, 2007 Zebrafish: an emerging model system for human disease and drug discovery. Clin Pharmacol Ther 82**:** 70-80.
Kettleborough, R. N., E. M. Busch-Nentwich, S. A. Harvey, C. M. Dooley, E. de Bruijn *et al.*, 2013 A systematic genome-wide analysis of zebrafish protein-coding gene function. Nature 496**:** 494-497.
Khatri, S. B., and A. K. Groves, 2013 Expression of the Foxi2 and Foxi3 transcription factors during development of chicken sensory placodes and pharyngeal arches. Gene Expr Patterns 13**:** 38-42.
Kimmel, C. B., W. W. Ballard, S. R. Kimmel, B. Ullmann and T. F. Schilling, 1995 Stages of embryonic development of the zebrafish. Dev Dyn 203**:** 253-310.
Koo, C. Y., K. W. Muir and E. W. Lam, 2012 FOXM1: From cancer initiation to progression and treatment. Biochim Biophys Acta 1819**:** 28-37.
Koshiba-Takeuchi, K., J. K. Takeuchi, K. Matsumoto, T. Momose, K. Uno *et al.*, 2000 Tbx5 and the retinotectum projection. Science 287**:** 134-137.
Kruse-Bend, R., J. Rosenthal, T. S. Quist, E. S. Veien, S. Fuhrmann *et al.*, 2012 Extraocular ectoderm triggers dorsal retinal fate during optic vesicle evagination in zebrafish. Dev Biol 371**:** 57-65.
Lagutin, O., C. C. Zhu, Y. Furuta, D. H. Rowitch, A. P. McMahon *et al.*, 2001 Six3 promotes the formation of ectopic optic vesicle-like structures in mouse embryos. Dev Dyn 221**:** 342-349.

Lam, E. W., J. J. Brosens, A. R. Gomes and C. Y. Koo, 2013 Forkhead box proteins: tuning forks for transcriptional harmony. Nat Rev Cancer 13**:** 482-495.
Larsson, C., M. Hellqvist, S. Pierrou, I. White, S. Enerback *et al.*, 1995 Chromosomal localization of six human forkhead genes, freac-1 (FKHL5), -3 (FKHL7), -4 (FKHL8), -5 (FKHL9), -6 (FKHL10), and -8 (FKHL12). Genomics 30**:** 464-469.
Lawson, N. D., and S. A. Wolfe, 2011 Forward and reverse genetic approaches for the analysis of vertebrate development in the zebrafish. Dev Cell 21**:** 48-64.
Le, H. G., J. E. Dowling and D. J. Cameron, 2012 Early retinoic acid deprivation in developing zebrafish results in microphthalmia. Vis Neurosci 29**:** 219-228.
Lehmann, O. J., N. D. Ebenezer, T. Jordan, M. Fox, L. Ocaka *et al.*, 2000 Chromosomal duplication involving the forkhead transcription factor gene FOXC1 causes iris hypoplasia and glaucoma. Am J Hum Genet 67**:** 1129-1135.
Lehmann, O. J., S. Tuft, G. Brice, R. Smith, A. Blixt *et al.*, 2003 Novel anterior segment phenotypes resulting from forkhead gene alterations: evidence for cross-species conservation of function. Invest Ophthalmol Vis Sci 44**:** 2627-2633.
Li, N., Y. Zhou, L. Du, M. Wei and X. Chen, 2011 Overview of Cytochrome P450 1B1 gene mutations in patients with primary congenital glaucoma. Exp Eye Res 93**:** 572-579.
Liu, W., O. V. Lagutin, M. Mende, A. Streit and G. Oliver, 2006 Six3 activation of Pax6 expression is essential for mammalian lens induction and specification. EMBO J 25**:** 5383-5395.
Loosli, F., W. Staub, K. C. Finger-Baier, E. A. Ober, H. Verkade *et al.*, 2003 Loss of eyes in zebrafish caused by mutation of chokh/rx3. EMBO Rep 4**:** 894-899.
Loosli, F., S. Winkler and J. Wittbrodt, 1999 Six3 overexpression initiates the formation of ectopic retina. Genes Dev 13**:** 649-654.
Lupo, G., G. Gestri, M. O'Brien, R. M. Denton, R. A. Chandraratna *et al.*, 2011 Retinoic acid receptor signaling regulates choroid fissure closure through independent mechanisms in the ventral optic cup and periocular mesenchyme. Proc Natl Acad Sci U S A 108**:** 8698-8703.
Maden, M., 2002 Retinoid signalling in the development of the central nervous system. Nat Rev Neurosci 3**:** 843-853.
Maden, M., A. Blentic, S. Reijntjes, S. Seguin, E. Gale *et al.*, 2007 Retinoic acid is required for specification of the ventral eye field and for Rathke's pouch in the avian embryo. Int J Dev Biol 51**:** 191-200.
Marsh-Armstrong, N., P. McCaffery, W. Gilbert, J. E. Dowling and U. C. Drager, 1994 Retinoic acid is necessary for development of the ventral retina in zebrafish. Proc Natl Acad Sci U S A 91**:** 7286-7290.
Martinez-Morales, J. R., V. Dolez, I. Rodrigo, R. Zaccarini, L. Leconte *et al.*, 2003 OTX2 activates the molecular network underlying retina pigment epithelium differentiation. J Biol Chem 278**:** 21721-21731.
Martinez-Morales, J. R., M. Signore, D. Acampora, A. Simeone and P. Bovolenta, 2001 Otx genes are required for tissue specification in the developing eye. Development 128**:** 2019-2030.
Mathers, P. H., A. Grinberg, K. A. Mahon and M. Jamrich, 1997 The Rx homeobox gene is essential for vertebrate eye development. Nature 387**:** 603-607.
Matsushima, D., W. Heavner and L. H. Pevny, 2011 Combinatorial regulation of optic cup progenitor cell fate by SOX2 and PAX6. Development 138**:** 443-454.

Matt, N., V. Dupe, J. M. Garnier, C. Dennefeld, P. Chambon *et al.*, 2005 Retinoic acid-dependent eye morphogenesis is orchestrated by neural crest cells. Development 132**:** 4789-4800.
Matt, N., N. B. Ghyselinck, I. Pellerin and V. Dupe, 2008 Impairing retinoic acid signalling in the neural crest cells is sufficient to alter entire eye morphogenesis. Dev Biol 320**:** 140-148.
McCaffery, P., M. O. Lee, M. A. Wagner, N. E. Sladek and U. C. Drager, 1992 Asymmetrical retinoic acid synthesis in the dorsoventral axis of the retina. Development 115**:** 371-382.
McCaffrery, P., K. C. Posch, J. L. Napoli, L. Gudas and U. C. Drager, 1993 Changing patterns of the retinoic acid system in the developing retina. Dev Biol 158**:** 390-399.
McMahon, C., G. Gestri, S. W. Wilson and B. A. Link, 2009 Lmx1b is essential for survival of periocular mesenchymal cells and influences Fgf-mediated retinal patterning in zebrafish. Dev Biol 332**:** 287-298.
Mercier, S., C. Dubourg, M. Belleguic, L. Pasquier, P. Loget *et al.*, 2010 Genetic counseling and "molecular" prenatal diagnosis of holoprosencephaly (HPE). Am J Med Genet C Semin Med Genet 154C**:** 191-196.
Meulemans, D., and M. Bronner-Fraser, 2004 Gene-regulatory interactions in neural crest evolution and development. Dev Cell 7**:** 291-299.
Mic, F. A., A. Molotkov, N. Molotkova and G. Duester, 2004 Raldh2 expression in optic vesicle generates a retinoic acid signal needed for invagination of retina during optic cup formation. Dev Dyn 231**:** 270-277.
Mirzayans, F., D. B. Gould, E. Heon, G. D. Billingsley, J. C. Cheung *et al.*, 2000 Axenfeld-Rieger syndrome resulting from mutation of the FKHL7 gene on chromosome 6p25. Eur J Hum Genet 8**:** 71-74.
Mitchell, S. M., J. P. Ross, H. R. Drew, T. Ho, G. S. Brown *et al.*, 2014 A panel of genes methylated with high frequency in colorectal cancer. BMC Cancer 14**:** 54.
Molotkov, A., N. Molotkova and G. Duester, 2006 Retinoic acid guides eye morphogenetic movements via paracrine signaling but is unnecessary for retinal dorsoventral patterning. Development 133**:** 1901-1910.
Morrison, D., D. FitzPatrick, I. Hanson, K. Williamson, V. van Heyningen *et al.*, 2002 National study of microphthalmia, anophthalmia, and coloboma (MAC) in Scotland: investigation of genetic aetiology. J Med Genet 39**:** 16-22.
Mory, A., F. X. Ruiz, E. Dagan, E. A. Yakovtseva, A. Kurolap *et al.*, 2014 A missense mutation in ALDH1A3 causes isolated microphthalmia/anophthalmia in nine individuals from an inbred Muslim kindred. Eur J Hum Genet 22**:** 419-422.
Murai, K. K., and E. B. Pasquale, 2003 'Eph'ective signaling: forward, reverse and crosstalk. J Cell Sci 116**:** 2823-2832.
Murali, D., S. Yoshikawa, R. R. Corrigan, D. J. Plas, M. C. Crair *et al.*, 2005 Distinct developmental programs require different levels of Bmp signaling during mouse retinal development. Development 132**:** 913-923.
Myatt, S. S., and E. W. Lam, 2007 The emerging roles of forkhead box (Fox) proteins in cancer. Nat Rev Cancer 7**:** 847-859.
Nasevicius, A., and S. C. Ekker, 2000 Effective targeted gene 'knockdown' in zebrafish. Nat Genet 26**:** 216-220.

Niederreither, K., and P. Dolle, 2008 Retinoic acid in development: towards an integrated view. Nat Rev Genet 9**:** 541-553.
Nishimura, D. Y., R. E. Swiderski, W. L. Alward, C. C. Searby, S. R. Patil *et al.*, 1998 The forkhead transcription factor gene FKHL7 is responsible for glaucoma phenotypes which map to 6p25. Nat Genet 19**:** 140-147.
Nissen, R. M., J. Yan, A. Amsterdam, N. Hopkins and S. M. Burgess, 2003 Zebrafish foxi one modulates cellular responses to Fgf signaling required for the integrity of ear and jaw patterning. Development 130**:** 2543-2554.
Nohe, A., E. Keating, P. Knaus and N. O. Petersen, 2004 Signal transduction of bone morphogenetic protein receptors. Cell Signal 16**:** 291-299.
Nornes, S., M. Clarkson, I. Mikkola, M. Pedersen, A. Bardsley *et al.*, 1998 Zebrafish contains two pax6 genes involved in eye development. Mech Dev 77**:** 185-196.
Nuckels, R. J., A. Ng, T. Darland and J. M. Gross, 2009 The vacuolar-ATPase complex regulates retinoblast proliferation and survival, photoreceptor morphogenesis, and pigmentation in the zebrafish eye. Invest Ophthalmol Vis Sci 50**:** 893-905.
Ohyama, T., and A. K. Groves, 2004 Expression of mouse Foxi class genes in early craniofacial development. Dev Dyn 231**:** 640-646.
Ojeda, A. F., R. P. Munjaal and P. Y. Lwigale, 2013 Expression of CXCL12 and CXCL14 during eye development in chick and mouse. Gene Expr Patterns 13**:** 303-310.
Oliver, G., F. Loosli, R. Koster, J. Wittbrodt and P. Gruss, 1996 Ectopic lens induction in fish in response to the murine homeobox gene Six3. Mech Dev 60**:** 233-239.
Onichtchouk, D., Y. G. Chen, R. Dosch, V. Gawantka, H. Delius *et al.*, 1999 Silencing of TGF-beta signalling by the pseudoreceptor BAMBI. Nature 401**:** 480-485.
Parker, S. E., C. T. Mai, M. A. Canfield, R. Rickard, Y. Wang *et al.*, 2010 Updated National Birth Prevalence estimates for selected birth defects in the United States, 2004-2006. Birth Defects Res A Clin Mol Teratol 88**:** 1008-1016.
Paulsen, M., S. Legewie, R. Eils, E. Karaulanov and C. Niehrs, 2011 Negative feedback in the bone morphogenetic protein 4 (BMP4) synexpression group governs its dynamic signaling range and canalizes development. Proc Natl Acad Sci U S A 108**:** 10202-10207.
Picker, A., and M. Brand, 2005 Fgf signals from a novel signaling center determine axial patterning of the prospective neural retina. Development 132**:** 4951-4962.
Picker, A., F. Cavodeassi, A. Machate, S. Bernauer, S. Hans *et al.*, 2009 Dynamic coupling of pattern formation and morphogenesis in the developing vertebrate retina. PLoS Biol 7**:** e1000214.
Pieper, A. A., S. Xie, E. Capota, S. J. Estill, J. Zhong *et al.*, 2010 Discovery of a proneurogenic, neuroprotective chemical. Cell 142**:** 39-51.
Pierrou, S., M. Hellqvist, L. Samuelsson, S. Enerback and P. Carlsson, 1994 Cloning and characterization of seven human forkhead proteins: binding site specificity and DNA bending. EMBO J 13**:** 5002-5012.
Prabhudesai, S. N., D. A. Cameron and D. L. Stenkamp, 2005 Targeted effects of retinoic acid signaling upon photoreceptor development in zebrafish. Dev Biol 287**:** 157-167.
Pratt, T., N. M. Tian, T. I. Simpson, J. O. Mason and D. J. Price, 2004 The winged helix transcription factor Foxg1 facilitates retinal ganglion cell axon crossing of the ventral midline in the mouse. Development 131**:** 3773-3784.

Quadro, L., W. S. Blaner, D. J. Salchow, S. Vogel, R. Piantedosi *et al.*, 1999 Impaired retinal function and vitamin A availability in mice lacking retinol-binding protein. EMBO J 18**:** 4633-4644.

Ragge, N. K., A. G. Brown, C. M. Poloschek, B. Lorenz, R. A. Henderson *et al.*, 2005 Heterozygous mutations of OTX2 cause severe ocular malformations. Am J Hum Genet 76**:** 1008-1022.

Raymond, P. A., L. K. Barthel, R. L. Bernardos and J. J. Perkowski, 2006 Molecular characterization of retinal stem cells and their niches in adult zebrafish. BMC Dev Biol 6**:** 36.

Raymond, P. A., L. K. Barthel and G. A. Curran, 1995 Developmental patterning of rod and cone photoreceptors in embryonic zebrafish. J Comp Neurol 359**:** 537-550.

Reddy, A. B., S. G. Panicker, A. K. Mandal, S. E. Hasnain and D. Balasubramanian, 2003 Identification of R368H as a predominant CYP1B1 allele causing primary congenital glaucoma in Indian patients. Invest Ophthalmol Vis Sci 44**:** 4200-4203.

Reis, L. M., R. C. Tyler, K. F. Schilter, O. Abdul-Rahman, J. W. Innis *et al.*, 2011 BMP4 loss-of-function mutations in developmental eye disorders including SHORT syndrome. Hum Genet 130**:** 495-504.

Reis, L. M., R. C. Tyler, A. Schneider, T. Bardakjian, J. M. Stoler *et al.*, 2010 FOXE3 plays a significant role in autosomal recessive microphthalmia. Am J Med Genet A 152A**:** 582-590.

Rembold, M., F. Loosli, R. J. Adams and J. Wittbrodt, 2006 Individual cell migration serves as the driving force for optic vesicle evagination. Science 313**:** 1130-1134.

Robu, M. E., J. D. Larson, A. Nasevicius, S. Beiraghi, C. Brenner *et al.*, 2007 p53 activation by knockdown technologies. PLoS Genet 3**:** e78.

Rodrigues, F. S., G. Doughton, B. Yang and R. N. Kelsh, 2012 A novel transgenic line using the Cre-lox system to allow permanent lineage-labeling of the zebrafish neural crest. Genesis 50**:** 750-757.

Sasagawa, S., T. Takabatake, Y. Takabatake, T. Muramatsu and K. Takeshima, 2002 Axes establishment during eye morphogenesis in Xenopus by coordinate and antagonistic actions of BMP4, Shh, and RA. Genesis 33**:** 86-96.

Schilter, K. F., A. Schneider, T. Bardakjian, J. F. Soucy, R. C. Tyler *et al.*, 2011 OTX2 microphthalmia syndrome: four novel mutations and delineation of a phenotype. Clin Genet 79**:** 158-168.

Schmitt, E. A., and J. E. Dowling, 1994 Early eye morphogenesis in the zebrafish, Brachydanio rerio. J Comp Neurol 344**:** 532-542.

Schmitt, E. A., and J. E. Dowling, 1996 Comparison of topographical patterns of ganglion and photoreceptor cell differentiation in the retina of the zebrafish, Danio rerio. J Comp Neurol 371**:** 222-234.

Schmitt, E. A., and J. E. Dowling, 1999 Early retinal development in the zebrafish, Danio rerio: light and electron microscopic analyses. J Comp Neurol 404**:** 515-536.

Semerci, C. N., E. Kalay, C. Yildirim, T. Dincer, A. Olmez *et al.*, 2014 Novel splice-site and missense mutations in the ALDH1A3 gene underlying autosomal recessive anophthalmia/microphthalmia. Br J Ophthalmol 98**:** 832-840.

Semina, E. V., I. Brownell, H. A. Mintz-Hittner, J. C. Murray and M. Jamrich, 2001 Mutations in the human forkhead transcription factor FOXE3 associated with anterior segment ocular dysgenesis and cataracts. Hum Mol Genet 10**:** 231-236.

Sen, J., S. Harpavat, M. A. Peters and C. L. Cepko, 2005 Retinoic acid regulates the expression of dorsoventral topographic guidance molecules in the chick retina. Development 132**:** 5147-5159.
Seo, H. C., Drivenes, S. Ellingsen and A. Fjose, 1998 Expression of two zebrafish homologues of the murine Six3 gene demarcates the initial eye primordia. Mech Dev 73**:** 45-57.
Seo, S., H. P. Singh, P. M. Lacal, A. Sasman, A. Fatima *et al.*, 2012 Forkhead box transcription factor FoxC1 preserves corneal transparency by regulating vascular growth. Proc Natl Acad Sci U S A 109**:** 2015-2020.
Seoane, J., H. V. Le, L. Shen, S. A. Anderson and J. Massague, 2004 Integration of Smad and forkhead pathways in the control of neuroepithelial and glioblastoma cell proliferation. Cell 117**:** 211-223.
Shaham, O., Y. Menuchin, C. Farhy and R. Ashery-Padan, 2012 Pax6: a multi-level regulator of ocular development. Prog Retin Eye Res 31**:** 351-376.
Shi, X., Y. Luo, S. Howley, A. Dzialo, S. Foley *et al.*, 2006 Zebrafish foxe3: roles in ocular lens morphogenesis through interaction with pitx3. Mech Dev 123**:** 761-782.
Shimozono, S., T. Iimura, T. Kitaguchi, S. Higashijima and A. Miyawaki, 2013 Visualization of an endogenous retinoic acid gradient across embryonic development. Nature 496**:** 363-366.
Sieber, C., J. Kopf, C. Hiepen and P. Knaus, 2009 Recent advances in BMP receptor signaling. Cytokine Growth Factor Rev 20**:** 343-355.
Skarie, J. M., and B. A. Link, 2009 FoxC1 is essential for vascular basement membrane integrity and hyaloid vessel morphogenesis. Invest Ophthalmol Vis Sci 50**:** 5026-5034.
Smith, A. N., L. A. Miller, G. Radice, R. Ashery-Padan and R. A. Lang, 2009 Stage-dependent modes of Pax6-Sox2 epistasis regulate lens development and eye morphogenesis. Development 136**:** 2977-2985.
Smith, R. S., A. Zabaleta, T. Kume, O. V. Savinova, S. H. Kidson *et al.*, 2000 Haploinsufficiency of the transcription factors FOXC1 and FOXC2 results in aberrant ocular development. Hum Mol Genet 9**:** 1021-1032.
Solomon, K. S., T. Kudoh, I. B. Dawid and A. Fritz, 2003a Zebrafish foxi1 mediates otic placode formation and jaw development. Development 130**:** 929-940.
Solomon, K. S., J. M. Logsdon, Jr. and A. Fritz, 2003b Expression and phylogenetic analyses of three zebrafish FoxI class genes. Dev Dyn 228**:** 301-307.
Sperry, R. W., 1963 Chemoaffinity in the Orderly Growth of Nerve Fiber Patterns and Connections. Proc Natl Acad Sci U S A 50**:** 703-710.
Sprague, J., D. Clements, T. Conlin, P. Edwards, K. Frazer *et al.*, 2003 The Zebrafish Information Network (ZFIN): the zebrafish model organism database. Nucleic Acids Res 31**:** 241-243.
Srour, M., D. Chitayat, V. Caron, N. Chassaing, P. Bitoun *et al.*, 2013 Recessive and dominant mutations in retinoic acid receptor beta in cases with microphthalmia and diaphragmatic hernia. Am J Hum Genet 93**:** 765-772.
Steingrimsson, E., N. G. Copeland and N. A. Jenkins, 2004 Melanocytes and the microphthalmia transcription factor network. Annu Rev Genet 38**:** 365-411.
Stevens, C. B., D. A. Cameron and D. L. Stenkamp, 2011 Plasticity of photoreceptor-generating retinal progenitors revealed by prolonged retinoic acid exposure. BMC Dev Biol 11**:** 51.

Takahashi, H., H. Sakuta, T. Shintani and M. Noda, 2009 Functional mode of FoxD1/CBF2 for the establishment of temporal retinal specificity in the developing chick retina. Dev Biol 331**:** 300-310.
Take-uchi, M., J. D. Clarke and S. W. Wilson, 2003 Hedgehog signalling maintains the optic stalk-retinal interface through the regulation of Vax gene activity. Development 130**:** 955-968.
Taranova, O. V., S. T. Magness, B. M. Fagan, Y. Wu, N. Surzenko *et al.*, 2006 SOX2 is a dose-dependent regulator of retinal neural progenitor competence. Genes Dev 20**:** 1187-1202.
Teng, L., N. A. Mundell, A. Y. Frist, Q. Wang and P. A. Labosky, 2008 Requirement for Foxd3 in the maintenance of neural crest progenitors. Development 135**:** 1615-1624.
Thiel, G., 2013 How Sox2 maintains neural stem cell identity. Biochem J 450**:** e1-2.
Thisse, C., and B. Thisse, 2008 High-resolution in situ hybridization to whole-mount zebrafish embryos. Nat Protoc 3**:** 59-69.
Tian, N. M., T. Pratt and D. J. Price, 2008 Foxg1 regulates retinal axon pathfinding by repressing an ipsilateral program in nasal retina and by causing optic chiasm cells to exert a net axonal growth-promoting activity. Development 135**:** 4081-4089.
Trousse, F., P. Esteve and P. Bovolenta, 2001 Bmp4 mediates apoptotic cell death in the developing chick eye. J Neurosci 21**:** 1292-1301.
Tsai, K. L., C. Y. Huang, C. H. Chang, Y. J. Sun, W. J. Chuang *et al.*, 2006 Crystal structure of the human FOXK1a-DNA complex and its implications on the diverse binding specificity of winged helix/forkhead proteins. J Biol Chem 281**:** 17400-17409.
Tumer, Z., and D. Bach-Holm, 2009 Axenfeld-Rieger syndrome and spectrum of PITX2 and FOXC1 mutations. Eur J Hum Genet 17**:** 1527-1539.
van Raamsdonk, C. D., and S. M. Tilghman, 2000 Dosage requirement and allelic expression of PAX6 during lens placode formation. Development 127**:** 5439-5448.
Veien, E. S., J. S. Rosenthal, R. C. Kruse-Bend, C. B. Chien and R. I. Dorsky, 2008 Canonical Wnt signaling is required for the maintenance of dorsal retinal identity. Development 135**:** 4101-4111.
Verma, A. S., and D. R. Fitzpatrick, 2007 Anophthalmia and microphthalmia. Orphanet J Rare Dis 2**:** 47.
Voronina, V. A., E. A. Kozhemyakina, C. M. O'Kernick, N. D. Kahn, S. L. Wenger *et al.*, 2004 Mutations in the human RAX homeobox gene in a patient with anophthalmia and sclerocornea. Hum Mol Genet 13**:** 315-322.
Wagner, E., P. McCaffery and U. C. Drager, 2000 Retinoic acid in the formation of the dorsoventral retina and its central projections. Dev Biol 222**:** 460-470.
Wargelius, A., H. C. Seo, L. Austbo and A. Fjose, 2003 Retinal expression of zebrafish six3.1 and its regulation by Pax6. Biochem Biophys Res Commun 309**:** 475-481.
Webb, T. R., M. Matarin, J. C. Gardner, D. Kelberman, H. Hassan *et al.*, 2012 X-linked megalocornea caused by mutations in CHRDL1 identifies an essential role for ventroptin in anterior segment development. Am J Hum Genet 90**:** 247-259.
Wehman, A. M., W. Staub, J. R. Meyers, P. A. Raymond and H. Baier, 2005 Genetic dissection of the zebrafish retinal stem-cell compartment. Dev Biol 281**:** 53-65.
Weigel, D., and H. Jackle, 1990 The fork head domain: a novel DNA binding motif of eukaryotic transcription factors? Cell 63**:** 455-456.

Weigel, D., G. Jurgens, F. Kuttner, E. Seifert and H. Jackle, 1989 The homeotic gene fork head encodes a nuclear protein and is expressed in the terminal regions of the Drosophila embryo. Cell 57**:** 645-658.
Weiss, O., R. Kaufman, N. Michaeli and A. Inbal, 2012 Abnormal vasculature interferes with optic fissure closure in lmo2 mutant zebrafish embryos. Dev Biol 369**:** 191-198.
Wen, J., Q. Hu, M. Li, S. Wang, L. Zhang *et al.*, 2008 Pax6 directly modulate Sox2 expression in the neural progenitor cells. Neuroreport 19**:** 413-417.
Westenskow, P., S. Piccolo and S. Fuhrmann, 2009 Beta-catenin controls differentiation of the retinal pigment epithelium in the mouse optic cup by regulating Mitf and Otx2 expression. Development 136**:** 2505-2510.
Westerfield, M., 1993 *The Zebrafish book : a guide for the laboratory use of zebrafish (Brachydanio rerio)*. University of Oregon Press, Eugene. Or.
Wijchers, P. J., M. F. Hoekman, J. P. Burbach and M. P. Smidt, 2005 Cloning and analysis of the murine Foxi2 transcription factor. Biochim Biophys Acta 1731**:** 133-138.
Willer, G. B., V. M. Lee, R. G. Gregg and B. A. Link, 2005 Analysis of the Zebrafish perplexed mutation reveals tissue-specific roles for de novo pyrimidine synthesis during development. Genetics 170**:** 1827-1837.
Williamson, K. A., and D. R. FitzPatrick, 2014 The genetic architecture of microphthalmia, anophthalmia and coloboma. Eur J Med Genet.
Wilson, J. G., C. B. Roth and J. Warkany, 1953 An analysis of the syndrome of malformations induced by maternal vitamin A deficiency. Effects of restoration of vitamin A at various times during gestation. Am J Anat 92**:** 189-217.
Wolbach, S. B., and P. R. Howe, 1925 Tissue Changes Following Deprivation of Fat-Soluble a Vitamin. J Exp Med 42**:** 753-777.
Woo, S., D. J. Rowan and T. M. Gomez, 2009 Retinotopic mapping requires focal adhesion kinase-mediated regulation of growth cone adhesion. J Neurosci 29**:** 13981-13991.
Wu, L. Y., M. Li, D. R. Hinton, L. Guo, S. Jiang *et al.*, 2003 Microphthalmia resulting from MSX2-induced apoptosis in the optic vesicle. Invest Ophthalmol Vis Sci 44**:** 2404-2412.
Wyatt, A. W., R. J. Osborne, H. Stewart and N. K. Ragge, 2010 Bone morphogenetic protein 7 (BMP7) mutations are associated with variable ocular, brain, ear, palate, and skeletal anomalies. Hum Mutat 31**:** 781-787.
Xuan, S., C. A. Baptista, G. Balas, W. Tao, V. C. Soares *et al.*, 1995 Winged helix transcription factor BF-1 is essential for the development of the cerebral hemispheres. Neuron 14**:** 1141-1152.
Yahyavi, M., H. Abouzeid, G. Gawdat, A. S. de Preux, T. Xiao *et al.*, 2013 ALDH1A3 loss of function causes bilateral anophthalmia/microphthalmia and hypoplasia of the optic nerve and optic chiasm. Hum Mol Genet 22**:** 3250-3258.
Yang, T., H. Vidarsson, S. Rodrigo-Blomqvist, S. S. Rosengren, S. Enerback *et al.*, 2007 Transcriptional control of SLC26A4 is involved in Pendred syndrome and nonsyndromic enlargement of vestibular aqueduct (DFNB4). Am J Hum Genet 80**:** 1055-1063.
Ye, M., K. M. Berry-Wynne, M. Asai-Coakwell, P. Sundaresan, T. Footz *et al.*, 2010 Mutation of the bone morphogenetic protein GDF3 causes ocular and skeletal anomalies. Hum Mol Genet 19**:** 287-298.

Yin, H. C., H. P. Tseng, H. Y. Chung, C. Y. Ko, W. S. Tzou *et al.*, 2008 Influence of TCDD on zebrafish CYP1B1 transcription during development. Toxicol Sci 103**:** 158-168.
Yuasa, J., S. Hirano, M. Yamagata and M. Noda, 1996 Visual projection map specified by topographic expression of transcription factors in the retina. Nature 382**:** 632-635.
Zacharias, A. L., and P. J. Gage, 2010 Canonical Wnt/beta-catenin signaling is required for maintenance but not activation of Pitx2 expression in neural crest during eye development. Dev Dyn 239**:** 3215-3225.
Zhang, X. M., and X. J. Yang, 2001 Temporal and spatial effects of Sonic hedgehog signaling in chick eye morphogenesis. Dev Biol 233**:** 271-290.
Zuber, M. E., G. Gestri, A. S. Viczian, G. Barsacchi and W. A. Harris, 2003 Specification of the vertebrate eye by a network of eye field transcription factors. Development 130**:** 5155-5167.